

Prediction of Shear/Peeling Failure In Plated R/C Beams

by

Mohammed Ashrafuddin

A Thesis Presented to the

FACULTY OF THE COLLEGE OF GRADUATE STUDIES
KING FAHD UNIVERSITY OF PETROLEUM & MINERALS
DHAHRAN, SAUDI ARABIA

In Partial Fulfillment of the
Requirements for the Degree of

MASTER OF SCIENCE

In

CIVIL ENGINEERING

June, 1995

INFORMATION TO USERS

This manuscript has been reproduced from the microfilm master. UMI films the text directly from the original or copy submitted. Thus, some thesis and dissertation copies are in typewriter face, while others may be from any type of computer printer.

The quality of this reproduction is dependent upon the quality of the copy submitted. Broken or indistinct print, colored or poor quality illustrations and photographs, print bleedthrough, substandard margins, and improper alignment can adversely affect reproduction.

In the unlikely event that the author did not send UMI a complete manuscript and there are missing pages, these will be noted. Also, if unauthorized copyright material had to be removed, a note will indicate the deletion.

Oversize materials (e.g., maps, drawings, charts) are reproduced by sectioning the original, beginning at the upper left-hand corner and continuing from left to right in equal sections with small overlaps. Each original is also photographed in one exposure and is included in reduced form at the back of the book.

Photographs included in the original manuscript have been reproduced xerographically in this copy. Higher quality 6" x 9" black and white photographic prints are available for any photographs or illustrations appearing in this copy for an additional charge. Contact UMI directly to order.

UMI

A Bell & Howell Information Company
300 North Zeeb Road, Ann Arbor, MI 48106-1346 USA
313/761-4700 800/521-0600

**PREDICTION OF SHEAR/PEELING FAILURE
IN PLATED R/C BEAMS**

BY

MOHAMMED ASHRAFUDDIN

A Thesis Presented to the
FACULTY OF THE COLLEGE OF GRADUATE STUDIES
KING FAHD UNIVERSITY OF PETROLEUM & MINERALS
DHAHRAN, SAUDI ARABIA

In Partial Fulfillment of the
Requirements for the Degree of

MASTER OF SCIENCE

In

CIVIL ENGINEERING

JUNE 1995

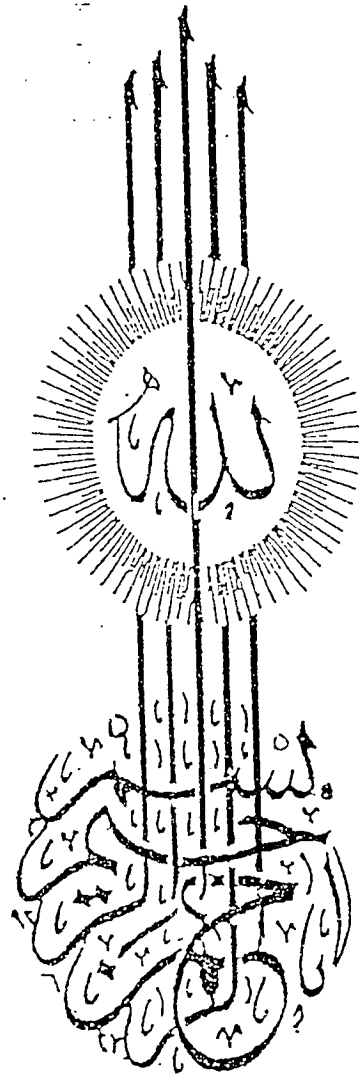
UMI Number: 1377137

UMI Microform 1377137
Copyright 1996, by UMI Company. All rights reserved.

This microform edition is protected against unauthorized
copying under Title 17, United States Code.

UMI

300 North Zeeb Road
Ann Arbor, MI 48103



سُبْحَانَكَ لَا عِلْمَ لَنَا إِلَّا مَا عَلَّمْتَنَا إِنَّكَ أَنْتَ الْعَلِيمُ الْحَكِيمُ

(Glory to Thee: Of knowledge we have none, save what Thou hast taught us: In truth; it is Thou who art perfect in knowledge and wisdom.)

(2:32)

KING FAHD UNIVERSITY OF PETROLEUM AND MINERALS
DHAHRAN 31261, SAUDI ARABIA

COLLEGE OF GRADUATE STUDIES

This Thesis, written by

Mohammed Ashrafuddin

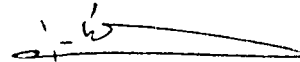
under the direction of his Thesis Advisor, and approved by his Thesis Committee, has been presented to and accepted by the Dean of the College of Graduate Studies, in partial fulfillment of the requirements for the degree of

Master of Science in Civil Engineering (Structures)

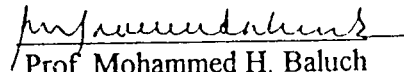
Thesis Committee



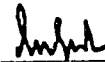
Prof. Ghazi J. Al-Sulaimani
Chairman



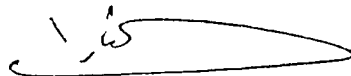
Dr. Al-Farabi M. Sharif
Co-Chairman



Prof. Mohammed H. Baluch
Member



Prof. Abul Kalam Azad
Member



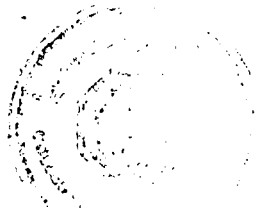
Dr. Al-Farabi M. Sharif
Department Chairman



Dr. Ala H. Al-Rabeh
Dean, College of Graduate Studies

17. 10. 95

Dated



This thesis is dedicated to

my parents

and

**all those noble and sublime personalities whose serenity, courage
and wisdom lead me to the *Path of Guidance***

ACKNOWLEDGMENTS

Firstly, I thank Almighty Allah, All praise is for Him, for bestowing me with the health, power and patience to complete this work. Then acknowledgment is due to KFUPM for the support given to this research work through its tremendous facilities, and the opportunity given to me to pursue graduate study with financial support.

I am greatly indebted to many for their invaluable assistance during my stay at KFUPM. I acknowledge, with deep gratitude and appreciation the inspiration, encouragement and guidance given to me by my major Advisor Prof. Sulaimani, Co-advisor Dr. Farabi, committee members Prof. Baluch and Prof. Azad, who have taken care and showed great interest in the work by assisting and giving constructive comments with patience.

My sincere thanks to Prof. Sulaimani for giving me an opportunity to work under him right after my first semester. Thanks to Dr. Farabi for showing special care and attention in all matters right from the day one of my admission. I am again thankful to Prof. Baluch for his concern, unending support, and encouragement. The credit for the good part of this thesis goes to Prof. Baluch. Thanks to Prof. Azad for all the help in different matters.

I would also like to express my thanks to Dr. Baghabra, Dr. Maslehuddin, Dr. Gadhib, Dr. Abdul Wahab, Dr. Aiban, Dr. Ahmedi, Dr. Musallam, Br. Affan Badar, Br. Sadat Ali Khan, Br. Rashiduddin for their moral support, guidance, encouragement and patronage.

Special thanks are due to all laboratory personnel (Omer, Nihash, Ahmed Nufeli, Mr. Mukarram, Hassan Zakaria, Abu-Jaffar, Abu-Abdullah, Tony and Farooq). All my friends and colleagues (Abbas Qureshi, Abdul Waris, Mujeeb, Sharfuddin, Saleem Parvez, Safder Khan, Ghouse Baig, Asif Sayani, Asad, Asad-ur-Rahman Khan and Arshad Chaudhry) who assisted me in the preparation of cages for the beams. Department secretaries (Mr. Mumtaz, Mr. Ooly and Mr. Affron) for their help at all times and all those, who without complaint of any omissions or commissions assisted me and stood by my side in this long journey of about three years stay at KFUPM.

I extend my heartfelt gratitude to Ibrahim Asi for his unlimited support and unwavering trust in me and above all his support and encouragement at all difficult times. I would like to acknowledge the continued support provided by the maintenance department. I also express my special thanks to Salman Naqvi, Ilyas, Lashari, Hadi, Younus and all other friends, teachers, colleagues for their help, moral support and memorable days we shared together.

Finally, without the able and continuing support, prayers, sacrifices, love, patience, encouragement and understanding of my beloved parents, wife, brother, sisters, in-laws and all well wishers the completion of this study would not have been a possibility.

THESIS ABSTRACT

Name of the Student : *Mohammed Ashrafuddin*

Title : *Prediction of Shear/Peeling Failure in Plated R/C Beams*

Major Field : *Civil Engineering (Structures)*

Date of Degree : *June 1995*

The work in this thesis focuses on an experimental investigation to characterize ultimate load levels and failure mode characteristics of reinforced concrete (R/C) beams strengthened or repaired by bonding external plates to the soffit of the R/C beam. The experimental investigation is designed so as to induce not only flexural failure and concrete rip-off failure in the repaired beams but also a diagonal tension failure similar to unplated R/C beams. Parametric constraints leading to diagonal tension failure in plated beams in contrast to flexural failure and rip-off failure are defined. A total of twenty eight R/C beams repaired by plate bonding were tested and data was generated to yield ultimate load levels, mode of failure and central beam deflection. Existing model for predicting rip-off failure was confirmed in terms of ultimate load levels and mode of failure, and a new predictor equation is proposed for determination of ultimate load for plated beams prone to fail under diagonal tension.

MASTER OF SCIENCE

KING FAHD UNIVERSITY OF PETROLEUM AND MINERALS

Dhahran, Saudi Arabia

ملخص الرسالة

إسم الطالب : محمد أشرف الدين
عنوان البحث : التنبؤ بإنهيارات القص أو الإنسلاخ في الكمرات المسلحة
والمدعمة بالصفائح
التخصص : هندسة مدنية (إنشاءات)
التاريخ : يونيو ، ١٩٩٥ م

يركز العمل في هذا البحث على التحليل العملي لمعرفة قوة تحمل ونوعية الإنهيارات التي تحدث للكمرات المسلحة والتي تم تدعيمها أو إصلاحها عن طريق لصق الصفائح الخارجية على باطن الكمرة المسلحة . تم تصميم البحث بحيث تكون الإنهيارات التي تتعرض لها الكمرات المدعمة بالصفائح إنهاءات ثني وإنهيارات إنسلاخ وكذلك، إنهاءات شد قطرية كتلك التي تحدث في الكمرات المسلحة الغير المدعمة بالصفائح. تمفي هذا البحث تعريف الحدود والضوابط التي تؤدي إلى حدوث إنهاءات الشد القطرية في الكمرات المدعمة والتي تختلف في طبيعتها عن تلك التي تؤدي إلى حدوث إنهاءات الثني والإنسلاخ . لقد تم إنشاء ثمانية وعشرون كمرة مسلحة ومن ثم تم إصلاحها باستخدام الصفائح المعدنية وبعد ذلك تم اختبار هذه الكمرات. إستخدمت نتائج إختبارات هذه الكمرات في تعريف أعلى قوة تتحملها هذه الكمرات، طبيعة الإنهيارات وكذلك الإنحناءات المركزية . جرى التأكد من أن المعادلات المستخدمة في إيجاد أعلى قوة تحمل وطبيعة الإنهيار موافقة النتائج التي تم الحصول عليها للكمرات ذات الإنسلاخ . كما تم إقتراح معادلات جديدة لإيجاد قوى تحمل الكمرات المعرضة للإنهيار عن طريق الشد القطري .

ماجستير علوم

جامعة الملك فهد للبترول والمعادن

الظهران ، المملكة العربية السعودية

Table of Contents

	Page No.
Acknowledgement	iv
Thesis Abstract (English)	v
Thesis Abstract (Arabic)	vi
List of Tables	ix
List of Figures	x
List of Plates	xiv
List of Symbols	xvii
Chapter I: INTRODUCTION	1
1.1 Repair and Rehabilitation of R/C Structures	1
1.2 Strengthening Techniques	3
1.3 Plate Bonding	3
1.4 Existing State-of-The-Art.....	5
1.5 Modes of Failure	6
1.5.1 Flexural Failure	6
1.5.2 Concrete/Glue/Steel Interface Separation	7
1.5.3 Concrete Rip-off Failure Mode	7
1.5.4 Diagonal Tension Failure Mode	8
1.6 Research Objectives	9
Chapter II: LITERATURE REVIEW	11
2.1 Use of Plate Bonding	11
2.2 Flexural and Shear Studies	
Chapter III: EXPERIMENTAL PROGRAM	25
3.1 Introduction	25
3.2 Materials	26
3.3 Preparation of Beams	27
3.4 Damaging of Beams	28
3.5 Repair of Beams	29
Chapter IV: THEORETICAL CALCULATIONS	45
4.1 Introduction	45

4.2	Unrepaired Beam	45
4.2.1	Flexural Capacity (P_f)	45
4.2.2	Shear Capacity (P_s)	46
4.3	Repaired Beam	47
4.3.1	Flexural Capacity (P_{flex})	47
4.3.2	Shear Capacity (P_{shear})	47
4.4	Expression for the Shear Capacity	49
4.4.1	Rip-off Failure	49
4.4.2	Diagonal Tension Failure	54
Chapter V: RESULTS AND DISCUSSION		58
5.1	Introduction	58
5.2	Flexural Beams	61
5.2.1	Effect of Stirrup Spacing	61
5.2.2	Effect of Plate Thickness	63
5.2.3	Effect of Curtailment Length of Plate	66
5.3	Shear Beams	69
Chapter VI: CONCLUSIONS AND RECOMMENDATIONS		133
6.1	Conclusions	133
6.1.1	For Plated with $P_f < P < P_s$	134
6.1.2	For Plated with $P_s < P < P_f$	135
6.2	Recommendations	136
Chapter VII: REFERENCES		137
APPENDIX-A (Solved Example)		142
APPENDIX-B (Mechanism)		162
Curriculum Vitae		184

List of Tables

Table		Page No.
3.1	Coarse Aggregate Grading	31
3.2	Maximum load, central deflection, residual deflection and crackwidth for Pre-damaged beams	32
5.1	Experimental and Predicted Ultimate Loads for all Beams Tested ...	71
5.2	Shear and Peeling Stresses based on Roberts [34] and KFUPM Research Group [38,41,44] approach	73

List of Figures

Figure	Page No.
3.1 Details of Experimental Program	33
3.2 Reinforcement Details	34
3.3 Details of Experimental variables for Beams of Flexure Group	35
3.4 Details of Experimental variables for Beams of Shear Shear Group ...	36
3.5 Coarse Aggregate Grading Curve (#67)	37
3.6 Sketch shows the load configuration used in testing the beam specimens	38
4.1 Internal Forces at Ultimate Conditions	56
4.2 Strain Distribution at Balanced Conditions	57
5.1 Load Vs Central Deflection for Beams repaired with 1100 mm long, 1 mm thick steel plates on the soffit of the beam having stirrups at 30,60 and 20 mm c/c respectively	74
5.2 Load Vs Central Deflection for Beams repaired with 1100 mm long, 2 mm thick steel plates on the soffit of the beam having stirrups at 30,60 and 120 mm c/c respectively	75
5.3 Load Vs Central Deflection for Beams repaired with 1100 mm long, 3 mm thick steel plates on the soffit of the beam having stirrups at 30, 60 and 120 mm c/c respectively	76
5.4 Load Vs Central Deflection for Beams repaired with 900 mm long, 1 mm thick steel plates on the soffit of the beam having stirrups at 30, 60 and 120 mm c/c respectively	77
5.5 Load Vs Central Deflection for Beams repaired with 900 mm long, 2 mm thick steel plates on the soffit of the beam having	

	stirrups at 30, 60 and 120 mm c/c respectively	78
5.6	Load Vs Central Deflection for Beams repaired with 900 mm long, 3 mm thick steel plates on the soffit of the beam having stirrups at 30, 60 and 120 mm c/c respectively	79
5.7	Load Vs Central Deflection for Beams repaired with 1100 mm long steel plates of thickness 1, 2, and 3 mm respectively on the soffit of beam having stirrups at 120 mm c/c each	80
5.8	Load Vs Central Deflection for Beams repaired with 1100 mm long steel plates of thickness 1, 2, and 3mm respectively on the soffit of beam having stirrups at 60 mm c/c each	81
5.9	Load Vs Central Deflection for Beams repaired with 1100 mm long steel plates of thickness 1, 2, and 3mm respectively on the soffit of beam having stirrups at 30 mm c/c each	82
5.10	Load Vs Central Deflection for Beams repaired with 900 mm long steel plates of thickness 1, 2, and 3mm respectively on the soffit of beam having stirrups at 120 mm c/c each	83
5.11	Load Vs Central Deflection for Beams repaired with 900 mm long steel plates of thickness 1, 2, and 3 mm respectively on the soffit of beam having stirrups at 60 mm c/c each	84
5.12	Load Vs Central Deflection for Beams repaired with 900 mm long steel plates of thickness 1, 2, and 3 mm respectively on the soffit of beam having stirrups at 30 mm c/c each	85
5.13	Load Vs Central Deflection for Beams repaired with 900 mm and 1100 mm long steel plates of 1mm thickness on the soffit of beam having stirrups at 120 mm c/c	86
5.14	Load Vs Central Deflection for Beams repaired with 900 mm and 1100 mm long steel plates of 2mm thickness on the soffit of beam having stirrups at 120 mm c/c	87
5.15	Load Vs Central Deflection for Beams repaired with 900 mm and 1100 mm long steel plates of 3mm thickness on the soffit of beam having stirrups at 120 mm c/c	88
5.16	Load Vs Central Deflection for Beams repaired with 900 mm and	

	1100 mm long steel plates of 1 mm thickness on the soffit of beam having stirrups at 60 mm c/c	89
5.17	.Load Vs Central Deflection for Beams repaired with 900mm and 1100 mm long steel plates of 2 mm thickness on the soffit of beam having stirrups at 60 mm c/c	90
5.18	Load Vs Central Deflection for Beams repaired with 900 mm and 1100 mm long steel plates of 3mm thickness on the soffit of beam having stirrups at 60 mm c/c	91
5.19	Load Vs Central Deflection for Beams repaired with 900 mm and 1100 mm long steel plates of 1mm thickness on the soffit of beam having stirrups at 30 mm c/c	92
5.20	Load Vs Central Deflection for Beams repaired with 900mm and 1100 mm long steel plates of 2 mm thickness on the soffit of beam having stirrups at 30 mm c/c	93
5.21	Load Vs Central Deflection for Beams repaired with 900 mm and 1100 mm long steel plates of 3 mm thickness on the soffit of beam having stirrups at 30 mm c/c	94
5.22	Load Vs Central Deflection for Beam (S11012) repaired with 1000 mm long steel plates of 1mm thickness on the soffit of beam having stirrups at 120 mm c/c	95
5.23	Load Vs Central Deflection for Beam (S11020) repaired with 1000 mm long steel plates of 1mm thickness on the soffit of beam having stirrups at 200 mm c/c	96
5.24	Load Vs Central Deflection for Beam (S31520) repaired with 900 mm long steel plates of 3 mm thickness on the soffit of beam having stirrups at 200 mm c/c	97
5.25	Effect of spacing of stirrups with the plate curtailed at 50 mm length (Theoretical and Experimental values)	98
5.26	Effect of spacing of stirrups with the plate curtailed at 150 mm length (Theoretical and Experimental values)	99
5.27	Effect of thickness of plate curtailed at 50 mm length (Theoretical and Experimental values)	100

5.28	Effect of thickness of plate curtailed at 150 mm length (Theoretical and Experimental values)	101
5.29	Effect of Plate curtailment with 120 mm c/c spacing of stirrups (Theoretical and Experimental values)	102
5.30	Effect of Plate curtailment with 60 mm c/c spacing of stirrups (Theoretical and Experimental values)	103
5.31	Effect of Plate curtailment with 30 mm c/c spacing of stirrups (Theoretical and Experimental values)	104
5.32	Theoretical and Experimental values for the Shear group beams based on KFUPM model [38,41,44]	105
5.33	Theoretical and Experimental values for the Shear group beams based on modified ACI shear strength expression [Present Work]	106
5.34	Peeling stress Vs Beam ID. based on Robert's [34] approach	107
5.35	Shear stress Vs Beam ID. based on Robert's [34] approach	108

List of Plates

Plate		Page No.
3.1	Photograph showing the close up of strain gauge connections on stirrups and spacers used	39
3.2	Photograph showing the test set up	40
3.3	Flexural cracks on beams	41
3.4	Cracks in the unrepaired beam at different load levels	42
3.5	Crushing of the concrete in the compression zone	43
3.6	Photograph showing the bonding of steel plate on the soffit of a beam	44
5.1	Photograph showing the mode of failure for beam F11512 strengthened by 1 mm thick, 100 mm wide and 900 mm long plate with 120 mm c/c spacing of stirrups	109
5.2	Photograph showing the mode of failure for beam F21512 strengthened by 2 mm thick, 100 mm wide and 900 mm long plate with 120 mm c/c spacing of stirrups	110
5.3	Photograph showing the mode of failure for beam F31512 strengthened by 3 mm thick, 100 mm wide and 900 mm long plate with 120 mm c/c spacing of stirrups	111
5.4	Photograph showing the mode of failure for beam F1512 strengthened by 1 mm thick, 100 mm wide and 1100 mm long plate with 120 mm c/c spacing of stirrups	112
5.5	Photograph showing the mode of failure for beam F2512 strengthened by 2 mm thick, 100 mm wide and 1100 mm long plate with 120 mm c/c spacing of stirrups	113
5.6	Photograph showing the mode of failure for beam F3512	

	strengthened by 3 mm thick, 100 mm wide and 1100 mm long plate with 120 mm c/c spacing of stirrups	114
5.7	Photograph showing the mode of failure for beam F1156 strengthened by 1 mm thick, 100 mm wide and 900 mm long plate with 60 mm c/c spacing of stirrups	115
5.8	Photograph showing the mode of failure for beam F2156 strengthened by 2 mm thick, 100 mm wide and 900 mm long plate with 60 mm c/c spacing of stirrups	116
5.9	Photograph showing the mode of failure for beam F3156 strengthened by 3 mm thick, 100 mm wide and 900 mm long plate with 60 mm c/c spacing of stirrups	117
5.10	Photograph showing the mode of failure for beam F156 strengthened by 1 mm thick, 100 mm wide and 1100 mm long plate with 60 mm c/c spacing of stirrups	118
5.11	Photograph showing the mode of failure for beam F256 strengthened by 2 mm thick, 100 mm wide and 1100 mm long plate with 60 mm c/c spacing of stirrups	119
5.12	Photograph showing the mode of failure for beam F356 strengthened by 3 mm thick, 100 mm wide and 1100 mm long plate with 60 mm c/c spacing of stirrups	120
5.13	Photograph showing the mode of failure for beam F1153 strengthened by 1 mm thick, 100 mm wide and 900 mm long plate with 30 mm c/c spacing of stirrups	121
5.14	Photograph showing the mode of failure for beam F2153 strengthened by 2 mm thick, 100 mm wide and 900 mm long plate with 30 mm c/c spacing of stirrups	122
5.15	Photograph showing the mode of failure for beam F3153 strengthened by 3 mm thick, 100 mm wide and 900 mm long plate with 30 mm c/c spacing of stirrups	123
5.16	Photograph showing the mode of failure for beam F153 strengthened by 1 mm thick, 100 mm wide and 1100 mm long plate with 30 mm c/c spacing of stirrups	124

5.17	Photograph showing the mode of failure for beam F253 strengthened by 2 mm thick, 100 mm wide and 1100 mm long plate with 30 mm c/c spacing of stirrups	125
5.18	Photograph showing the mode of failure for beam F353 strengthened by 3 mm thick, 100 mm wide and 1100 mm long plate with 30 mm c/c spacing of stirrups	126
5.19	Photograph showing the mode of failure for beam S11512 strengthened by 1 mm thick, 100 mm wide and 900 mm long plate with 120 mm c/c spacing of stirrups	127
5.20	Photograph showing the mode of failure for beam S11012 strengthened by 1 mm thick, 100 mm wide and 1000 mm long plate with 120 mm c/c spacing of stirrups	128
5.21	Photograph showing the mode of failure for beam S2512 strengthened by 2 mm thick, 100 mm wide and 1100 mm long plate with 120 mm c/c spacing of stirrups	129
5.22	Photograph showing the mode of failure for control beam with shear stirrups at 200 mm c/c	130
5.23	Photograph showing the mode of failure for beam S11012 strengthened by 1 mm thick, 100 mm wide and 1000 mm long plate with 200 mm c/c spacing of stirrups	131
5.24	Photograph showing the mode of failure for beam S11012 strengthened by 1 mm thick, 100 mm wide and 1000 mm long plate with 200 mm c/c spacing of stirrups	132

List of Symbols

- A_s = Area of conventional steel reinforcement
 b_a = Width of adhesive
 b_c = Width of concrete beam
 b_p = Width of bonded plate
 d_a = Thickness of adhesive layer
 d_c = depth of concrete beam
 t_p = Thickness of bonded plate
 E_a = Modulus of elasticity of adhesive
 E_c = Modulus elasticity of concrete
 E_p = Modulus of elasticity of bonded plate
 E_s = Modulus of elasticity of steel
 G_a = Shear modulus of adhesive
 V = Global shear force at end of plate
= Distance from top of beam to the neutral axis of the equivalent transformed steel section
 h_s = Effective depth of conventional reinforcement
 h_p = Effective depth of bonded steel plate
 I = Second moment of inertia of fully composite transformed equivalent steel section
 I_p = Moment of inertia of steel plate about its own centroid
 K_s = Shear stiffness of joint per unit length
 K_n = Normal/peeling stiffness of adhesive per unit length
 M^* = Bending moment at distance of $(d_c+d_s)/2$ from end of plate
 X = Distance between support of beam and end of plate
 τ_o = Shear stress at end of plate
 σ_o = Normal/peeling stress at end of plate
 M_u = Ultimate moment capacity
 d_s = Distance to centroid of tension steel
 f_c = Concrete compressive strength
 f_{ys} = Yield strength of internal steel
 f_{yp} = Yield strength of steel plate
 f_{yst} = Yield strength of stirrups
 s = Spacing of stirrups
 V_c = Shear capacity of plain concrete
 V_s = Shear capacity of stirrups
 V_u = Experimentally measured ultimate shear capacity of the section
 L_c = M_o/V_o at plate cutoff location
 M_o = Moment at the location of plate cutoff
 V_o = Shear force at the location of plate cutoff

Chapter I

INTRODUCTION

1.1 Repair and Rehabilitation of R/C Structures

The repair and maintenance of concrete structures is a major challenge to the construction industry. The need for repair and maintenance stems from lack of durability and serviceability. In addition to alarming degree of deterioration in concrete structures and it also stems from the fact that it is too difficult to replace buildings, dams, bridges, highways and other structures by new structures, because of time factor and high cost. The strengthening and repair of structures or their replacement becomes necessary when their performance with respect to ultimate load and serviceability becomes unsatisfactory. Therefore, strengthening and repair of structures has become as important as the design of new structures.

Concrete structures built during the peak period of construction are now showing defects. There are various reasons for the unsatisfactory performance of the structures, such as the use of inferior materials, inadequate construction practices, poor workmanship, prevailing weather conditions, defective designs and improper detailing of reinforcement, damage due to fire, blast and earthquakes, change in the function of structure from a lower service load to a higher service

load and reinforcement corrosion resulting in its decrease in the cross-sectional area, thus reducing the load carrying capacity of the structure. To regain its original load carrying capacity, strengthening becomes essential.

As the structures with unsatisfactory performance are never accepted because of the safety and public acceptance, therefore, such structures should either be replaced by new ones or the defective structural member of the building should be strengthened. The choice between the two alternatives of either to replace or to strengthen the member depends on various factors such as the material cost, labor cost, time duration for which the structure shall be out of use and disruption in the other facilities like plumbing, electrical and HVAC facilities in the building. As the replacement of the structure is very expensive, it is done only in the case when the problem is severe and there is no other solution. But, in this economical era, it is more rational to go for strengthening the members, particularly with the availability of many attractive, simple and quick techniques. The suitability of repair techniques, and repair materials can be selected considering economy, compatibility and efficiency. Cost, ease of application and efficiency are the major considerations in choosing the repair materials and repair techniques. Some repair materials are very expensive, some are fair and some are cheap. Similarly, some repair techniques require expensive equipment's and skilled labor for placement and some do not.

1.2 Strengthening Techniques

A number of strengthening techniques have been used in the past to achieve desired improvements. The following is a list of some of the commonly used techniques to repair structurally distressed components:

1. Replacing non-structural toppings with structural toppings, or lighter material.
2. Provide extra supports to reduce the span length.
3. Add extra reinforcement by stapling and guniting **Steel Plates** externally.
4. Using external or internal prestressing.
5. Using Ferro-cement mortar.

1.3 Plate Bonding

With the invention of epoxy adhesives, another technique of strengthening of structures has been added to the repair world, which is plate bonding. This technique has gained popularity in a short interval of time because of its vast advantages.

In Plate bonding, a steel plate of relatively small thickness, of just a few millimeters, is bonded with epoxy glue to the reinforced concrete beams and slabs for improving their structural behavior and strength. Full composite action is

achieved between a concrete member and a steel plate by the use of a suitable epoxy glue. Plate bonding can be used to increase flexural capacity of RC beams weak in flexure due to inadequate main reinforcement, or to increase shear capacity of RC beams weak in shear due to inadequate stirrup provision.

The advantages of Plate Bonding Techniques are as follows:

1. Site disruption is minimum as compared to other repair techniques. Here, only the surface of the structural member is abraded by sand blasting to make the structural member rough for proper adhesion.
2. Size of the structural member increases by just a few millimeters when strengthened by plate bonding. There is a negligible reduction in the clear span or the ceiling height of the structure.
3. Minimum scaffolding and shuttering is required.
4. Simple to implement
5. Quick in installation
6. The structure can be strengthened by plate bonding when the building is in operation, as there is no vibration, no noise. Hence, the normal activities can go unaffected.

The most important shortcoming of plate bonding technique, using steel plates, is the danger of corrosion at the steel/glue interface, which adversely affects the bond strength. The use of epoxy bonded external plates for strengthening and

repair of reinforced concrete (R/C) members is an attractive alternative to structural engineers due to above mentioned advantages for the use of structures in question. However, prior to establishing full confidence in the use of external plates as reinforcement, the behavior of such elements must be fully understood, especially in relation to behavioral characteristics that are not observed in ordinary R/C members. Considerable research has been carried out on repair and strengthening of R/C beams using plate bonding by University groups at Sheffield [30-33] and at King Fahd University of Petroleum and Minerals (KFUPM) [37-38] leading to identification of a horizontal rip-off failure in concrete - a phenomenon not known in unplated R/C beams.

1.4 Existing State-of-The-Art

One of the most important factors in the externally bonded plated beams is the development of high peeling and shear stresses at the location of plate curtailment which under certain combinations of plate geometry and other parameters can lead to a highly brittle mode of failure.

This research focuses on behavior of plated R/C beams in order to better understand the failure modes of such structural elements. The work has direct impact on the design for strengthening and repair of R/C beams using plate bonding. Although the use of external reinforcement for strengthening and repair

of reinforced concrete (R/C) members subjected to bending and shear has attractive features, structural engineers need to fully understand the behavior of such elements under loading prior to recommending adoption of the technique.

1.5 Modes Of Failure

R/C beams when strengthened externally by plates bonded on the tension side failed in a variety of ways, depending on the plate thickness. The modes of failure were:

1.5.1 Flexural failure

This failure is characteristic of under reinforced R/C beams externally reinforced by thin plates and of sufficient length such that conditions at failure are marked by yielding of internal reinforcement and external plate, there is crushing of concrete in the compression zone and flexural cracks intrude to the very top of the beam (Plate). The counterpart of this mode in ordinary R/C beams is the flexural failure of underreinforced beams. Ideally speaking, the external reinforcement for R/C beams should be designed so as to yield a ductile flexural failure under ultimate load conditions.

1.5.2 Concrete/Glue/Steel Interface Separation

As the plate thickness increases, the interface shear and peeling stresses at the plate curtailment zone increase and, if the allowable strength values for the interface are exceeded, the plate may separate, resulting in premature failure. If the bonding adhesive is weak or gluing is not properly done, this type of failure may be characterized by plate debonding initially emanating from the plate curtailment. As the plate debonding proceeds away from the support and as the effective plate length is reduced, the peak peeling stresses progressively increase to a value where a secondary rip-off crack develops, leading to sudden failure. In order to preempt the likelihood of plate separation in the design process, the stresses at the region of plate cutoff are checked to insure that plate separation does not occur. Premature separation of the plate at concrete/glue/steel interface, starting from the zone of plate curtailment separation leading to a reduced bonded plate length with ultimate failure resulting from the formation of a diagonal crack proceeding from inward and moving delamination at the interface, to the point of loading.

1.5.3 Concrete Rip-off Failure Mode

If gluing is strong enough to prevent plate debonding, cracking emanates from the location of plate curtailment. The existence of peak peeling and shear stresses at the plate curtailment zone, in addition to the bending stress, results in a biaxial tensile stress state, forcing the crack to move in an essentially horizontal

direction just below the level of internal flexural and shear reinforcement where the section is the weakest initiated at the point of plate curtailment. Failure ensues when the moving horizontal crack joins an existing highly stressed flexural crack, leading to a brittle and explosive failure at external plate stress levels below yield [38,41,44].

1.5.4 Diagonal Tension Failure Mode

Another independent mode of failure of plated R/C beams, which like the flexural failure has its counterpart in unplated R/C beams, is one of failure by diagonal tension. This mode of failure is similar to that in unplated R/C beams, with failure precipitated by a diagonal crack emanating from near the plate curtailment zone or support region and traversing across the stirrups at approximately 45 degrees.

It is believed that the development of flexural cracks beyond the plate curtailment produce high localized bond stress concentrations at the tension steel and consequently magnify the actual shear stress leading to steeper diagonal cracks. A diagonal crack connects the existing flexural cracks, these cracks become wider and wider at higher loads, open up resulting in the failure of the beam. This type of the failure is often encountered when the principle tensile stress

exceeds the tensile strength of concrete. Tension crack forms where the tensile stresses are largest and will immediately cause the beam to fail.

1.5.5 Flexure/Rip-off Failure Mode

A mixed type of failure where the internal steel and the external plate yield before failure, with actual failure being precipitated by the horizontal tearing of concrete cover below the level of main reinforcement. This is called Flexure/Rip-off failure.

1.6 Research Objectives

Not much work has been done to study the possibility of highly brittle mode of failure called the shear failure for certain combinations of plate geometry and other parameters, which play a primary role in shear or concrete rip-off failure. Also, the ultimate load for certain plated RC beams failing in shear are overestimated by ACI expression for shear strength of unplated RC beams by virtue of crack profile, rendering stirrup inefficient.

This research focuses on behavior of plated R/C beams in order to better understand the failure modes of such structural elements. The work has direct impact on the design for strengthening and repair of R/C beams using plate bonding. The main objectives of this research are to study and predict the

shear/peeling failure of plated reinforced concrete beams. The broad objectives of this research are:

1. To study the overall behavior of RC beams reinforced with external steel plate bonded to the soffit by varying
 - Plate Thickness (t_p),
 - Curtailment Length (L_c),
 - Spacing of Stirrups (s).
2. To study efficiency of stirrups in plated beams in which
 - Flexural capacity of unrepaired beam is less than the shear capacity.
($P_f < P_s$).
 - Shear capacity of unrepaired beam is less than the flexural capacity.
($P_s < P_f$).
3. To predict mode of failure as being brittle or ductile, based on characteristics of unrepaired beam and geometric and material details of external reinforcement and bonding agent.
4. To delineate the range of validity of expression for rip-off failure as presented by KFUPM research group for plated RC beams.

Chapter II

LITERATURE REVIEW

2.1 Use of Plate Bonding

Though very little data is available on the performance of RC members repaired by plate bonding techniques, but it has been extensively used to strengthen various structures like buildings and bridges through out the world, particularly in Belgium [1], France [2,3], Japan [4], Poland [5], South Africa [6], Switzerland [7,8] and United Kingdom [9,10,11]. Investigations into the performance of plate bonding technique started in 1960s [12-14]. External strengthening of existing buildings and bridges using epoxy bonded steel plates are now being accepted as an efficient and convenient way of improving the serviceability performance and/or ultimate strength of concrete structures. In Japan [15], over 200 bridges have been strengthened by this technique. The repair and reinforcement of French 'Route Nationale 186' bridge, crossing Saint Denis Canal, [16], Swanley Bridges in Great Britain [17], Interchange of four bridges on M5 motorway at Quinton in United Kingdom [18], repair of Hottingerstrasse Telephone Exchange in Zurich [19], expansion and renovation of Fusslistrasse Telephone Exchange in Zurich [20], the shopping center at Spreitenbach,

Switzerland, air conditioning system in the Neue Hard Development Building Zurich, ALBA, Aluminium Smelter Bahrain [21] are, but a few examples.

2.2 Flexural and Shear Studies

Extensive work has been carried out on behavior of plated R/C beams with the work encompassing experimental, analytical and numerical modelling by various researchers [22-38] around the world. It was found that RC beams repaired with thin strips of steel bonded on the tension face indicated improved behavior both at service and the ultimate load levels. But when a relatively thicker plate was used, there was a separation of steel plate at the terminate ends "peeling of steel plate", and beams failed not only before reaching the theoretically predicted ultimate strengths but it exhibited lack of ductility.

It is a must for safety that, structural members should have enough ductility to give sufficient warning before failure. The separation of plates at the terminate ends takes place due to high concentrations of shear and normal stresses (peeling stresses). In order to overcome this problem of separation of plates at the terminate ends, Jones [22] made a study by using anchor bolts and angle plates. He found that anchor bolts improved ductility, but separation of plate at the terminate ends could not be prevented. On the other hand, angle plates proved to be the best anchorage system as they improved ductility and prevented plate separation. But

angle plates were not suitable for wider beams and cannot be used for slabs. His findings were not confirmed by others as it did not clearly explain the stress behavior at terminate ends of the plate.

In 1975, Irwin [23] reported from his experimental study that, the crack width in RC beams repaired with steel bonded plate was significantly less than that of unrepaired beam. The failure of former group of beams took place due to separation of the plate. Plated beams had higher moment capacity during the first cycle of loading, but it suddenly dropped due to plate separation.

In 1979, Calder [24] from his experimental results reported bending tests and shear tests of glues in unreinforced concrete beams, when exposed to atmosphere under different environmental conditions for a period of two years, indicated that corrosion of plates took place at the steel/glue interface in all specimens which were exposed to natural environments thus reducing the strength of the specimens. Corrosion of plates in exposed specimens was due to the migration of moisture from concrete to steel plate passing through the glue layer. The analysis of results indicated that there were significant differences of results for beams which were exposed to different environments and between loaded and unloaded specimens. No significant difference in the results of beams were found, which were tested after one or two years of exposure. The load applied to beams decreased to about 70% of the original value after first 8 months of exposure. The

load carrying capacity of glue reduced significantly after two years of exposure, but it was still greater than that of concrete. A significantly higher area of steel plate was rusted after two year of exposure as compared to one year of exposure.

In 1980, Jones et.al [25] reported the results of an experimental study on the behavior and strength of plain and RC beams strengthened by steel plates bonded by epoxy glue on the soffit of beams. Two types of glues and two types of steel plates with different yield strengths were used, and the effects of glue thickness, plate lapping, multiple plates and of precracking prior to bonding were investigated. The effects of above variables on deflection, concrete strain distribution, cracking behavior, steel strain, mode of failure, load at first crack and ultimate strength were presented. It was shown that gluing and lapping operations can be carried out efficiently and successfully, and that the technique can be extended to provide a reliable method of strengthening insitu structures. But, the long-term performance of glue or the effects of environment on corrosion are not reported.

Cusens and Smith [26] in 1980, studied the structural performance of four epoxy adhesives by subjecting them to shear in three types of specimens: (i) a steel-steel double lap specimen, (ii) a concrete prism with scarfed joint, and (iii) a concrete beam with external steel plate reinforcement. Specimens were tested under simple and sustained static load, and in fatigue. They were cured between 20

and 80° C. The shear strength of adhesion to steel was about 13 MPa. A marked difference was observed in the performance of different adhesives after immersion in water for 8 weeks. Beams exhibited ductile behavior, with the yielding of steel plate when the thickness of adhesive was maintained at 1 mm.

Macdonald [27] in 1982, carried out a testing program on 17, 3.5 m long RC beams with epoxy bonded external reinforcement subjected to 4 point loading. The variables included different adhesives, plate geometry's, a jointed plate, glue-line thickness, partial bonding and multi-layered plates. Beams were also tested As-cast (for reference), plated without concrete being cracked (plated As-cast) and plated after cracking (plate precracked). It was found that addition of plates increased the maximum sustained load required to produce the first visible crack by 80 %, stiffnesses were found to be increased by about 190 % for plated As-cast condition and 250 % when plate was added after the beam had been cracked to a width of 0.1 mm. When wide plates were used, it was seen that the type of failure that can occur while the plates are separated from the beam by horizontal shear failure in concrete did not occur. The experimental and calculated values of loads for various conditions were found to be in good agreement.

In 1982, Lloyd and Calder [28] presented experimental investigation of exposure tests conducted on concrete specimens strengthened by epoxy bonded steel plates. Visual examination showed that corrosion of steel plate can take place

at steel/glue interface and existence of chlorides in corrosion product were detected. A micro-structural analysis of concrete/resin system using marker solutions and electron microscopy revealed cracks and pores in both concrete and resin. It was shown that these cracks act as routes for corrosive liquids to reach the steel plate and cause corrosion. It was observed that, use of primer on steel plates has been successful in inhibiting corrosion.

In 1982, Jones et al. [29] conducted an experimental test to study the strength and deformational characteristics in flexure for under and over reinforced concrete beams with glued steel plates. The composite behavior of beams, interaction of plate/glue/concrete and influence of glued plate on stiffness, cracking, plate slip, interface shear stress and ultimate strength of beams were described. The ultimate strength of beams were theoretically predicted and was found to be in good agreement with experimental results. A detailed information about plate separation were presented, which is related to interface shear stress. Tests showed that composite action can be achieved in glued RC beams.

In 1987, Swamy et al. [30] presented comprehensive test data on the effect of glued steel plates on first crack load, cracking behavior, structural deformation, serviceability loads and ultimate strengths of RC beams strengthened with steel plates on tension face. The results indicated that plated beams enhanced flexural

stiffness which control cracking and deformation at all load levels until failure. However, the stiffening effect was much greater in controlling cracking. The structural effect was found to be far greater than if the bar area had been increased by the same area as that of plates, provided adhesives are chosen carefully and proper gluing techniques are followed. The plated beams showed beam action and composite behavior right upto failure. The glued plates increased ultimate flexural strength by about 15%. However, there is a limit on plate thickness over which premature shear/bond failure occurs without the beams achieving its full flexural strength. Though, such beams still controls cracking and deformation upto failure, two tentative design criteria were suggested to ensure full flexural capacity and ductile failure of plated RC beams.

In 1987, Jones et al. [31] presented the test results of 24 epoxy bonded steel plated beams. Variables studied were effect of glued steel plates on the first crack load, cracking behavior, structural deformation, serviceability loads and ultimate strength of strengthened reinforced concrete beams. The stiffness of beams increased with increase in thickness of glueline. The stiffening effect was much more influential in reducing rebar strain and plate strain than on reducing deflection. The rebar strain controlled cracking in concrete and steel plates provided restraining medium to crack initiation. The strain measurements in all beams showed yielding of plates in case of 1.5 and 3mm thick plates. On

unloading, plastically deformed plates warped away from concrete, and failure took place in concrete but not in glue/concrete interface or plate/glue interface.

The externally bonded plates substantially reduced deflections and rotations, steel bar strain and cracking. The load carrying capacity at serviceability limit state increased with increase in plate thickness. But serviceability loads increased with an increase in plate thickness for precracked beams. The experimental ultimate loads for plated and unplated beams were compared. Beams with 1.5 mm and 3.0 mm thick plates tolerated higher ultimate loads compared to unplated beams. But beams with 6mm thick plates gave less ultimate load compared to beams with 1.5 mm and 3.0 mm thick plates because of premature failure due to plate separation. Beams with 1.5 mm thick plates ($b/t = 83.3$) exhibited pure flexure failure. Beams with 3 mm thick plates ($b/t = 40.3$) indicated a combination of shear/bond failure. However, flexural type of failure was predominant due to the separation, after yielding of plates and rebars. However, with 6 mm plates failure took place due to separation of plates. To obtain pure flexural failure it was therefore, recommended to keep the width to depth ratio of plates equal to 50 and depth of neutral axis to effective depth of beam equal to 0.4.

In 1988, Jones et al. [32] presented a theoretical study based on the simple elastic theory to determine average bond stresses anywhere along the plate

interface. It was shown that bond stress at glue/plate interface and glue/concrete interface is almost equal. The bond stress in the end region, taking into account the effect of plate cut-off was also determined. At the plate end, bond stresses were high compared to interior region. Also, tapering of plates at the end and using multiple plates with curtailment, did not reduce average bond stress. An expression for peeling force at the interface was derived.

In order to investigate the problem of sudden failure by plate separation, seven beams were tested by loading at two points, at 1/3rd distance apart. The L-shaped anchor plates were the most effective anchoring system used and the beams reached full theoretical ultimate capacities. Curtailed multiple plates and tapered plates did not help in changing the mode of failure from tearing mode to pure flexure failure as exhibited by the analysis of test results. With anchor bolts, ductility was improved, but tearing of concrete could not be prevented. However, flexural failure was achieved. With angle plates, not only ductility improved, but also no tearing of concrete cover at the terminate ends of the plates was observed. Very high shear stresses were produced at the terminate ends of the plate with a limiting value equal to $\sqrt{2} \times$ (tensile splitting strength of concrete).

Comparison of load-deflection curves of plated beams indicated that, this technique can be used to strengthen structures which are pre-cracked. Some beams

had more deflection because of creeping effect due to sustained loading. Hence, it was concluded that, this technique can be used to strengthen the damaged structures while under load. Bonded plates controlled the crack width effectively in structurally damaged RC beams strengthened in loaded and unloaded state.

In 1989, Swamy et al. [33] carried out an experimental study, to examine the applicability of plate bonding technique to strengthen, structurally damaged RC beams. Two types of strengthened beams were tested. First beam was loaded upto 70% of its flexural capacity, then unloaded and strengthened in the unloaded state. Second beam was also loaded upto 70% of its flexural strength, and strengthened with plates while under load. The structural behavior of these two types of strengthened beams was reported in terms of deflection, concrete and steel strain, cracking behavior, flexural stiffness and strength. It was observed that repaired beams were efficient structurally and that plated beams were restored to stiffness and strength values superior, to those of original unplated beams. The data indicated that complete confidence and reliability can be placed in applying the technique to structurally damaged beams. The repaired composite beams were able to preserve their structural integrity and maintain composite action until failure and the composite structural system followed the simple laws of mechanics upto failure.

In 1989, Robert's [34] provided a simple, approximate procedure for predicting the shear and normal stress concentrations, in the adhesive layer of plated RC beams. The analysis was performed in three stages. During the first stage, stresses were determined assuming full composite action between RC beam and epoxy bonded steel plate. During the second and third stages, analysis was modified to take into account actual boundary conditions at the terminate ends of the steel plate. The complete solution was obtained by superposition. The solutions for shear and normal stresses were simplified.

Alan and Arumugam [35] used four specimens having a plate with a square-end, a plate tapered in elevation, a plate with a short taper in plan and a plate with a long taper in plan. A laboratory specimen was introduced to model strain distributions local to the ends of externally bonded steel plates to RC beams. The model was validated by comparing with the finite element predictions and it was used to demonstrate that, tapering of plates in plan or in elevation reduces the stress concentrations in concrete. It was also suggested to extend the work to include additional end configuration.

Van and Vanden [36] carried out a study on the behavior of glued connection under atmospheric conditions which showed no considerable influence on mechanical characteristics. However, this depended on the preparation of concrete and steel plate surface and gluing operation. They suggested that, for an

optimum and durable result, more specialized personnel and an intense control of surface preparation works is required. The glue connection exhibited a poor behavior at high temperatures. As such they suggested more research to improve the fire resistance, and its behavior in cyclic thermal loading.

Macdonald studied the use of glued steel plates, for strengthening four reinforced concrete beams. Plates were bonded to the tension flanges of beams by epoxy-resin. This study focused on the effects of variation in adhesive properties, joint in plates, plate thickness variation and load cycling. Results indicated that, the load to produce a crack of a certain width in a plated beam was approximately twice, that to produce the same size-crack in unplated beam, but with no significant increase in load carrying capacity.

Experimental and theoretical studies were conducted by Hussain [37] on plate bonding technique. A large number of RC beams were damaged in flexure by inducing 10 mm central deflection. Then, these beams were repaired by bonding steel plates of different thicknesses on the bottom faces of beams. In a few beams, end anchorage to plates was provided by anchor bolts. Beams repaired by 1.0 mm and 1.5 mm thick plates reached the theoretically predicted ultimate flexural strengths, while, the beams with 2.0 and 3.0 mm thick plates did not. In general, ductility was improved by providing end anchorage to the plates. The modes of

failure for beams repaired by 1.5 mm, 2.0 mm and 3.0 mm thick Plates with and without end anchorage were due to plate separation. Theoretical study based on partial interaction theory was conducted to determine the shear and peeling stresses at the interface in epoxy bonded plated beams. RC beams under shear group having insufficient shear reinforcement were damaged in shear, under four point loading. These shear beams were then repaired by bonding jackets, U-strips, straight strips and wings in the shear spans. All the shear repaired beams indicated improvement in strength and ductility, however, the load sustained by the beams, repaired by full encasement in the shear span were found to be maximum.

Ziraba [38] in 1993 presented a non-linear finite element model for the flexure, shear response of RC beams strengthened externally by epoxy bonded steel and fiber glass plates. The salient features included the introduction of a thin, six-noded element to simulate behavior of concrete/epoxy glue/plate interface, loading a virgin RC beam to a prescribed displacement to simulate damage, unloading and then reloading the damaged RC beam repaired by an external plate. Results were presented for RC beams repaired by plates of varying thickness and the failure mode was noted from flexure, for the case of external reinforcement in the form of thin plates to a unique concrete cover rip off failure, for thicker plates. Using experimental-numerical approach, and based on data from a specially designed half beam specimen and experimental results from other specimen geometry's, combined with their respective non-linear finite element idealization, a

classical Mohr-Coulomb failure law together with a tension cut-off was suggested for the material characterization of the steel/glue/concrete interface. Based on the results of numerical and experimental studies, a rational design approach for plated RC beams was presented by interpreting major modes of failure including flexure, interface separation and concrete cover rip-off. New expressions for peak interface shear and peeling stresses, as well as a predictor equation for shear resistance of plated RC beams were presented, for use as a design tool.

Chapter III

EXPERIMENTAL PROGRAM

3.1 Introduction

The work studies response of plated R/C beams as divided into two broad categories:

1. Beams in which the flexural capacity P_f is less than the shear capacity P_s of the unplated section. Such beams are referred to as the Flexure Group beams (F).
2. Beams in which the shear capacity P_s is less than the flexural capacity P_f of the unplated section. These beams are referred to as the shear group beams (S).

Twentyeight reinforced concrete beams were cast in this study. All the 28 R/C beams tested were 1250 mm long and 150 x 150 mm in cross section containing 2-10 mm diameter bars as internal flexural reinforcement bars for flexure group (F) and 3-12 mm diameter bars for shear group of beams. In addition, 6 mm diameter bars were provided as compression steel with shear reinforcement in the form of 6 mm diameter plain steel stirrups spaced at 30, 60 and 120 mm for

flexure group and 120 and 200 mm for shear group of beams as shown in Figure 3.1. Spacing of the stirrups was varied to flexure and shear beams as shown in Figure 3.2. In every set of a particular shear stirrup spacing, one beam was left unplated to act as control beam and the remaining were modified using mild steel plates of different thicknesses and curtailment lengths, having 100 mm width (Figure 3.3 and Figure 3.4). Instrumentation of the beams consisted of mounting Electrical strain gauges at the middle of main reinforcement, middle of stirrups at different locations, on top, at the center of concrete beam and the steel plate, in the middle and under the application of loads.

The acronym designation adopted for beams tested was as follows: First letter is the word character F or S designating flexure or shear group beam. The first number appearing after F or S represents plate thickness (t_p) in millimeters (1,2 and 3), the number following t_p indicates the curtailment length of plate L_c in centimeters (5,10 and 15) and the last number gives the spacing of stirrups (s) in centimeters (3,6,12 and 20).

3.2 Materials

The concrete used for casting the beams was made using ASTM C 150 Type V Sulphate Resisting Portland cement. Coarse aggregate was crushed limestone procured from the quarries in Abu-Hadriya, and fine aggregate was beach sand.

The concrete mixes were made with a cement content of 350 Kg/m^3 . The grading of coarse aggregate was selected confirming to ASTM C-33 as shown in Table 3.1. The chosen grading curve lies between the lower and upper limits for 12.5 mm (1/2") max size, (Figure 3.5). Potable water was used to mix the constituents. A water-cement ratio of 0.55 and coarse to fine aggregate ratio of 1.63 was kept invariant for all the mixes. The workability of concrete mixes was 2.0 to 3.5 inches slump. The yield strength of main reinforcement was 414 MPa, Shear stirrups was 380 MPa and that of mild steel plates was 276 Mpa. The elastic modulus of rebars and steel plates was 200 GPa. The shear and elastic modulus of the epoxy glue was 120.1 and 278.6 MPa, respectively.

3.3 Preparation of Beams

The steel cages consisting of longitudinal, compressive and shear reinforcement for both flexure and shear group of beams were prepared, installed with strain gauges and placed into the molds maintaining a clear cover of 25 mm from all the three sides as shown in Plate 3.1. The constituents containing cement, sand and coarse aggregate were thoroughly mixed in a revolving drum type concrete mixer. The mixing was done for about 5 minutes till the concrete was uniform. Slump was measured for each batch of concrete. Concrete was placed into the molds in three layers, taking special care to protect the strain gauges and the wires connecting them. All the specimens cast were thoroughly vibrated after each

layer in accordance with ASTM C192, using electrical vibrator till complete consolidation was achieved and the entrapped air eliminated. After casting, surface of the specimens were uniformly leveled and for each batch of casting, three cylinders of size 150 x 300 mm were cast to measure the compressive strength of concrete. The specimens were remolded after 24 hours and then, both the beams and cylinders were moist cured for 28 days under laboratory conditions. Cylinders were then tested after capping with sulphur according to ASTM C-39, using a hydraulic compression testing machine.

3.4 Damaging of Beams

All the beams were tested over a span of 1200 mm with loading at mid-third points. All the beams were preloaded (damaged) to a predetermined level to simulate badly damaged beams in practice. The preloading levels for both flexure (F) and shear (S) group of beams were decided upon after testing control beams to failure. It was then decided to load flexural beams to obtain 10 mm central deflection, while shear beams were preloaded to obtain 5 mm central deflection or the appearance of first shear crack.

All the beams were marked at supports, at span and at third points to facilitate the placing of supports, distribution beam and the Linear Variable Differential Transformer (LVDT's). The beam were damaged under four point

loading. Two point loads were applied at the ends of middle third and reactions were set at a span of 25 mm from the ends of beam (Figure 3.6). For loading, a 25 ton capacity INSTRON machine was used. A portable data logger and a personnel computer were used to record outputs directly from the load cell as shown in the Plate 3.2. The readings were taken for the strains on concrete surface, steel plate, main steel and the shear stirrups. After loading the beams to 10 mm central deflection, it was gradually released. The rate of loading and unloading was kept at 2mm/min for flexure group and 1 mm/min for shear group of beams. Developing cracks were marked, measurements were taken and crack widths measured at the level of main steel, at various load levels as shown in Plates 3.3 and 3.4. The load Vs Central deflection curves were plotted for all the three sets of beams. Readings were taken at every 5 kN interval. Table 3.2 shows the maximum load obtained during the damaging process and the residual deflections after unloading for all the beams. Control beams were reloaded upto failure, as shown in Plate 3.5.

3.5 Repair of Beams

This part of the research was conducted to evaluate the repair scheme followed for beams, and to study the mode of failure after repair. After damaging, eighteen beams of flexure group and five beams of shear group were strengthened by mild steel plates on the soffit of beams by varying curtailment length and thickness. In order to achieve a good bond, damaged concrete beams and steel

plates were roughened by sand blasting. Concrete beams were sand blasted till the aggregate was exposed and steel plates were sand blasted till all the grease was removed. Then both the surfaces were cleaned by air pressure. The adhesive used to bond concrete surface with steel plates was two part epoxy glue consisting of resin and hardener. The two components of epoxy glue were stirred by mixing thoroughly two parts of resin to one part of hardener by weight till the paste became homogeneous giving a grey colour.

The thoroughly mixed glue was applied at appropriate places of the beam and steel plate using a paint brush. The glue was spread such that the entire area to be bonded was fully wet with glue. Copper wire spacers of 1.5 mm were spread evenly on the freshly glued surface to maintain a uniform glueline thickness. Then glued steel plates were loaded on the glued concrete beams at marked locations. The plates were then clamped and excessive glue squeezed out which was later cleaned with the help of a brush. Clamps were removed after curing the glue for 15 days as shown in Plate 3.6. After curing for the glue, repaired beams were finally tested. The loading operation was similar to that discussed earlier. The beams were loaded upto failure, which was indicated by a drop in the load.

Maximum Size of Aggregate	% Passing
1/2"	40
3/8"	35
#4	20
#8	5

Table 3.1: Coarse Aggregate Grading

Pre-damaged Beams							
Group	Beam ID	Max Load (kN)	Central Deflection (mm)	Residual Deflection (mm)	Average Crack Width at Max. Central Deflection (mm)	Average Crack Width at residual Deflection (mm)	Remarks
Flexure	F0012	47.379	23.146	5.994	2.5	1.0	Control Beam
	F11512	42.664	10.02	5.88	1.5	1.0	
	F21512	41.24	9.882	5.878	2.0	1.0	
	F31512	58.92	5.77	5.938	1.5	1.0	
	F1512	44.349	9.536	5.914	1.0	0.7	
	F2512	39.37	9.788	5.85	1.5	1.5	
	F3512	39.305	8.57	5.918	0.7	1.0	
	F006	40.922	10.098	5.898	2.5	1.0	Control Beam
	F1156	43.733	10.128	6.042	1.0	1.0	
	F2156	43.05	10.038	5.93	1.0	0.6	
	F3156	41.913	10.018	5.964	1.5	1.0	
	F156	42.445	10.01	5.854	1.5	1.0	
	F256	44.076	10.096	6.08	1.0	1.0	
	F356	41.914	10.038	5.704	1.5	1.0	
	F003	43.459	10.036		1.5	0.7	Control Beam
	F1153	41.311	10.026	5.934	0.9	0.45	
F2153	43.278	10.046	5.888	0.9	0.5		
F3153	44.853	9.842	5.91	0.9	0.6		
F153	43.617	10.064	5.954	1.0	0.9		
F253	40.364	9.848	5.792	1.5	1.0		
F353	43.546	10.066	5.64	1.0	0.8		
Shear	S0012	66.3	5.21	1.09	0.1		Control Beam
	S11012	65.134	6.088	1.29	0.2		
	S2512	64.34	6.1	4.964	0.15		
	S11512	64.54	5.462	5.462	0.2		
	S0020	82.22	7.32	1.168	0.2	0.05	Control Beam
	S11020	64.259	5.68	1.074	0.2	0.05	
S31520	53.2	3.886	1.614	0.3	0.1		

Table 3.2: Maximum Load, Central deflection, Residual Deflection and Crack width for Pre-damaged beams

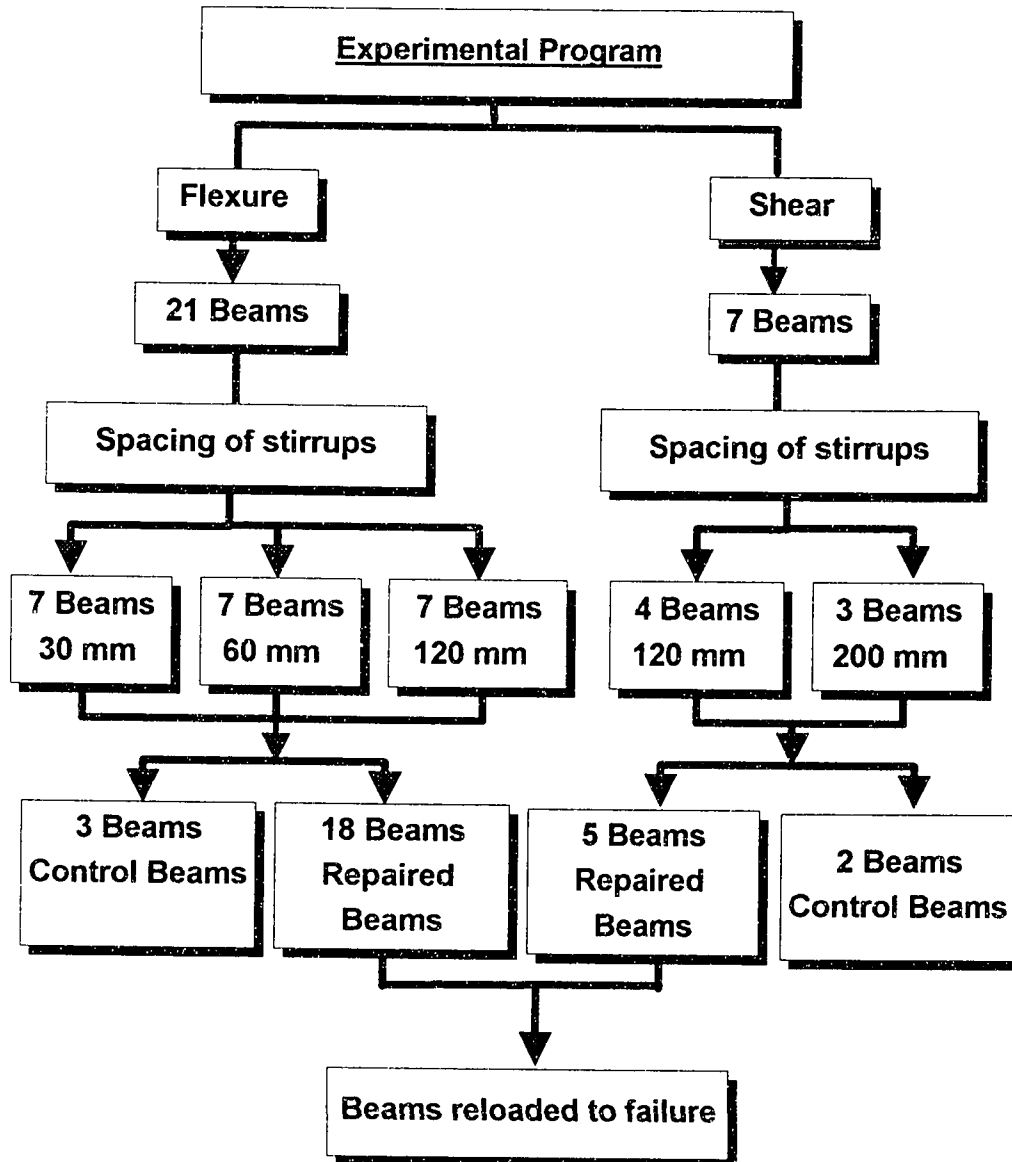


Figure 3.1: Details of Experimental Program

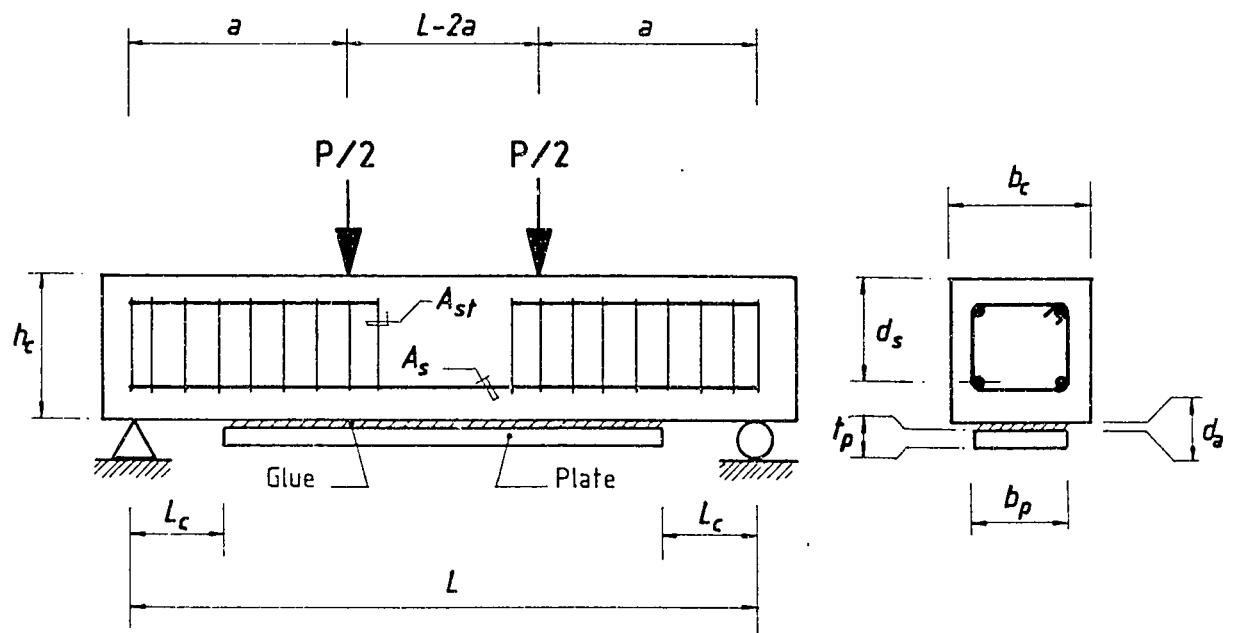


Figure 3.2: Reinforcement details

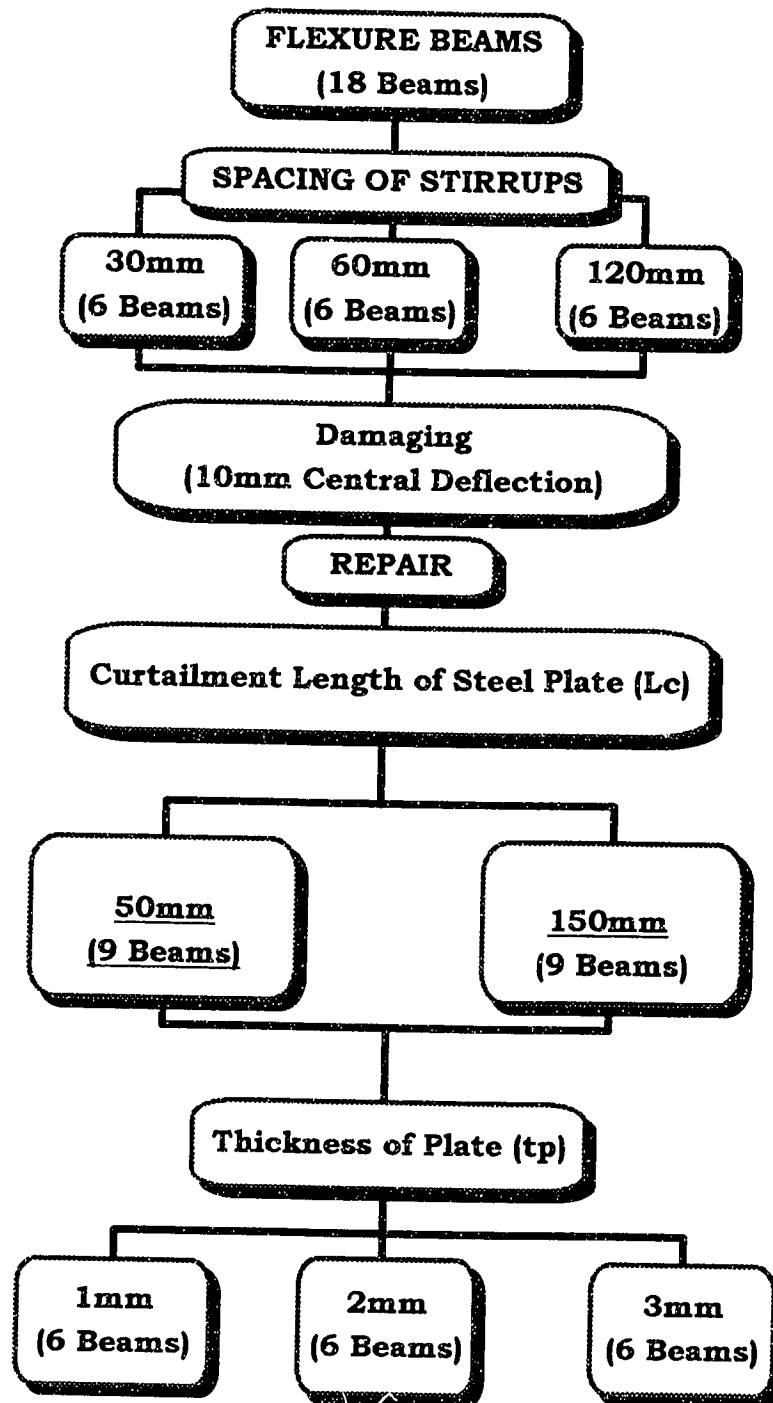


Figure 3.3: Details of Experimental variables for Beams of Flexure group

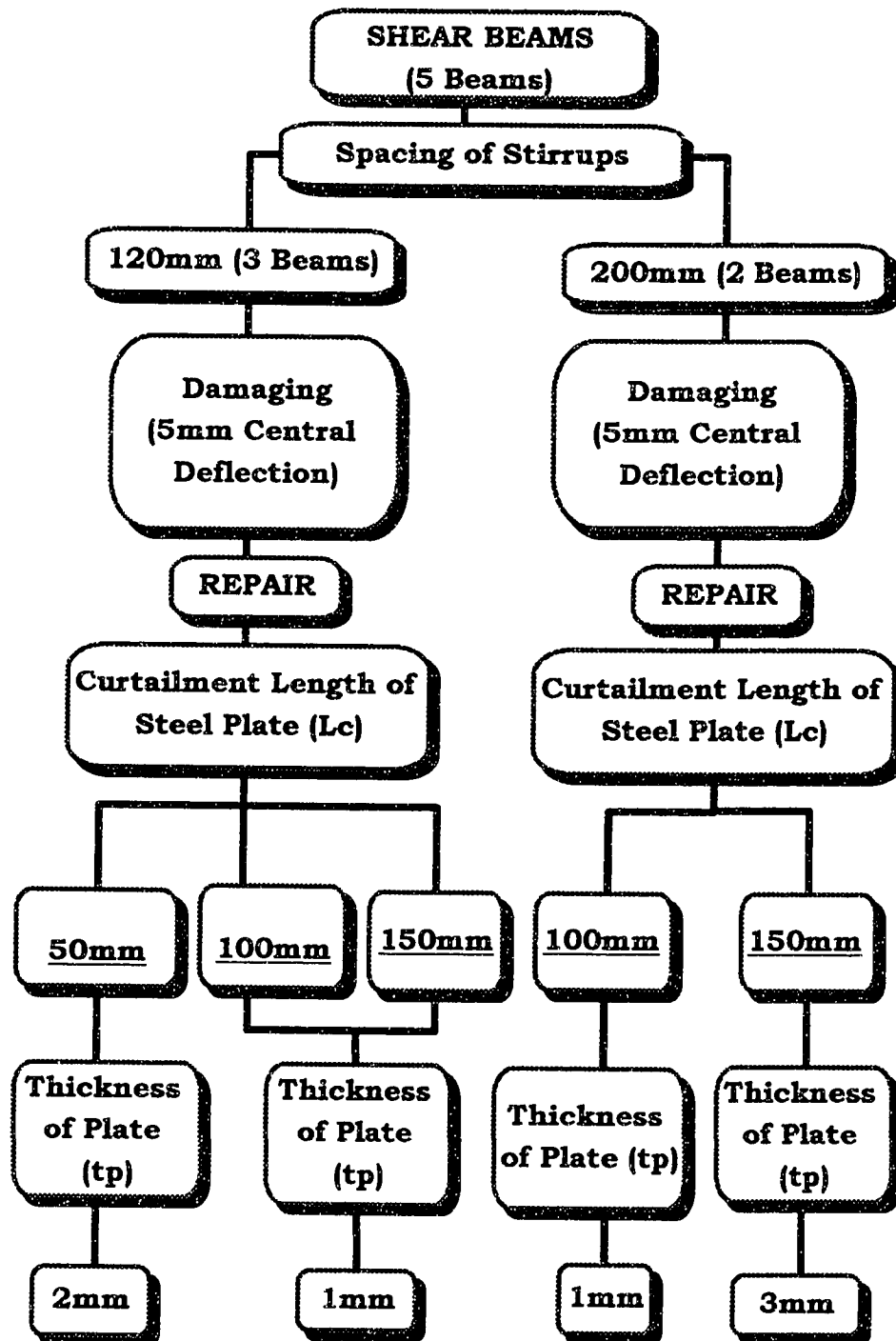


Figure 3.4: Details of Experimental variables for Beams of Shear group

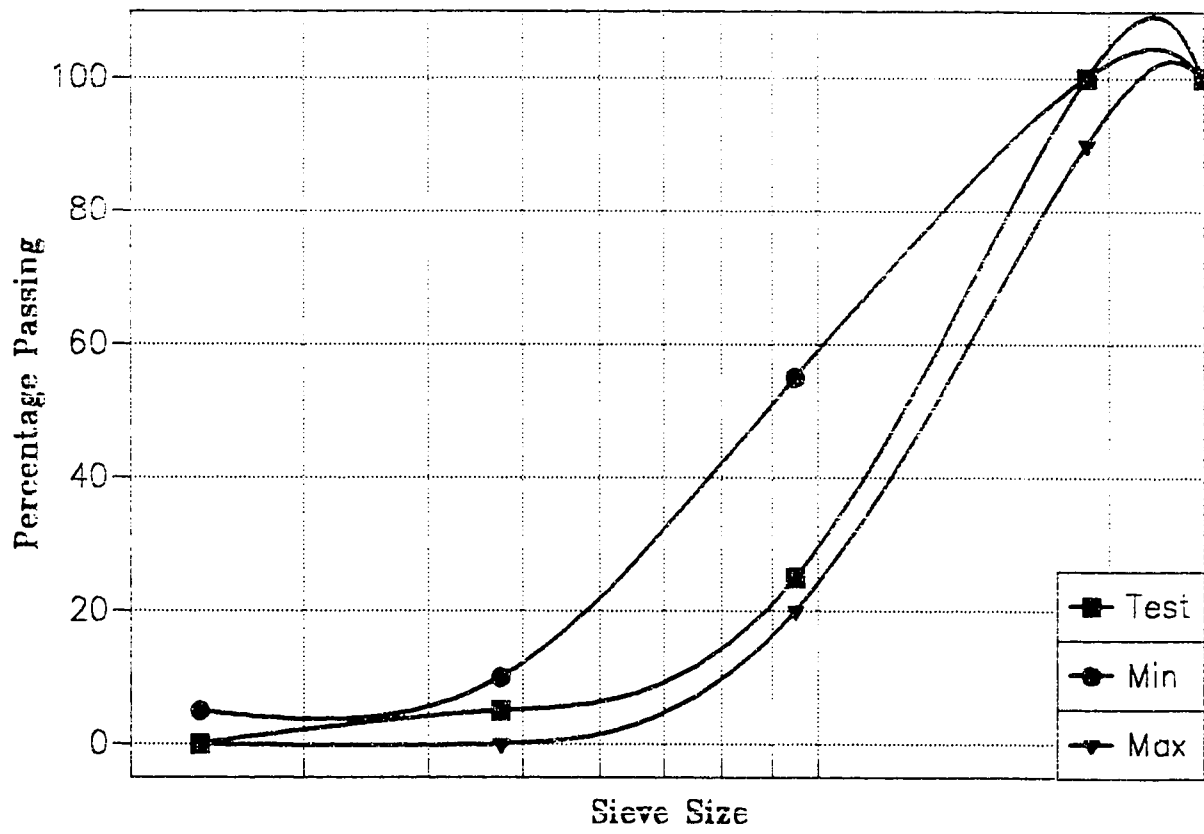
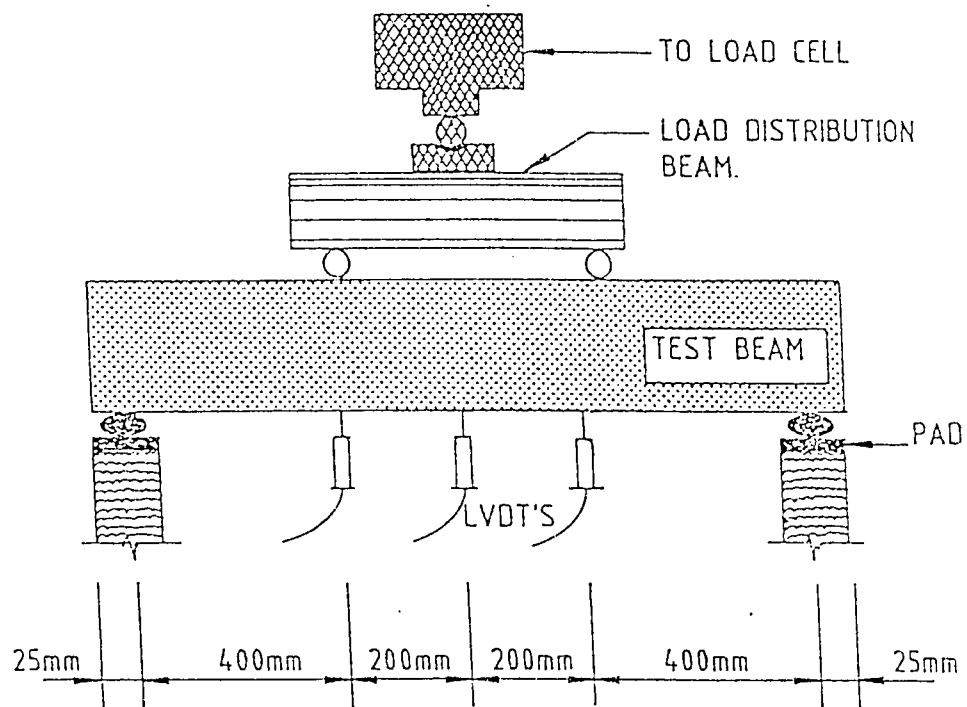


Figure 3.5: Coarse Aggregate Grading Curve (#67)



3.6: Sketch shows the load configuration used in testing the beam specimens



Plate 3.1: Photograph showing the close up of strain gauge connections on stirrups and spacers used

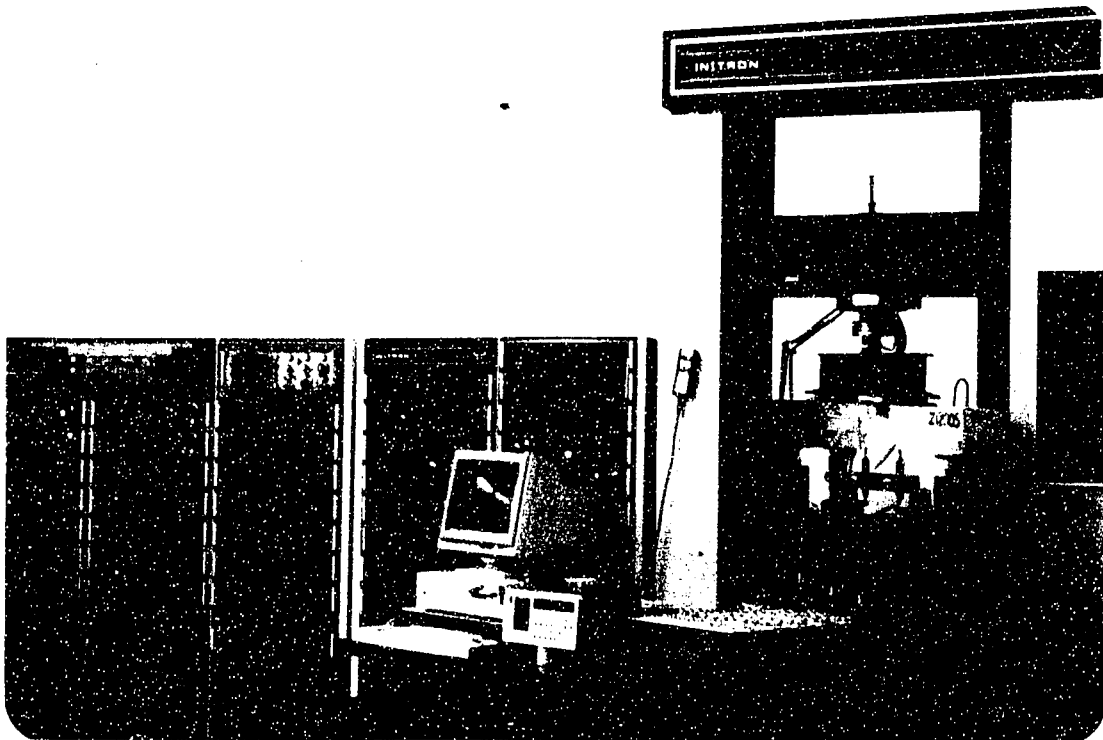


Plate 3.2: Photograph showing the test set up

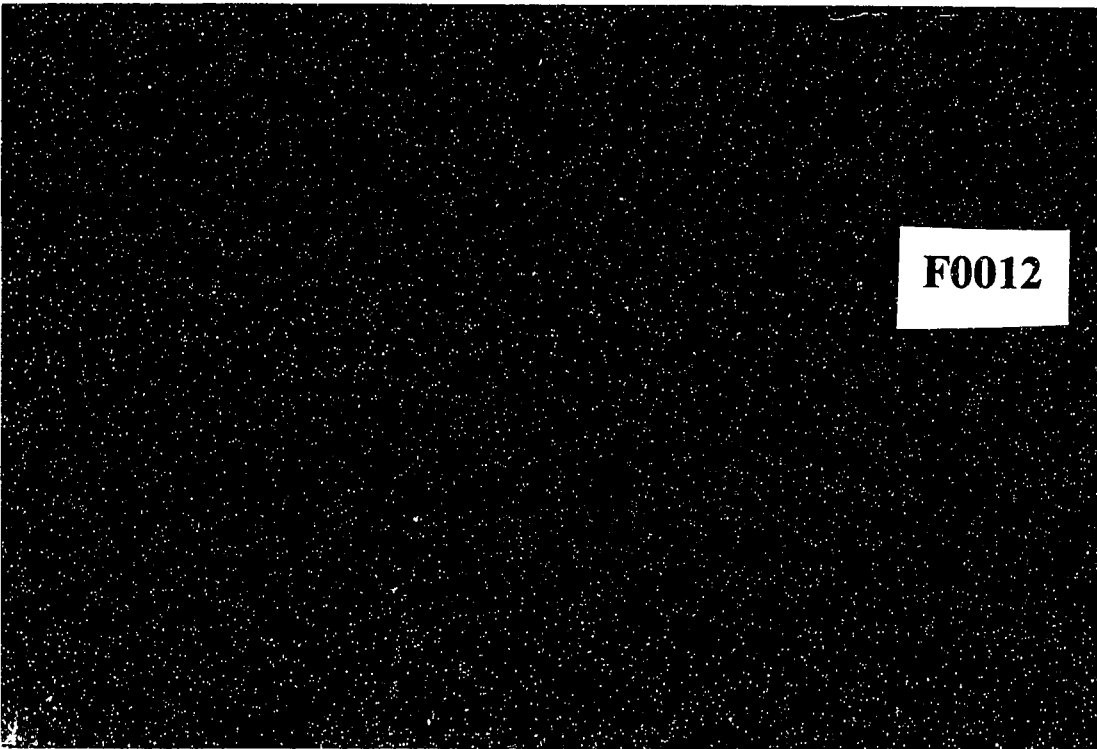
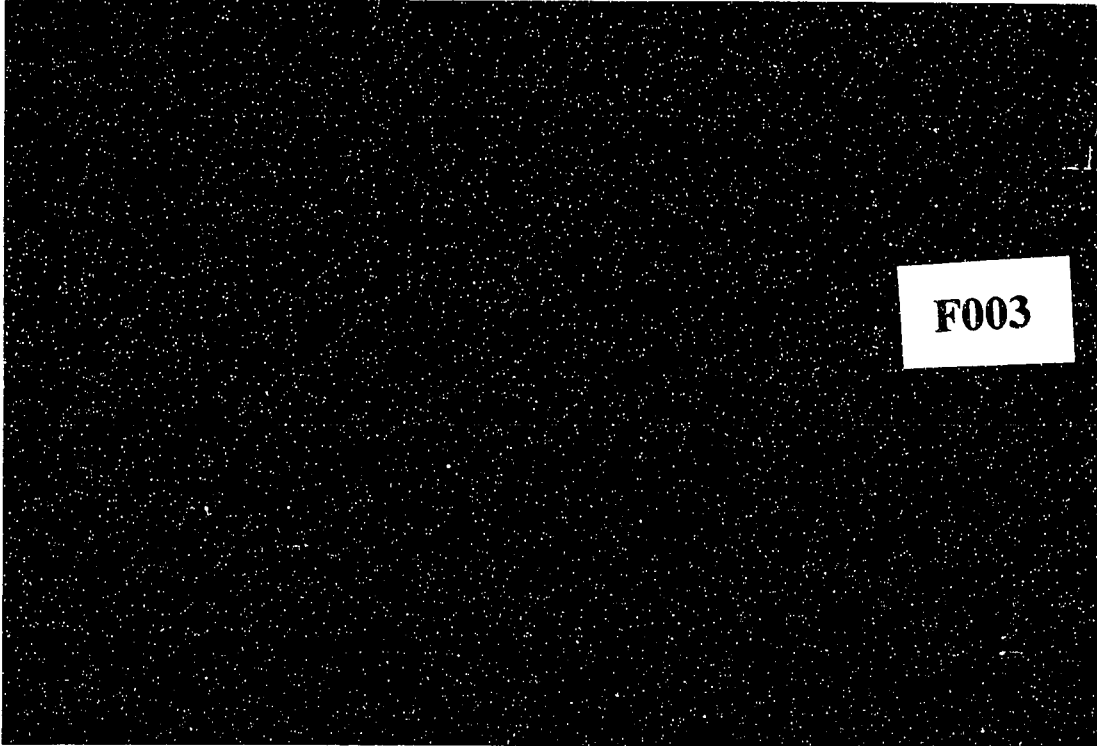


Plate 3.3: Flexural cracks on beams

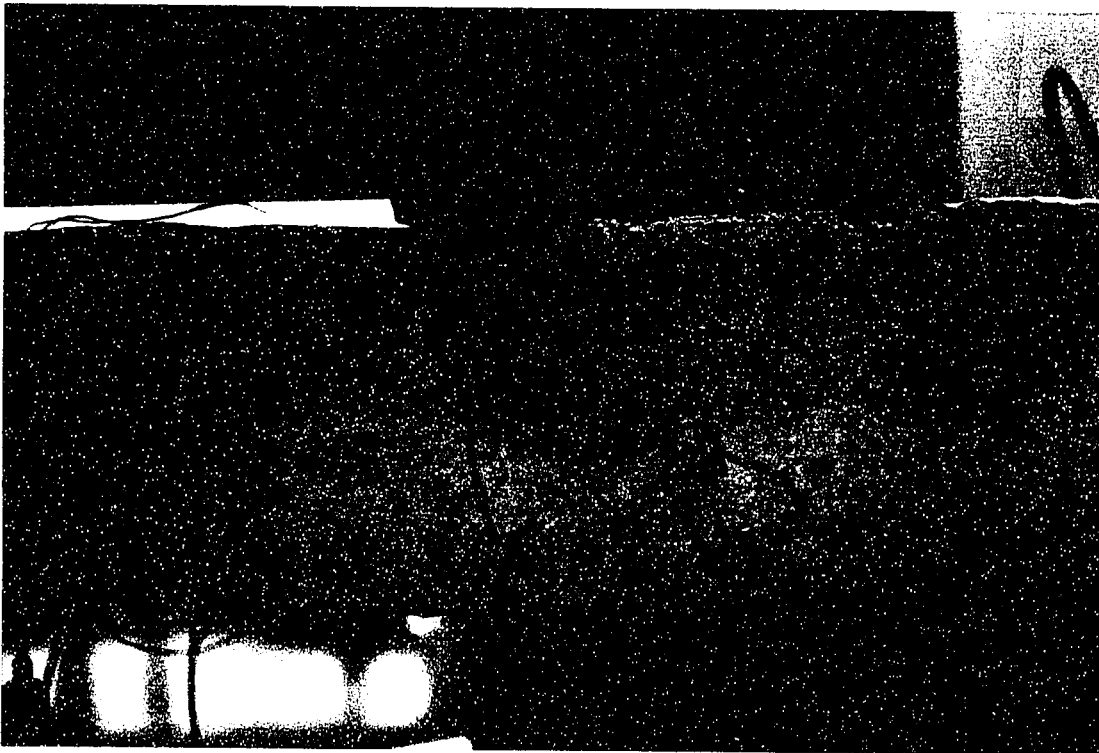
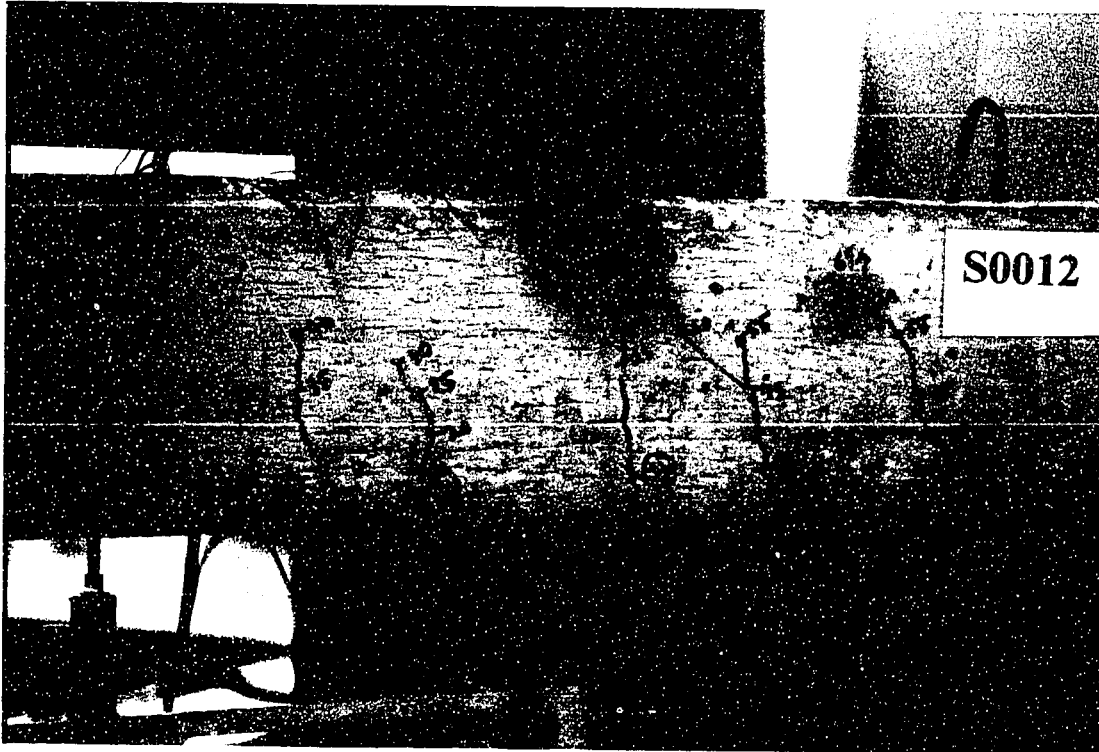


Plate 3.4: Cracks in the unrepaired beam at different load levels

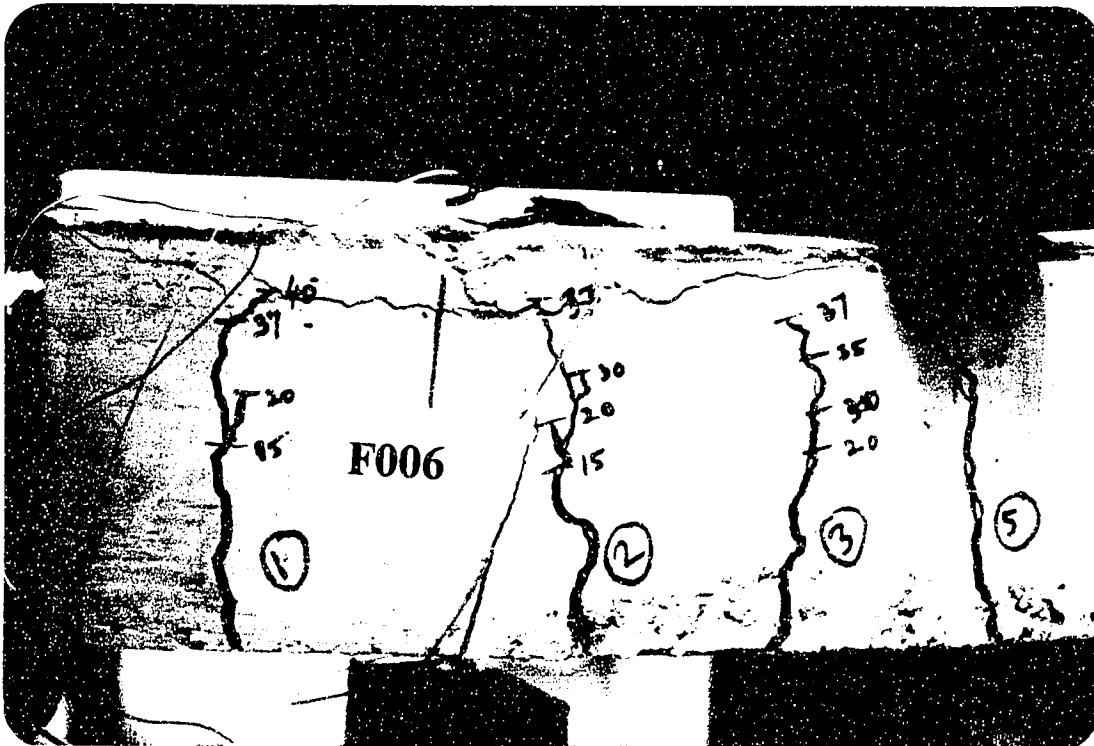


Plate 3.5: Crushing of the concrete in the compression zone



Plate 3.6: Photograph showing the bonding of steel plate on the soffit of a beam

Chapter IV

THEORETICAL CALCULATIONS

4.1 Introduction

In this chapter the procedures used for the calculations of theoretical ultimate loads for flexure and shear are presented. For the flexural design of repaired and unrepaired beams, calculations were based on strain compatibility and use of rectangular compression stress block given by ACI-318 code (Figure 4.1). Shear design for repaired beams was based on the predictor equation suggested by KFUPM model [38,41,44]. Peeling and shear stresses for repaired beams are calculated according to methods suggested by KFUPM [38,41,44] and Robert's approach [34], respectively.

4.2 Unrepaired Beam

Calculations for P_f and P_s based on Unplated beam properties:

4.2.1 Flexural Capacity (P_f)

For all members designed according to ACI strength method, $f_s = f_y$ at failure and the nominal flexural strength is given by:

$$M_n = A_s f_{ys} \left(d_s - \frac{a}{2} \right) \quad (4.1)$$

$$A_s = \frac{\pi}{4} d^2$$

The depth of the concrete rectangular stress block is given by

$$\frac{a}{d} = \left(\frac{A_s f_{ys}}{0.85 f'_c b_c} \right)$$

The load corresponding to flexure is given by

$$\frac{P_f}{2} a' = M_n \quad (4.2)$$

$$P_f = \frac{2M_n}{a'}$$

4.2.2 Shear Capacity (P_s)

Shear strength provided by concrete V_c is given by

$$V_c = \frac{1}{6} \left[\sqrt{f'_c} + 100 \rho_w \left(\frac{V_u d_s}{M_u} \right) \right] b_c d_s \quad (4.3)$$

$$\rho_w = \frac{A_s}{b_c d_s} \quad (4.4)$$

Shear strength in the web steel is given by

$$V_s = \frac{A_v f_{ys} d_s}{s} \quad (4.5)$$

Total shear force V_n applied at a given section is given by

$$V_n = V_c + V_s \quad (4.6)$$

The load corresponding to shear

$$P_s = 2 V_n \quad (4.7)$$

4.3 Repaired Beam

4.3.1 Flexural Capacity (P_{flex})

Assuming yielding of both internal and external reinforcement at failure, moment equilibrium at ultimate load conditions requires:

$$M_n = A_s f_{ys} \left(d_s - \frac{\bar{a}}{2} \right) + t_p b_p f_{yp} \left(h_p - \frac{\bar{a}}{2} \right) \quad (4.8)$$

The depth of the concrete rectangular stress block is given by:

$$\bar{a} = \frac{A_s f_{ys} + b_p t_p f_{yp}}{0.85 f'_c b_c} \quad (4.9)$$

$$h_p = h_c + d_s + \frac{t_p}{2}$$

$$P_{flex} = \frac{2M_n}{a} \quad (4.10)$$

4.3.2 Shear Capacity (P_{shear})

Investigation for Concrete Rip-off

In order to check on the shear capacity of the plated R/C beams, the following quantities are computed according to ACI strength method:

Shear strength provided by concrete V_c is given by

$$V_c = \frac{1}{6} \left[\sqrt{f'_c} + 100 \rho_w \left(\frac{V_u d_s}{M_u} \right) \right] b_c d_s \quad (4.11)$$

$$\rho_w = \frac{A_s}{b_c d_s}$$

Shear strength in the web steel is given by

$$V_s = \frac{A_v f_{ys} d_s}{s}$$

Total shear force V_n applied at a given section is given by

$$V_n = V_c + V_s$$

The load corresponding to shear

$$P_s = 2 V_n$$

To check the efficiency of the stirrups associated with the crack resulting from concrete rip-off failure or below the level of reinforcement prior to a steep vertical ascent to the point of loading, the quantity K_{sf} is computed for the beams which shall be identified as to have failed in Rip-off or Flexure/Rip-off.

$$K_{sf} = \frac{\left(\left(\frac{P_{\text{expt}}}{2} \right) - V_c \right)}{V_s} \quad (4.12)$$

If $K_{sf} = 0$, It implies no participation of stirrups in resisting concrete rip off failure.

If $K_{sf} > 1.0$, It implies ACI shear strength for such beams could be conservative.

If $K_{sf} < 1.0$, then modified expression suggested by KFUPM [38,41,44] is used to estimate the shear capacity of plated R/C beams.

4.4 Expression for Shear Capacity

4.4.1 Rip-Off Failure

The horizontal cracking is precipitated by the biaxial tension field induced at the location of plate curtailment due to creation of the traverse normal stress or more commonly known as the peeling stress. Using the strength of materials approach, the maximum shear and peeling stresses at the interface for the beam using Robert's approach [34] at the maximum load sustained by the beam is calculated from the following formula:

The maximum shear stress at interface τ_o at the point of plate curtailment is given by:

$$\tau_o = \left(V_n + \sqrt{\left(\frac{K_s}{E_p b_p d_p} \right) M^*} \right) b_p t_p \left(\frac{h_p - h}{b_a I} \right) \quad (4.13)$$

The maximum peeling (normal) stress at interface σ_o is given by:

$$\sigma_o = \tau_o t_p \left(\frac{K_n}{4E_p I_p} \right)^{1/4} \quad (4.14)$$

In addition to the material properties and beam dimension, the other parameters are determined as follows:

$$A = \frac{E_c b_c}{2E_p}$$

$$B = \frac{E_s A_s}{E_p} + b_p t_p$$

$$C = \frac{A_s d_s E_s}{E_p} + h_p b_p t_p$$

$$X = \frac{-B + (B^2 + 4AC)^{1/2}}{2A} \quad (4.15)$$

$$M^* = \frac{P}{2y} \left(X + \frac{d_c + t_p}{2} \right)$$

$$V = \frac{P}{2}$$

$$I_p = \frac{b_p t_p^3}{12} \quad (4.16)$$

The second moment of Inertia (I) of the fully composite transformed equivalent steel section is given by

$$I = \frac{E_c b_c X^3}{3E_p} + \frac{A_s E_s (h_s - X)^2}{E_s} + b_p t_p (h_p - X)^2 \quad (4.17)$$

The shear stiffness of the interface layer

$$K_s = \frac{G_a b_a}{d_a} \quad (4.18)$$

Normal stiffness of the interface layer

$$K_n = \frac{E_a b_a}{d_a} \quad (4.19)$$

In order to preempt the likelihood of plate separation in the design process, the stresses at the region of plate cutoff are checked to insure that plate separation does not occur. The design formulas are presented in such a way that, for a given level of allowable coefficient of cohesion of the steel/glue/concrete interface c_{all} ,

a maximum cutoff distance from the beam support is evaluated. In general, the interface stresses for a given load increase as the plate thickness and plate cross-sectional area enlarge. For a plate of required cross-sectional area, the minimum thickness is achieved by selecting the largest plate width, which is limited by the width of the beam.

The interface stresses τ_o , σ_o at the plate cutoff region are limited to an acceptable level, if [38]

$$\tau_o + \sigma_o \tan 28^\circ \leq c_{all} \quad (4.20)$$

Where c_{all} is the allowable coefficient of shear cohesion, MPa, for the epoxy concrete/steel surface. The peak shear stress τ_o is given as

$$\tau_o = \alpha_1 f'_t \left(\frac{C_{r1} V_o}{f'_c} \right)^{5/4} \quad (4.21)$$

Where,

α_1 = 35, an empirical regression coefficient determined

from numerical parametric study

f'_t = tensile strength of concrete, MPa

V_o = global shear force at location of plate cutoff

In contrast, using a linear strength of materials model, Robert's [34] suggested use of the following expression to evaluate the peak shear interface stress

$$\overline{\tau_o} = C_{r1} V_o \quad (4.22)$$

Where

$$C_{r1} = \left[1 + \left(\frac{K_s}{E_p b_p d_p} \right)^{1/2} L_c \right] \frac{b_p d_p}{I b_a} (h_p - h) \quad (4.23)$$

Where,

- L_c = M_o / V_o at plate cutoff location
- h = depth to neutral axis of cracked section of plated beam
- I = second moment of area of equivalent transformed steel section about neutral axis for cracked section
- G_a, b_a, d_a shear modulus, width, and depth of adhesive

The peak peeling stress σ_o required is given by

$$\overline{\sigma_o} = C_{R2} \overline{\tau_o} \quad (4.24)$$

The factor C_{R2} is calculated using

$$C_{R2} = d_p \left(\frac{K_n}{4E_p I_p} \right)^{1/4} \quad (4.25)$$

Where,

- I_p = second moment of area of steel plate about its own centroid
- E_a = elastic modulus of adhesive

The capacity of a plated R/C beam prone to concrete rip-off failure has been detailed in Ref [38,41,44] and can be approximated (in N-mm) as

$$V_u = (V_c + kV_s) \quad (4.26)$$

$$V_c = \frac{1}{6} \left(\sqrt{f'_c} + 100 \rho_w \frac{V_u d_s}{M_u} \right) b_c d_s \quad (4.27)$$

$$V_s = \frac{A_v f_{yst} d_s}{s} \quad (4.28)$$

$$k = 2.4 e^n \quad (4.29)$$

$$n = -0.08 C_{R1} C_{R2} * 10^6 \quad (4.30)$$

Where

f'_c = concrete strength, MPa

b_w, d_s = width and effective depth of unplated R/C section

A_v = amount of shear reinforcement

f_{yst} = stirrup yield strength

s = stirrup spacing

$$\rho_w = \frac{A_s}{b_c d_s}$$

$$\frac{V_u d_s}{M_u} > 1.0$$

The coefficient (k) is obtained as a regression of experimental data of several plated beams, reported by different researchers to have failed after concrete cover rip-off [38,41,44]. This expression for rip-off capacity of plated R/C beams has been further verified in the present experimental investigation in which eighteen beams were designed to fail in a concrete rip-off mode.

4.4.2 Diagonal Tension Failure

The ultimate shear capacity when diagonal tension failure is anticipated in the plated R/C beam is found to be well predicted by:

$$V_u = \frac{1}{6} \left\{ \sqrt{f'_c} + 100 \left(\rho_w + \rho_p \right) \frac{V_u d_s}{M_u} \right\} b_c d_s + \frac{A_v f_{yst} d_s}{s} \quad (4.31)$$

The above expression is simply the ACI equation for shear strength of R/C members modified to account for the increase in the shear capacity of the beam due to the external plate reinforcement. As per ACI requirements,

$$\frac{V_u d_s}{M_u} > 1.0$$

and

$$s > \frac{d_s}{2}$$

Where

$$\rho_w = \frac{A_s}{b_c d_s}$$

$$\rho_p = \frac{A_{sp}}{b_c d_s}$$

b_c = width of beam

d_s = distance from top of beam to centroid of internal reinforcement

s = spacing of stirrups

A_v = area of cross-section of a stirrup

f_{yst} = yield stress of stirrups

V_u, M_u shear and moment at critical section of distance d_s from face of support

In beams with $P_s < P_f$, although initial cracks emanate from location of plate curtailment due to existence of high peeling and shear stresses, these cracks are arrested due to presence of high amount of flexural reinforcement and the rip-off failure is preempted. Thus, loads based on rip-off model underestimate the capacity of such beams, whose actual failure is precipitated in a classical diagonal tension mode. These loads are predicted with reasonable accuracy by modifying the ACI expression for shear strength of R/C beams to account for the beneficial effect of the steel plate on the shear capacity of the beam.

The peeling stress plays a significant role in shear capacity of plated RC beams. For beams with low values of $C_{R1}C_{R2}$, the shear cracking remains similar to the diagonal tension cracking of unplated R/C beams, enabling sufficient number of stirrups to be mobilized to intercept cracking. As $C_{R1}C_{R2}$ increases, the extent of horizontal cracking increases, with the final movement of the crack being quite steep close to the point of loading.

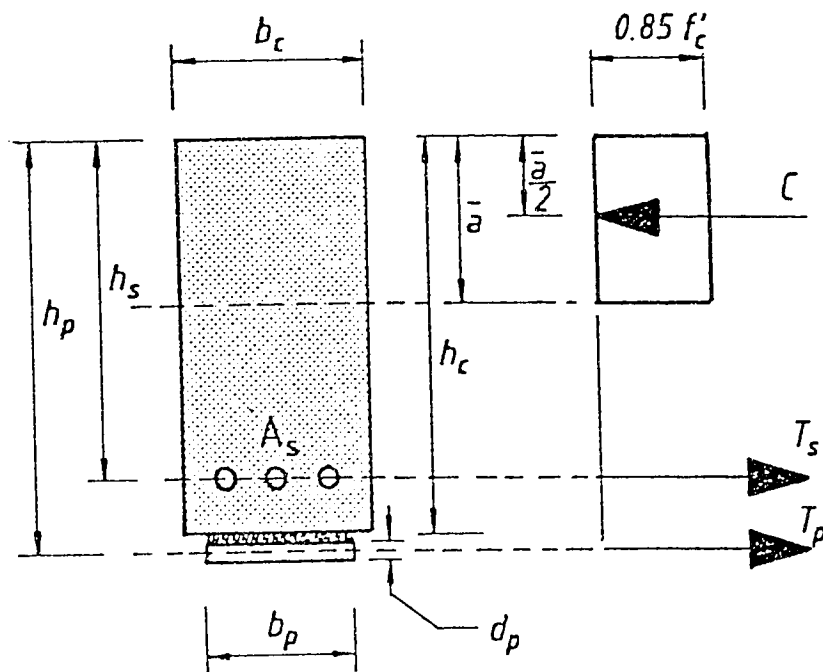


Figure 4.1 Internal forces at Ultimate conditions

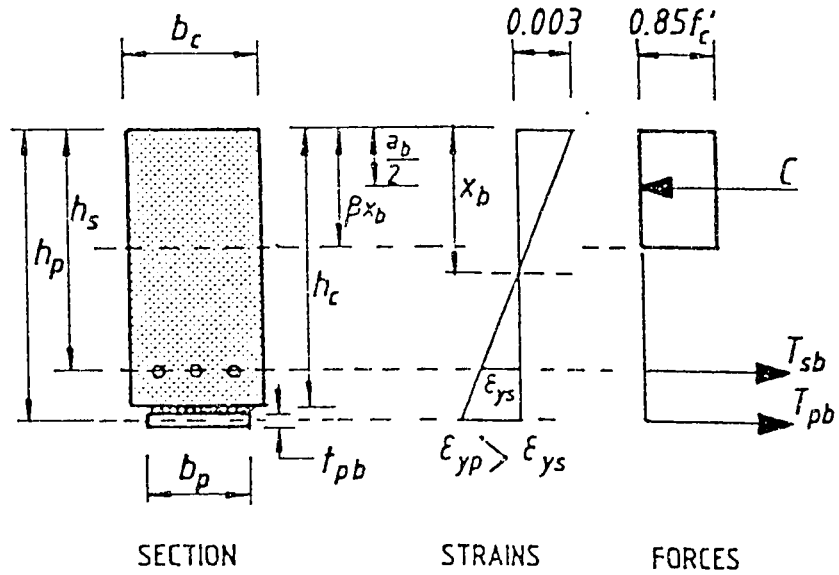


Figure 4.2 Strain distribution at balanced conditons

Chapter V

RESULTS AND DISCUSSION

5.1 Introduction

Control beams for flexure group (F0012, F006 and F003) and for shear group (S0012 and S0020) were loaded to 10 and 5 mm central deflection, representing 85 % of ultimate capacity, respectively, unloaded and then reloaded to failure. The experimental load obtained for the flexure group control beams is approximately 35 % greater than that predicted by the strength method (Table 5.1), since no account was made for increase in yield stress of internal reinforcement by virtue of strain hardening. Similar observation is made about control beam S0012 which failed by diagonal tension, although the flexural capacity based on perfect elasto-plastic behavior of reinforcement is slightly lower than the shear reinforcement. Results are presented in the form of load-deflection plots (Figures 5.1 to 5.24). Table 5.1 is an overall summary of predicted and experimentally observed ultimate loads together with modes of failure for the 23 repaired beams tested, of which 18 belong to the flexure group category ($P_f < P_s$) and five to the shear group ($P_s < P_f$). Shown in columns (2) and (3) of Table 5.1 are the predicted flexural and shear capacities of the beams using the ACI strength method. The ultimate loads based on concrete rip-off failure as predicted by the KFUPM model [38,41,44] are shown in column (4). The ultimate loads listed in column (5) are

based on the following predictor equation and is to be used when diagonal tension failure is anticipated in the plated R/C beam. Equation (4.31) is simply the ACI equation for shear strength of R/C member modified to account for the increase in the shear capacity of the beam due to the external plate reinforcement. As per ACI requirements,

$$V_u = \frac{1}{6} \left\{ \sqrt{f'_c} + 100 (\rho_w + \rho_p) \frac{V_u d_s}{M_u} \right\} b_c d_s + \frac{A_v f_{yst} d_s}{s} \quad (4.31)$$

As noted in the results outlined in Table 5.1, all the plated R/C beams have failed in one of the three modes as discussed in the section of state-of-the-art and modes of failure. Load based on flexure failure mode can be found readily from ACI strength method taking into account the contribution of the external plate. Load for rip-off failure appears to be well predicted by the existing KFUPM model [38,41]. It is to be noted that for beams in which $P_f < P_s$, rip-off is the most likely failure mode if the ultimate load predicted based on the KFUPM model is less than the predicted by the ACI strength method based on yielding of internal and external reinforcement and crushing of concrete in the compression zone. Ultimate loads predicted by the KFUPM model [38,41,44] for the S-series beams ($P_s < P_f$) are very much on the conservative side and also do not predict the actual failure mode which is diagonal tension in contrast to concrete rip-off. Inspection of these beams reveals that although initial cracks emanate from location of plate curtailment, the rip-off failure does not take place since these

beams have sufficient internal and external flexural reinforcement that prevents the horizontally developing rip-off crack from joining existing flexural cracks and to proceed upwards. After the arrest of any crack from plate curtailment zone, the load picks up to a magnitude that is sufficient to cause a classical diagonal tension failure of the plated beam in contrast to the rip-off failure. It is not surprising that this load is well predicted by the proposed ACI modified equation for shear failure (Eq. 4.31) as values in column (5) of Table 5.1 indicate.

It is to be noted that ultimate load values in column (2) are underestimated, since flexural failure is assumed to occur at perfect elasto-plastic conditions in reinforcement, ignoring effects of strain hardening, e.g. beam F153 failed in flexure at 71.7 kN whereas, the flexural model predicted failure at 54.3 kN and similarly for all other beams.

An illustrative example for evaluating ultimate loads and maximum shear and peeling stresses at the interface for the beams are given in Appendix A. The effect of thickness of bonded plate, shear stirrups and the curtailment length on ultimate loads, and modes of failure in repaired beams are discussed in this Chapter. Results in Table 5.1 indicate an excellent correlation between theoretical and experimental ultimate loads for all repaired beams (Figure 5.15 to Figure 5.25). Maximum values of shear and normal (peeling) stresses at the plate curtailment or interface were evaluated for repaired beams using Robert's [34]

approximate analytical solution assuming full elastic behavior and compared with KFUPM [38,41,44] model as presented in Table 5.2. Peeling and shear stress based on Robert's [34] suggested expression are plotted for each beam as presented in figures 5.34 and 5.35. It is observed that the beams failing in flexure exhibited a peeling stress of 0.7 and a shear stress of about 3.0. Rest of the beams failing in either rip-off, flexure/rip-off or diagonal tension showed higher values. The beams failing in different modes are depicted in plates 5.1 to 5.24.

5.2 Flexural Beams

5.2.1 Effect of Stirrup Spacing

The effect of stirrup spacing for beams of 1 mm plate thickness and 50 mm curtailment length are shown in Figure 5.1. It is observed that, all the beams with different spacing of stirrups behaved almost in a similar manner at all load levels till failure. It is clear that, spacing of shear reinforcement has no great influence on the behavior of these beams which failed in flexure dominated mode of failure with ductility. This is because the flexural capacity of repaired beam was less than the shear capacity.

When the thickness of steel plate was increased to 2 mm, it was observed that the mode of failure for the beams changed from flexure to shear. The shear capacity of these beams was less than the flexural capacity. Beams F2512, F256

and F253 showed highly brittle type of Rip-off failure. All three beams as shown in Figure 5.2 behaved essentially in the same fashion at all load levels up to failure. Thus, it is inferred that the spacing of stirrups does not increase the load capacity, however the mode of failure may change depending on the spacing of stirrups. Further, from a comparison of load-deflection curves in Figure 5.1 and 5.2, it can be hypothesised that the failure is dependent on both the stirrup spacing and plate thickness.

Figure 5.3 shows the effect of spacing of stirrups when the plate thickness was 3 mm and curtailment length was 50 mm. All the beams failed in shear, exactly in a way similar as that in the case of beams with 2 mm thick plate, except that the spacing of stirrups had a visible effect on the ultimate load. The ultimate load increasing with a decrease in the spacing of stirrups. Beams F3512, F356 and F353, with a stirrup spacing of 120, 60 and 30 mm failed in shear exhibiting a rip-off failure.

In the beams with a curtailment length of 150 mm, the effect of stirrup spacing and plate thickness on the ultimate load and failure mechanism was as follows. When the plate thickness was 1 mm, (Figure 5.4) the spacing of shear reinforcement influenced the load carrying capacity and the failure mechanism. The mode of failure changed drastically from a highly brittle type to a mixed type, as the spacing of stirrups decreased from 120 mm to 30 mm. Beam F11512 which

had stirrups at 120 mm failed in shear exhibiting a Rip-off failure. When the spacing of stirrups was reduced to 60 mm, beam carried some additional load and the mode of failure was again rip-off, with the horizontal tearing of concrete cover. In the Beam F1153 with stirrups at 30 mm, the failure load increased further and a mixed mode of failure (Flexure/Rip-off) with greater amount of ductility was recorded.

In the beam with a plate thickness of 2 mm, the spacing of stirrups (Figure 5.5) significantly affected the load carrying capacity. The spacing of stirrups had a significant effect. As the spacing of stirrups increased the load carrying capacity of these beams decreased. Beam F21512 showed a reduced load carrying capacity as compared to Beams F2156 and F2153. All the beams F21512, F2156 and F2153 showed a highly brittle mode of failure with a horizontal tearing of concrete cover rip off. In the beams with a plate thickness of 3 mm, (Figure 5.6) the spacing of shear reinforcement has a considerable influence on the behavior of beams with regard to the ultimate load capacity. All the beams F31512, F3156 and F3153 exhibited a Rip-off mode of failure.

5.2.2 Effect of Plate Thickness

Figures 5.7 through Figure 5.12 show the load vs central deflection for the repaired beams strengthened with steel plates of thickness 1,2 and 3 mm,

respectively. These data indicate that the thickness of plate considerably influences mode of failure and the ultimate load carrying capacity.

Figure 5.7 shows the effect of plate thickness for beams with a stirrup spacing of 120 mm and curtailment length of 50 mm. In Beam F1512, with 1 mm thick plate, curtailed near the support, pure flexural failure with ductility was observed. But beams F2512 and F3512 indicated a Rip-off failure. This shows that, as the plate thickness is increased from 1 mm to 3 mm, the mode of failure changes from pure flexure to a highly brittle mode of rip-off failure. From these data it can be inferred that when the steel plate is curtailed near the support, a thickness of 1 mm induces a flexure cum ductile failure, whereas, when 2 and 3 mm thick plates are used, a brittle failure was noted. Therefore, in such situations, a minimum plate thickness, 1 mm per se, is more desirable.

Figure 5.8 shows the load-deflection curves for beams with stirrups at 60 mm spacing. These curves indicate flexure cum ductile failure in the beam repaired with 1 mm thick plate. Whereas, in beams with thicker plates, of 2 and 3 mm thickness exhibited shear failure, with a horizontal tearing of concrete cover rip-off. However, the ultimate load in all these beams was more or less similar.

The load-deflection curves for beams with stirrups at 30 mm spacing are plotted in Figure 5.9. As seen in the previous two cases, as the plate thickness increased, mode of failure changed from flexure to shear. Beam F153,

strengthened with 1 mm thick plate, showed flexural failure with greater amount of ductility as compared to Beams F253 and F353 showing shear failure with a horizontal tearing of concrete cover rip-off.

Further, when the length of curtailment was increased from 50 to 150 mm, the plate thickness was still found to have a major influence on both the mode of failure and ultimate load carrying capacity of the beams. Figure 5.10 shows that all the beams (F11512, F21512 and F31512) failed in rip-off. Beam with the thickest plate, carried more load compared to beams with thinner plates.

In the beams F1156, F2156 and F3156, with spacing of stirrups at 60 mm, Figure 5.11, rip-off failure mode was noticed in all the beams, irrespective of the plate thickness. Also, the ultimate load was not significantly different from each other. Figure 5.12 shows the effect of thickness of plates on the load-deflection behavior for beams with a stirrup spacing of 30 mm. From these curves it can be seen that the thickness of plate considerably influences the behavior of beams with respect to the mode of failure. Beam F1153 with 1 mm thick plate exhibited a mixed type of failure (Flexure/rip-off) with greater amount of ductility before failure as compared to beams F2153 and F3153 containing 2 and 3 mm thick plates. But, Beam F3153 showed a highly brittle mode of shear failure with the horizontal tearing of concrete cover rip-off.

5.2.3 Effect of Curtailment Length of Plate

The effect of curtailment length on the load carrying capacity and failure mechanism for varying plate thickness and stirrup spacing is presented in Figures 5.13 through Figure 5.21. The load-deflection curves for beams strengthened with 1 mm thickness plate, and stirrup spacing at 120 mm, are plotted in Figure 5.13. These curves indicate that the length of curtailment has a visible effect on the mode of failure and the ultimate load. In Beam F1512, in which a curtailment length of 50 mm was maintained, pure flexure failure with a ductile behavior was noted. In Beam F11512, repaired with 150 mm curtailment length a brittle mode of rip-off failure was recorded. Further, the ultimate load decreased with an increase in the curtailment length. The ultimate load of the beam with a curtailment length of 50 mm was 1.5 times that of beam with a curtailment length of 150 mm.

In beams with 2 mm thick plate and 120 mm stirrups spacing, Beam F2512, sustained a larger load compared to beam F21512 with a shorter plate (Figure 5.14). This shows that the curtailment length has a great influence on the load carrying capacity and the mode of failure of the beams. The mode of failure for both the beams was rip-off. However, the beam with a larger curtailment length exhibited a large deflection. In the beams with a plate thickness of 3 mm (Figure 5.15), curtailment length did not influence the mode of failure. Both Beams, F3512 and F31512 showed a highly brittle mode of rip-off failure. The ultimate load,

however, did change with the length of plate. The beam with a longer plate could bear a higher load than the one with a shorter plate, and the latter deflected more than the former.

Figure 5.16 shows the load-deflection curves for beams repaired with 1 mm thick plate and curtailment lengths of 50 and 150 mm, and stirrup spacing of 60 mm. The length of curtailment was found to have a significant role with respect to the mode of failure and ultimate load capacity of the beams. Beams F156 with longer plate exhibited pure flexural failure with ductility and large deflection, whereas, Beam F1156 with a shorter plate exhibited a rip-off failure. Further, Beam F156 was able to sustain larger ultimate load than Beam F1156 and the ductility of the former was more than that of the latter.

In the beams with a plate thickness of 2 mm, the mode of failure changed completely from flexure to shear. Figure 5.17 shows that Beam F2156 with a shorter plate was more ductile than Beam F256. But beam with a larger plate was able to sustain considerably very high load than beam with a smaller plate. Both the beams F256 and F2156 failed in shear with the horizontal tearing of concrete cover rip-off.

In the beams with a plate thickness of 3 mm, the effect of plate curtailment is reflected from the failure behavior. Figure 5.18 shows that both the beams

F3156 and F356 failed in shear with the horizontal tearing of the concrete cover rip-off. Though Beam F356 was able to bear a higher load than Beam F3156, it exhibited a sudden drop in the load carrying capacity indicating a highly brittle mode of failure. Further, beam F3156 indicated a more ductile behavior.

Figure 5.19 shows beams repaired with 1 mm plate thickness with a stirrup spacing of 30 mm. Plate curtailment was found to have an effect with respect to the mode of failure. Beam F153 with longer plate failed in pure flexure and Beam F1153 with a shorter plate exhibited mixed type of failure. The mode of failure changed completely from flexure to flexure/rip-off as the length of curtailment increased. It is seen that there is slight fall in the ultimate load capacity of the beam with a shorter plate.

Figure 5.20 indicates that when the thickness of plate was increased to 2 mm, the length of plate could only effect the beam in carrying more load, but the mode of failure remained same. Both Beams F253 and F2153 showed rip-off failure with the horizontal tearing of concrete cover. Beam F253 which was bonded with a longer plate was able to sustain a very high load as compared to beam F2153 bonded with a shorter plate. The curtailment length affected both the ultimate load and mode of failure in plates bonded with a 3 mm thick plate as shown in Figure 5.21. Beams F3153 and F353 showed a brittle failure with the horizontal tearing of concrete cover rip-off.

5.3 Shear Beams

Figure 5.22 to Figure 5.24 show the load vs central deflection curves for beams S110512, S11020, S31520 strengthened with steel plates of 1, 1 and 2 mm thickness and curtailment lengths of 100, 100 and 150 mm, respectively. All these beams when loaded to failure showed shear failure with the formation of diagonal tension cracks in between the shear stirrups initiating from the point of curtailment of the plate and proceeding towards the point of application of loading. Also S11512 and S 2512 exhibited a similar mode of failure, i.e. diagonal tension.

However, the design of this experiment has isolated and identified the occurrence of failure by diagonal tension in contrast to the rip-off failure. Specially, for beams in which $P_f < P_s$ (F-series in Table 3), failure will occur by either flexure, rip-off or flexure-rip off. However, for beams in which $P_s < P_f$ (S-series in Table 5.1), the beam will fail in a diagonal tension mode.

An apparent anomaly in Table 5.1 is Beam S31520 which failed in diagonal tension at 66.2 kN, considerably below the predicted value of 84.2 kN. Close visual inspection of this beam revealed that the primary crack initiated at location of plate curtailment, traveled under a stirrup immediately in the vicinity, and went up at approximately 45 degrees without meeting any shear reinforcement- since the spacing of the stirrups was 200 mm. The other shear beam with the same

stirrup spacing, beam S11020, had a different L_c which ensured interception of diagonal tension crack by atleast one stirrup. For a practical situation, maximum spacing of the stirrups 's' should be as designated by the ACI code of $d_s/2$.

Beam ID	Compressive strength of concrete (MPa/psi) (1)	Predicted load based on ACI strength method		Predicted load based on KFUPM model [38,41] for rip-off failure (4)	Predicted load based on proposed expression for diagonal tension failure [Eq. 4.31] (5)	Experimental load (6)	Remarks (7)
		Flexural (2)	Shear (3)				
F0012	41.2/5970	35*	81.6	-	-	48	Flexure
F11512	41.2/5970	53.6	81.6	45.8	-	50	Rip-off
F21512	49.1/7114	73.1	84.9	47.1	-	48.5	Rip-off
F31512	41.2/5970	91.1	81.6	53	-	58.9	Rip-off
F1512	47.0/6812	54.1	84.1	64.5	-	74.6	Flexure
F2512	41.2/5970	71.9	81.6	53.8	-	77	Rip-off
F3512	43.6/6324	90.3	82.7	51.8	-	65.7	Rip-off
F006	47.7/6914	35*	124.4	-	-	48	Flexure
F1156	50.1/7269	54.4	125.4	54	-	58.9	Rip-off
F2156	47.7/6914	72.9	124.4	48.8	-	56	Rip-off
F3156	47.7/6914	91.1	124.4	47.6	-	54	Rip-off
F156	50.1/7269	54.4	125.4	86.4	-	71.2	Flexure
F256	47.1/6830	72.8	124.2	68.9	-	77.2	Rip-off
F356	47.8/6933	91.1	124.4	63	-	66.8	Rip-off

*The five values of P_f for control beams are marked with an asterisk to indicate that the actual flexural capacity will be higher due to strain-hardening of internal reinforcement.

Table 5.1 -- Experimental & predicted ultimate loads for all beams tested

Table 5.1 (contd.)

Beam ID	Compressive strength of concrete (MPa/psi) (1)	Predicted load based on ACI strength method		Predicted load based on KFUPM model [38,41] for rip-off failure (4)	Predicted load based on proposed expression for diagonal tension failure [Eq. 4.31] (5)	Experimental load (6)	Remarks (7)
		Flexural (2)	Shear (3)				
F003	45/6526.8	35*	203.4	—	—	50.5	Flexure
F1153	45/6526.8	54	203.4	65	—	69.3	Flexure/Rip-off
F2153	47.7/6911	72.9	204.5	54.4	—	58	Rip-off
F3153	49.9/7237	91.5	205.5	52	—	69.1	Rip-off
F153	49.9/7237	54.3	205.5	127.4	—	71.7	Flexure
F253	42.0/6087	72.1	202.1	80	—	78.2	Rip-off
F353	42.0/6087	90	202.1	79	—	74.5	Rip-off
S0020	45.4/6588	71*	73.4	—	—	84	Diagonal tension
S11020	45.4/6588	88.1	73.4	60.5	76.7	80.9	
S31520	47.4/6881	122.1	74.3	52.1	84.2	66.2	
S0012	39.5/5735	70*	86.9	—	—	70	Diagonal tension
S11512	39.5/5735	86.3	86.9	57.3	90.2	88.0	
S11012	39.5/5736	86.3	86.9	65.1	90.2	85	
S2512	39.5/5737	102.5	86.9	65.2	93.6	97.6	

*The five values of P_r for control beams are marked with an asterisk to indicate that the actual flexural capacity will be higher due to strain-hardening of internal reinforcement.

Beam Id.	Robert's Approach [34]		KFUPM Model [38,41,44]		Failure Mode
	Shear Stress	Peeling Stress	Shear Stress	Peeling Stress	
F11512	4.2312	0.972	7.967	2.0134	Rip-off
F21512	4.175	1.407	7.835	2.345	Rip-off
F31512	3.487	0.78	6.256	1.54	Rip-off
F1512	3.138	0.721	5.079	1.284	Flexure
F2512	3.625	0.99	6.566	1.973	Rip-off
F3512	3.181	0.962	5.395	1.794	Rip-off
F1156	4.953	1.137	8.905	2.25	Rip-Off
F2156	4.791	1.309	8.543	2.567	Rip-off
F3156	4.512	1.364	7.927	2.636	Rip-off
F156	2.995	0.688	4.784	1.209	Flexure
F256	3.613	0.987	6.05	1.818	Rip-Off
F356	3.222	0.974	5.197	1.728	Rip-Off
F1153	5.827	1.338	10.92	2.795	Flexure/Rip-off
F2153	4.962	1.355	8.932	2.684	Rip-Off
F3153	5.778	1.747	10.804	3.593	Rip-off
F153	3.03	0.696	5.191	1.311	Flexure
F253	3.677	1	6.61	1.986	Rip-Off
F353	3.613	1.092	6.467	2.15	Rip-Off
S11020	3.997	0.918	7.01	1.771	Diagonal Tension
S31520	4.959	1.499	9.179	3.052	Diagonal Tension
S11012	4.233	0.972	8.164	2.063	Diagonal Tension
S15112	5.708	1.311	11.865	2.998	Diagonal Tension
S2512	3.942	1.077	7.47	2.245	Diagonal Tension

5.2: Shear and Peeling Stresses based on Robert's [34] and KFUPM Research Group [38,41,44] approach

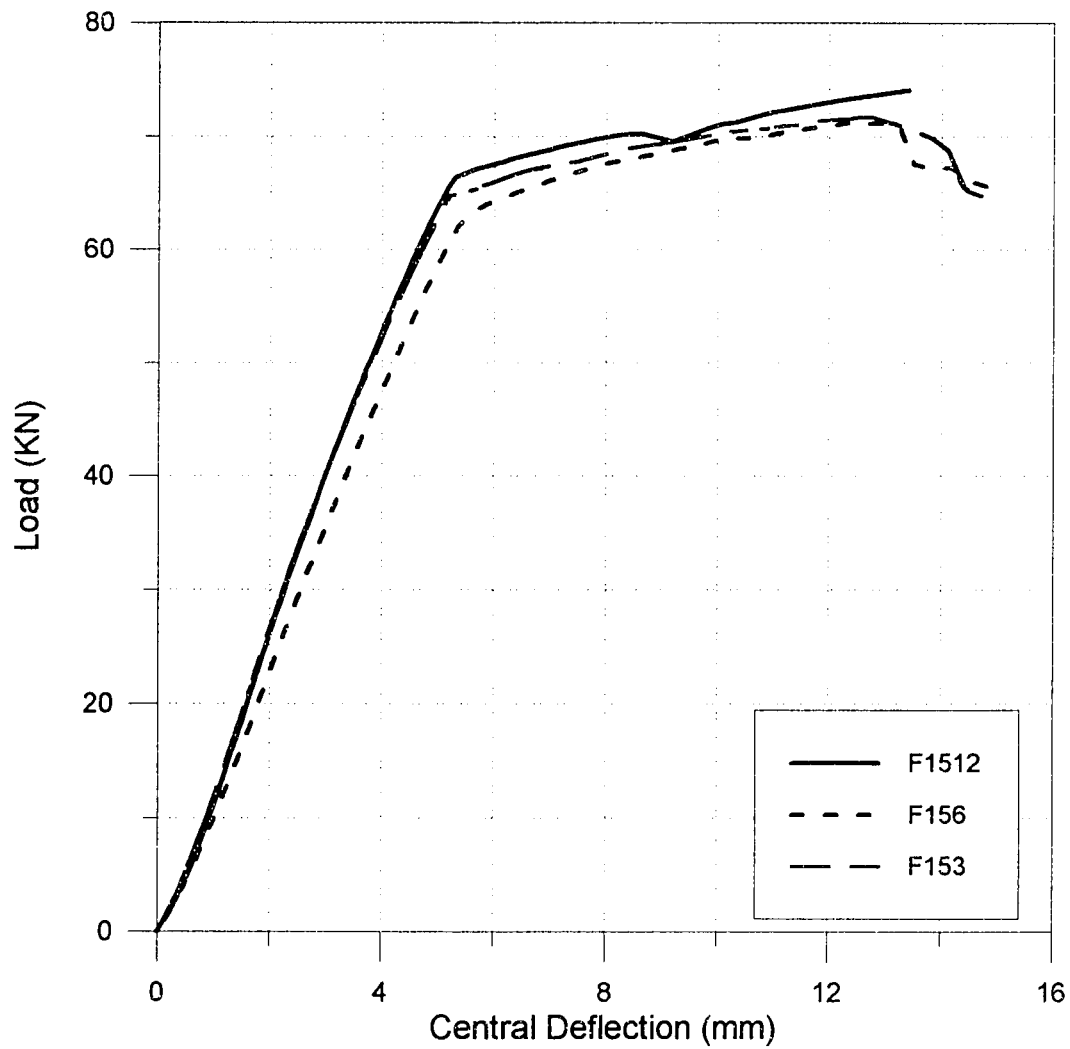


Figure 5.1: Load Vs Central Deflection for Beams repaired with 1100 mm long, 1 mm thick steel plates on the soffit of the beam having stirrups at 30,60 and 20 mm c/c respectively

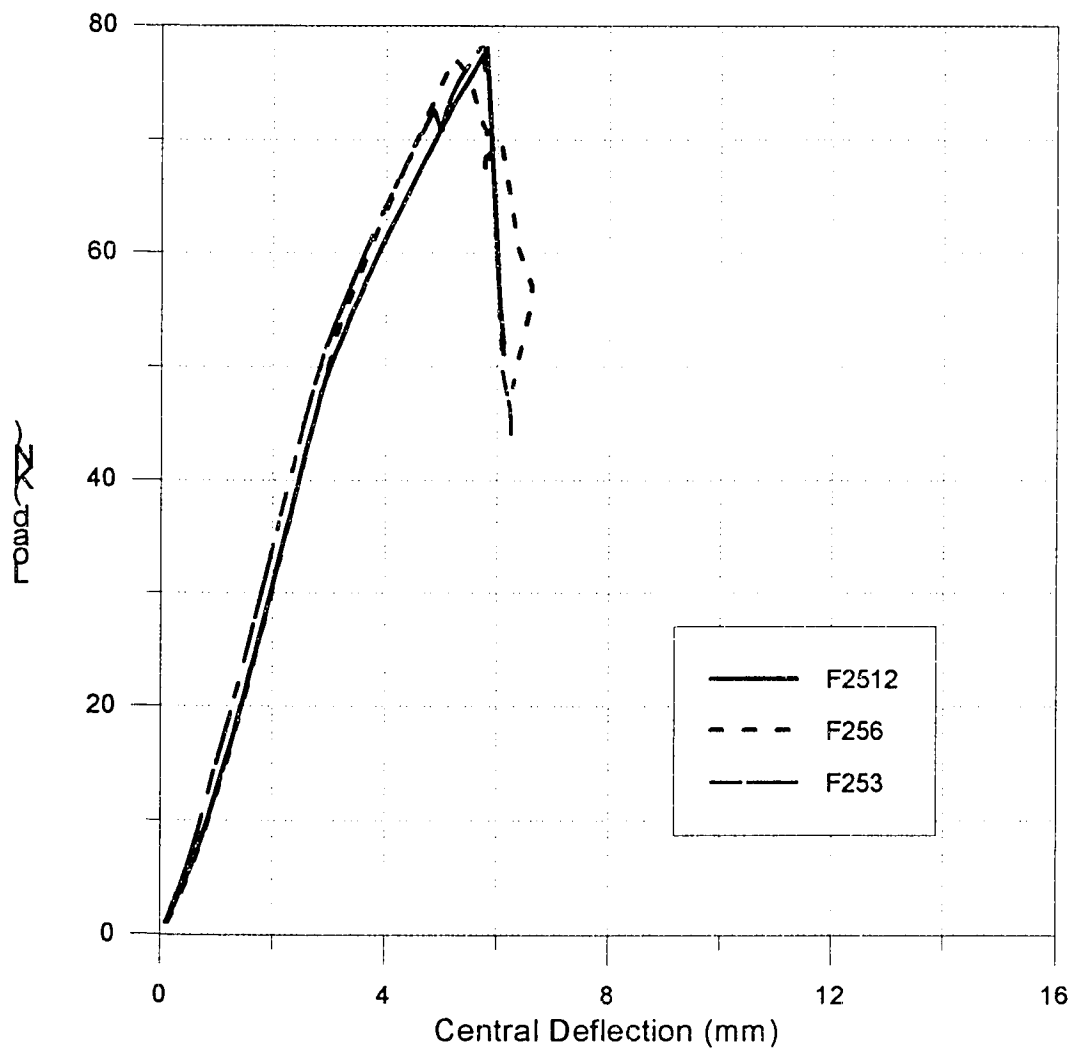


Figure 5.2: Load Vs Central Deflection for Beams repaired with 1100 mm long, 2 mm thick steel plates on the soffit of the beam having stirrups at 30,60 and 120 mm c/c respectively

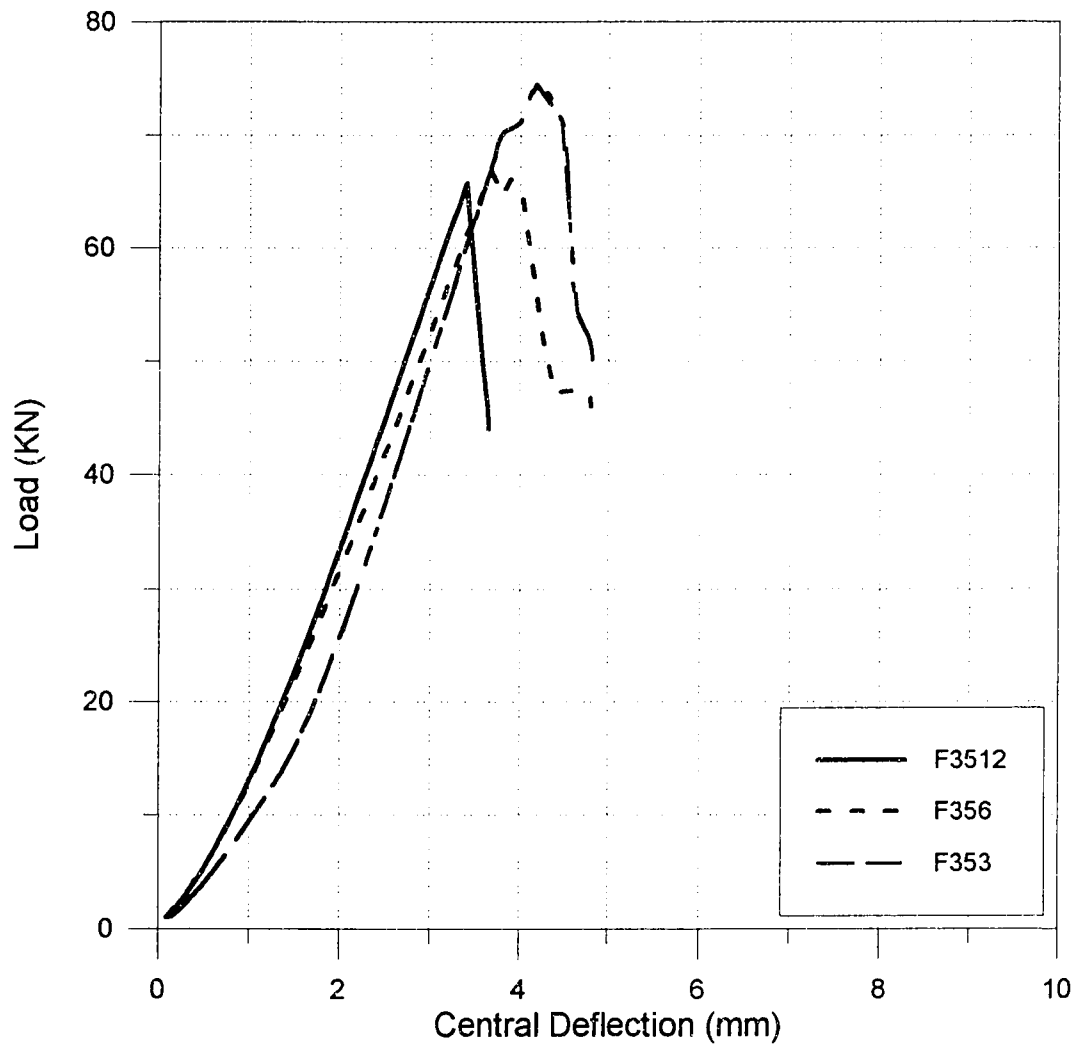


Figure 5.3: Load Vs Central Deflection for Beams repaired with 1100 mm long, 3 mm thick steel plates on the soffit of the beam having stirrups at 30, 60 and 120 mm c/c respectively

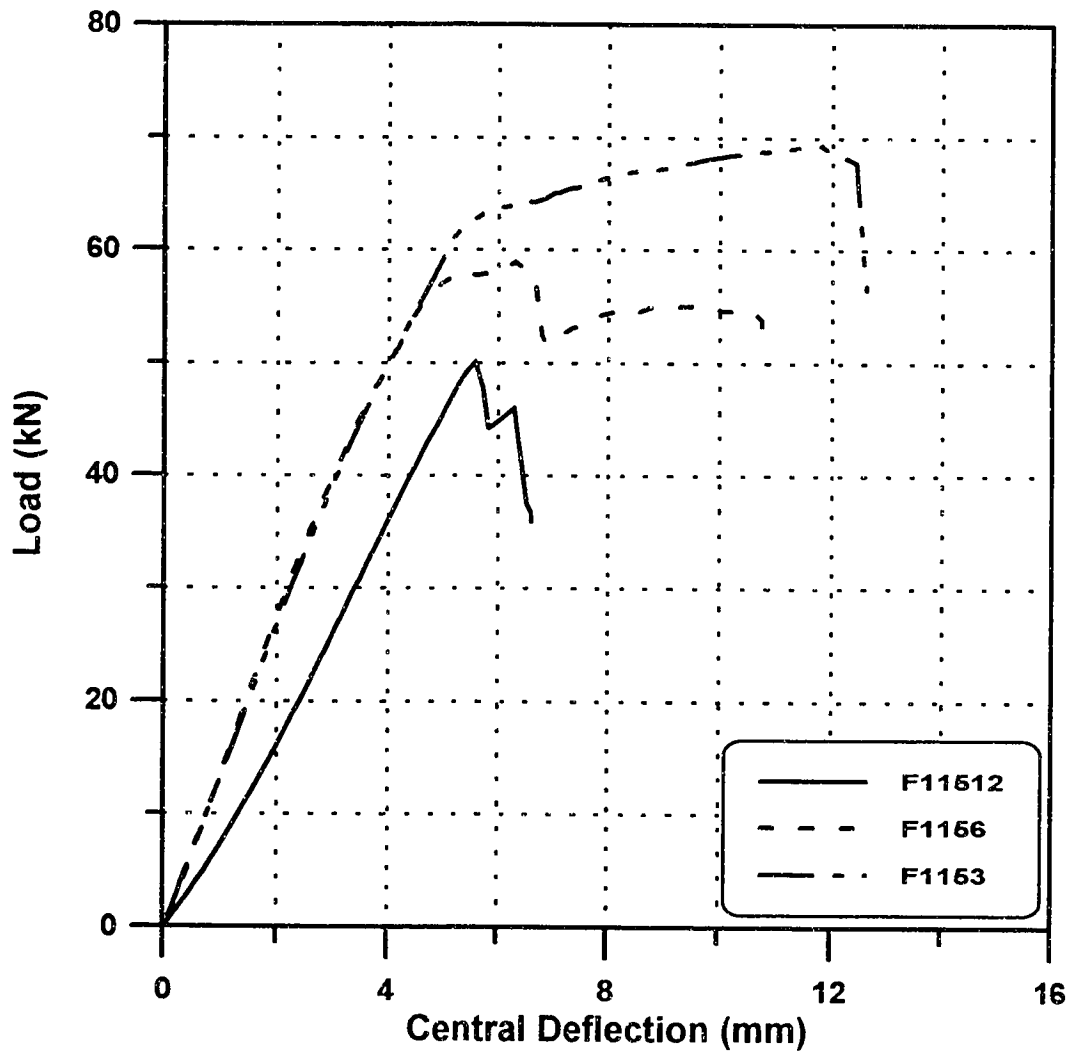


Figure 5.4: Load Vs Central Deflection for Beams repaired with 900 mm long, 1 mm thick steel plates on the soffit of the beam having stirrups at 30, 60 and 120 mm c/c respectively

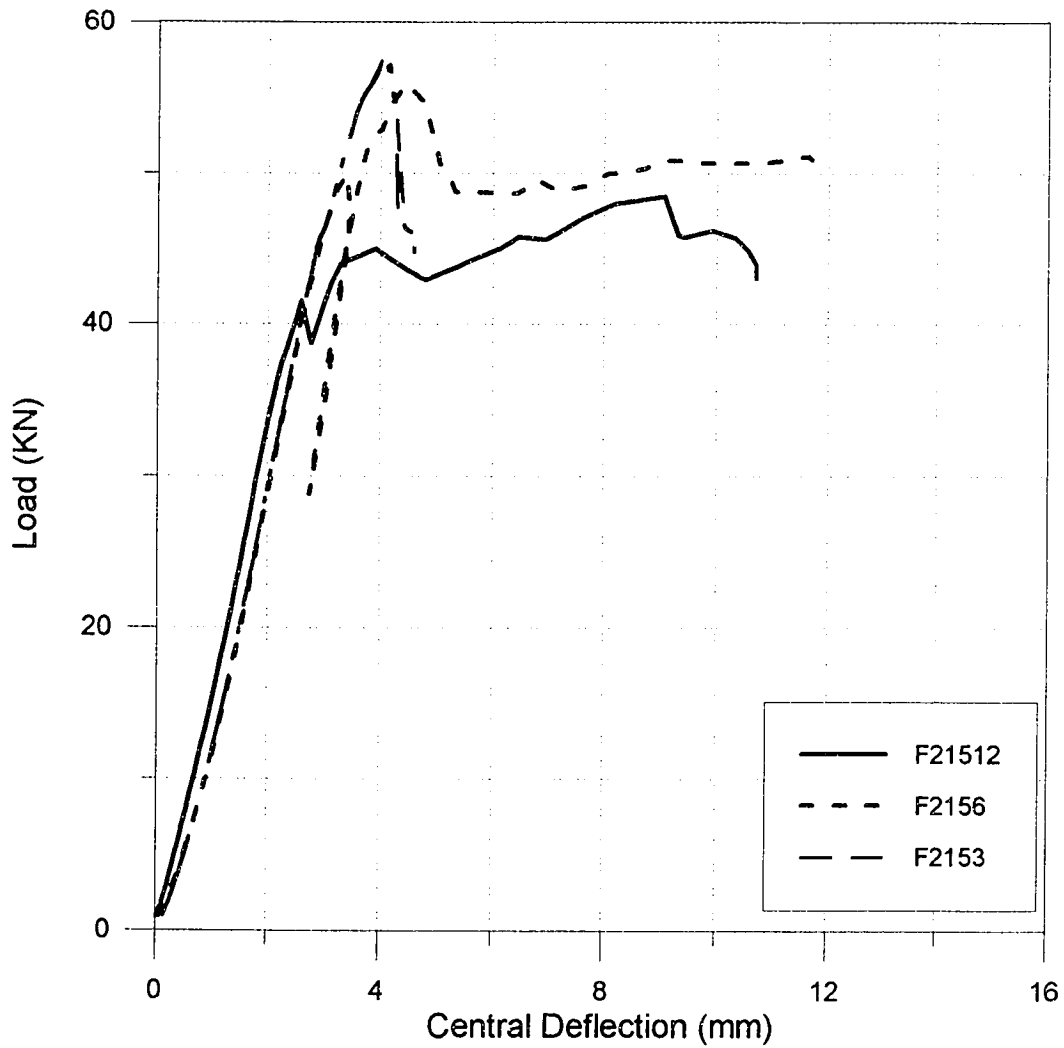


Figure 5.5: Load Vs Central Deflection for Beams repaired with 900 mm long, 2 mm thick steel plates on the soffit of the beam having stirrups at 30, 60 and 120 mm c/c respectively

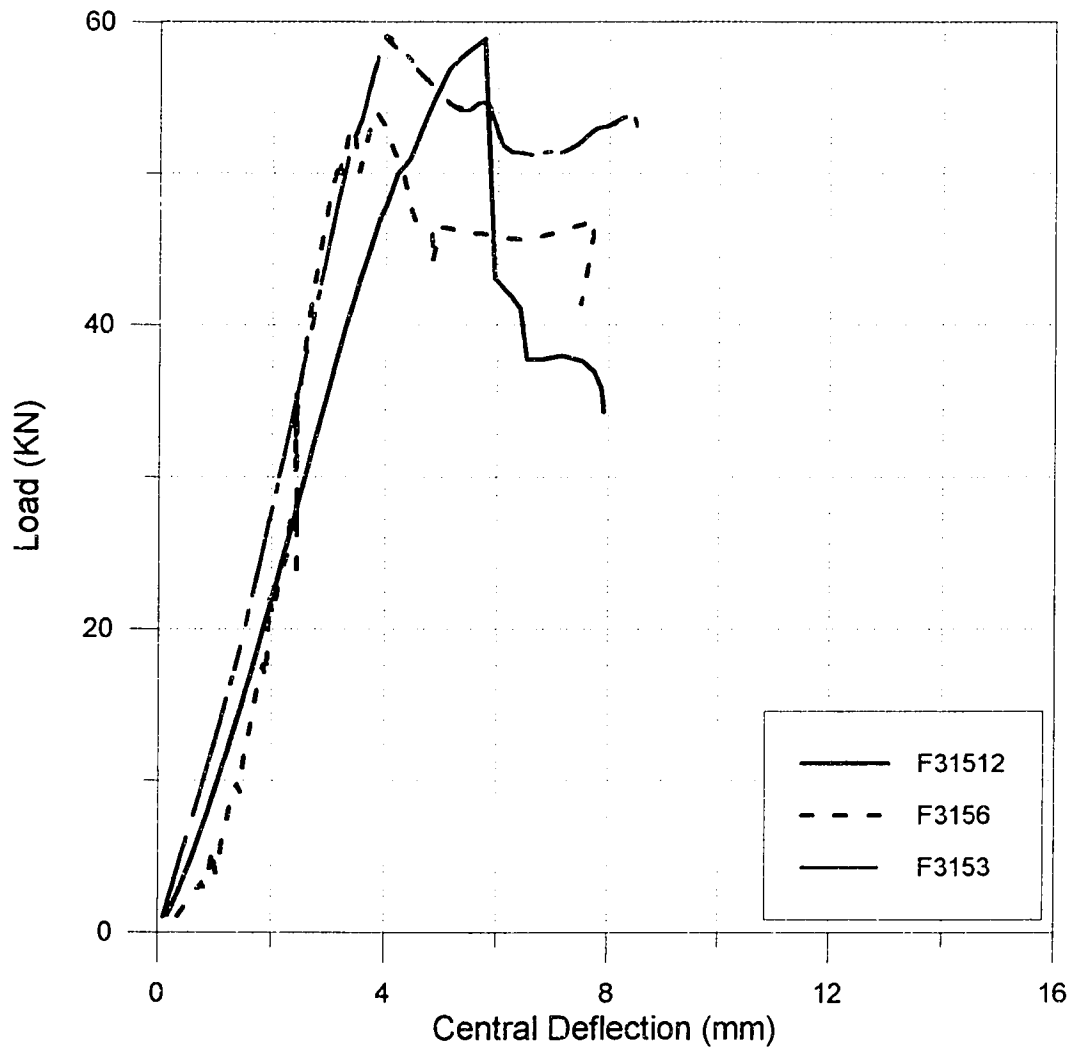


Figure 5.6: Load Vs Central Deflection for Beams repaired with 900 mm long, 3 mm thick steel plates on the soffit of the beam having stirrups at 30, 60 and 120 mm c/c respectively

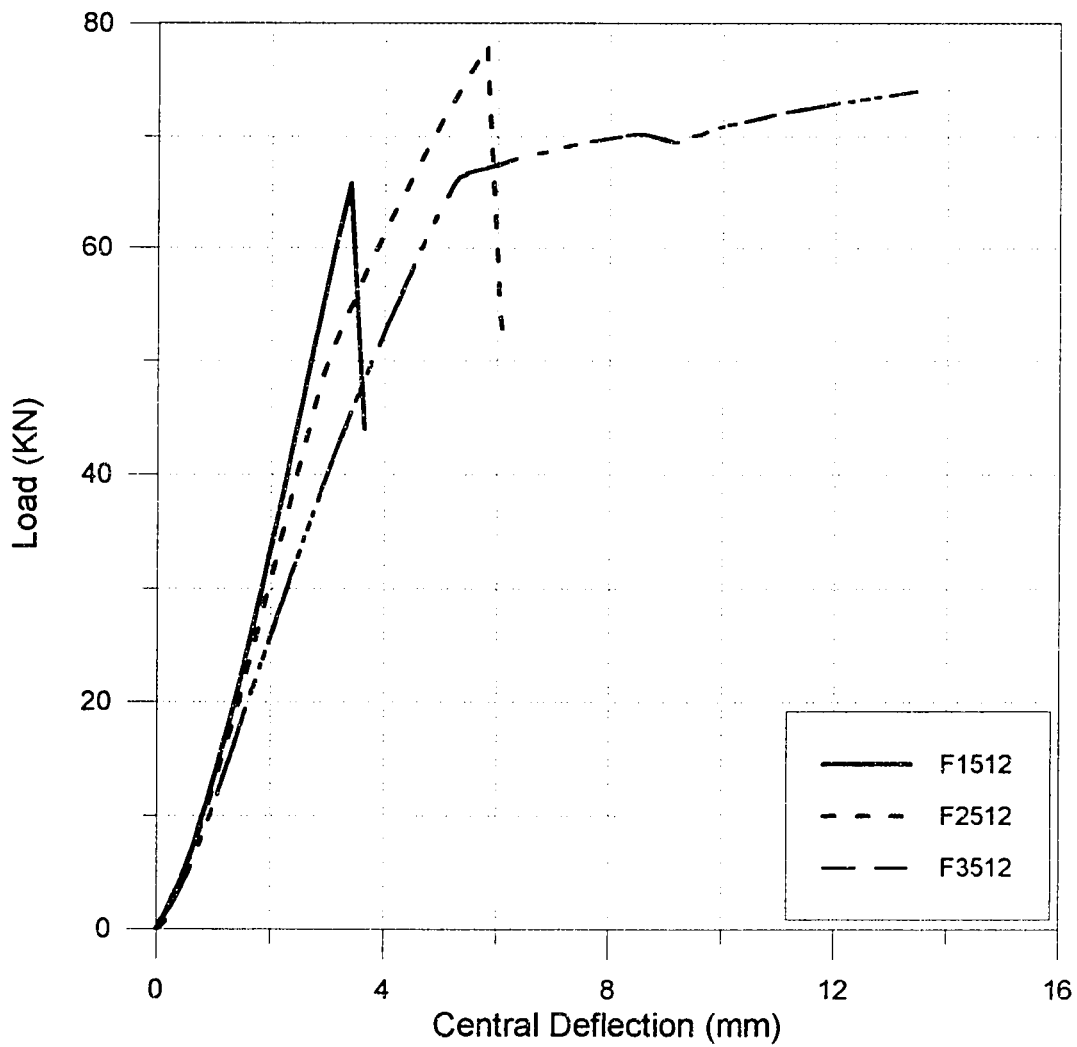


Figure 5.7: Load Vs Central Deflection for Beams repaired with 1100 mm long steel plates of thickness 1, 2, and 3 mm respectively on the soffit of beam having stirrups at 120 mm c/c each

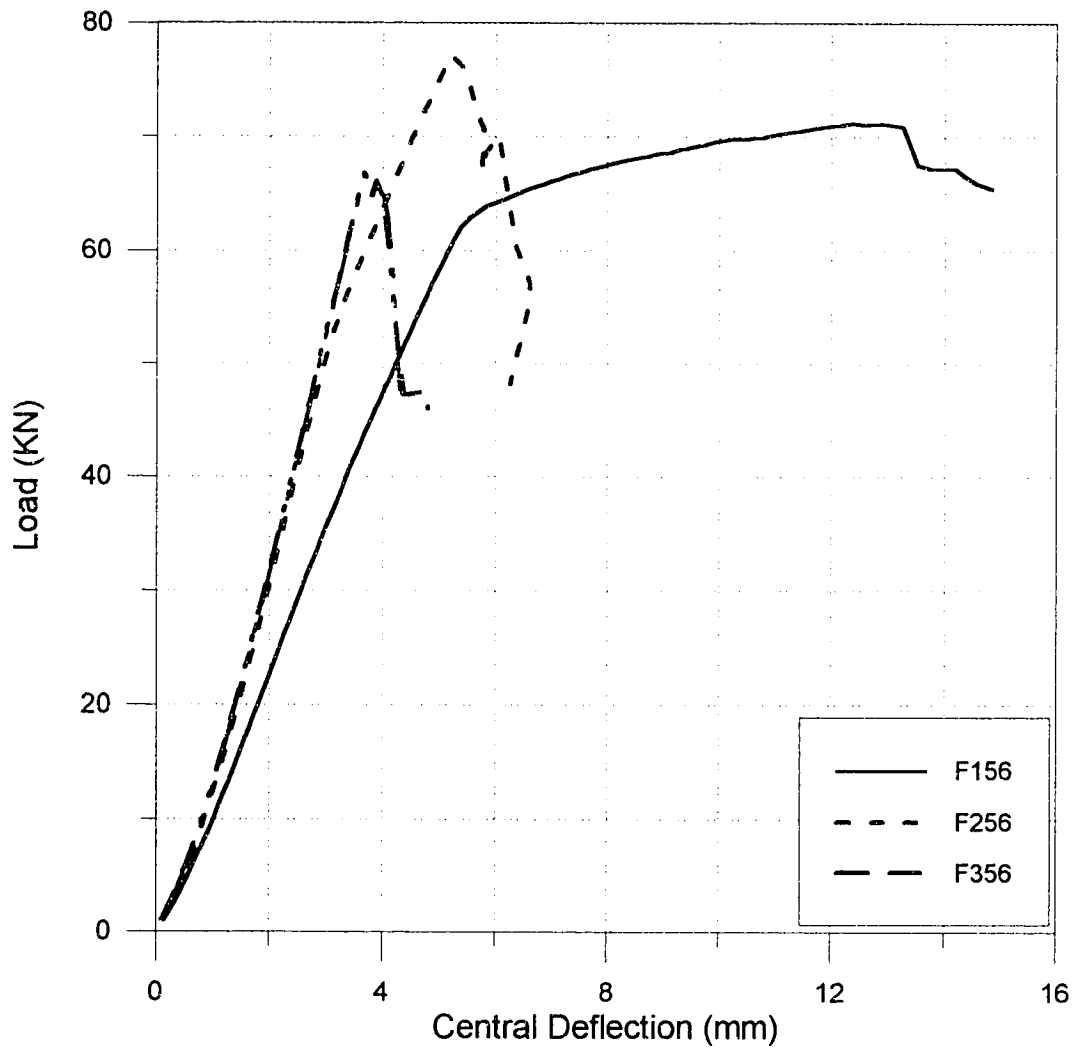


Figure 5.8: Load Vs Central Deflection for Beams repaired with 1100 mm long steel plates of thickness 1, 2, and 3 mm respectively on the soffit of beam having stirrups at 60 mm c/c each

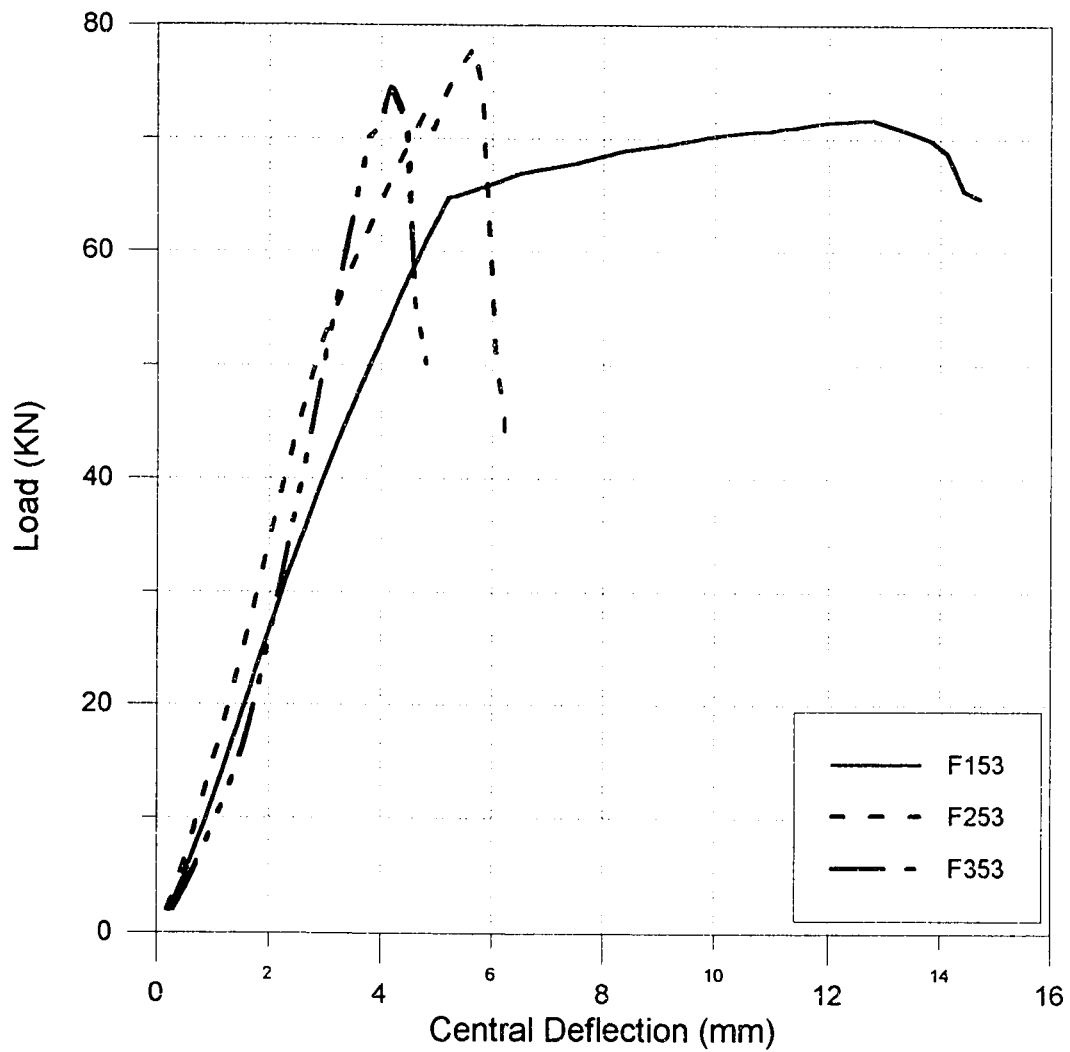


Figure 5.9: Load Vs Central Deflection for Beams repaired with 1100 mm long steel plates of thickness 1, 2, and 3 mm respectively on the soffit of beam having stirrups at 30 mm c/c each

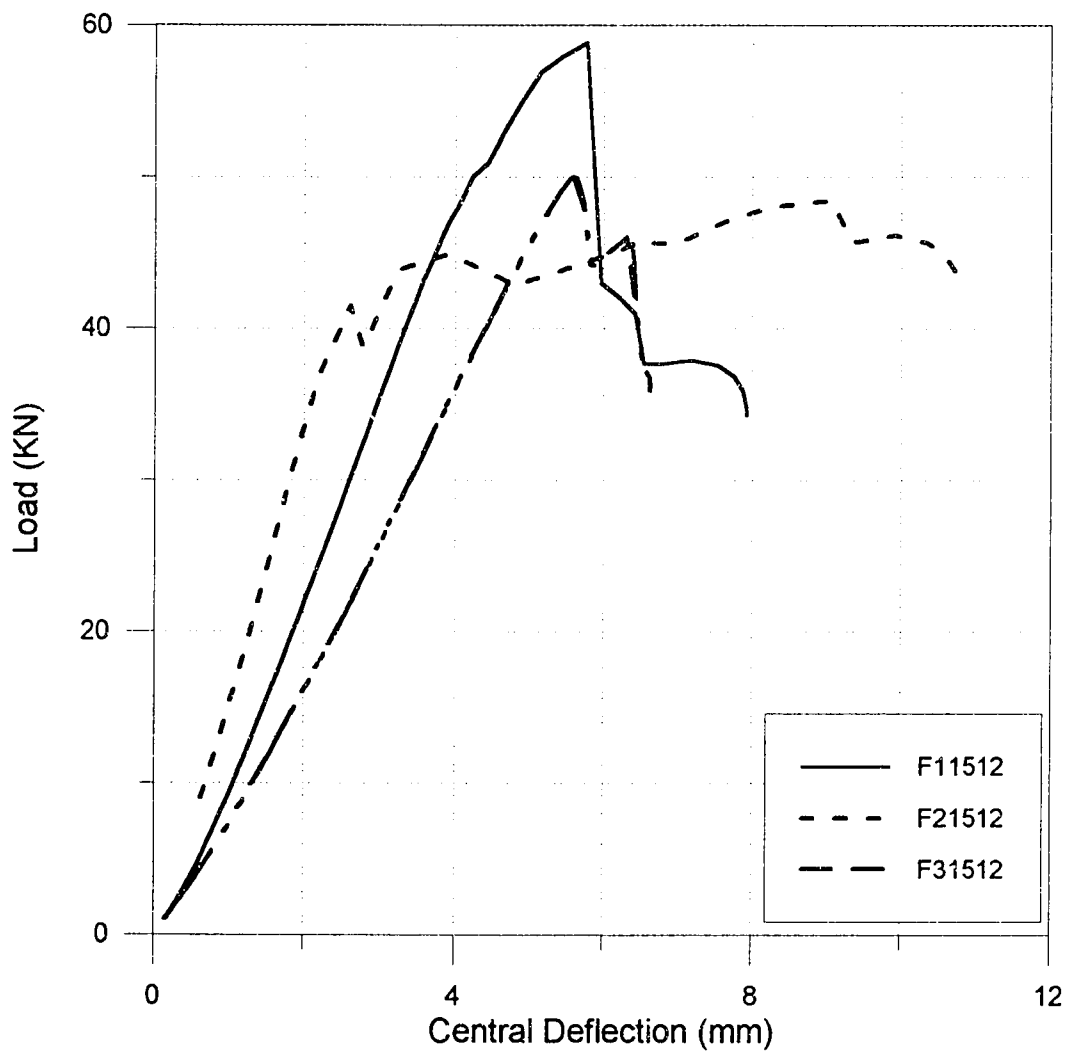


Figure 5.10: Load Vs Central Deflection for Beams repaired with 900 mm long steel plates of thickness 1, 2, and 3 mm respectively on the soffit of beam having stirrups at 120 mm c/c each

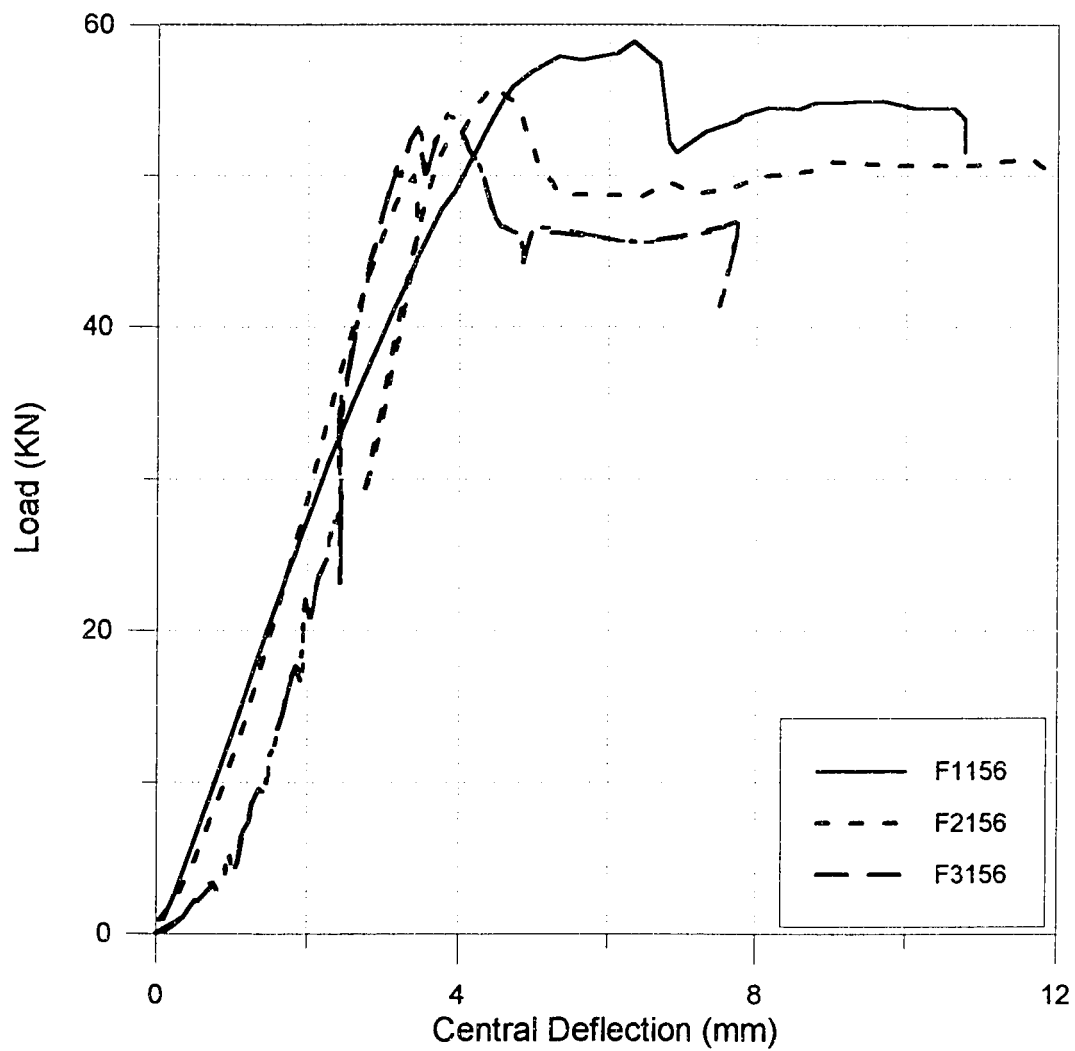


Figure 5.11: Load Vs Central Deflection for Beams repaired with 900 mm long steel plates of thickness 1, 2, and 3 mm respectively on the soffit of beam having stirrups at 60 mm c/c each

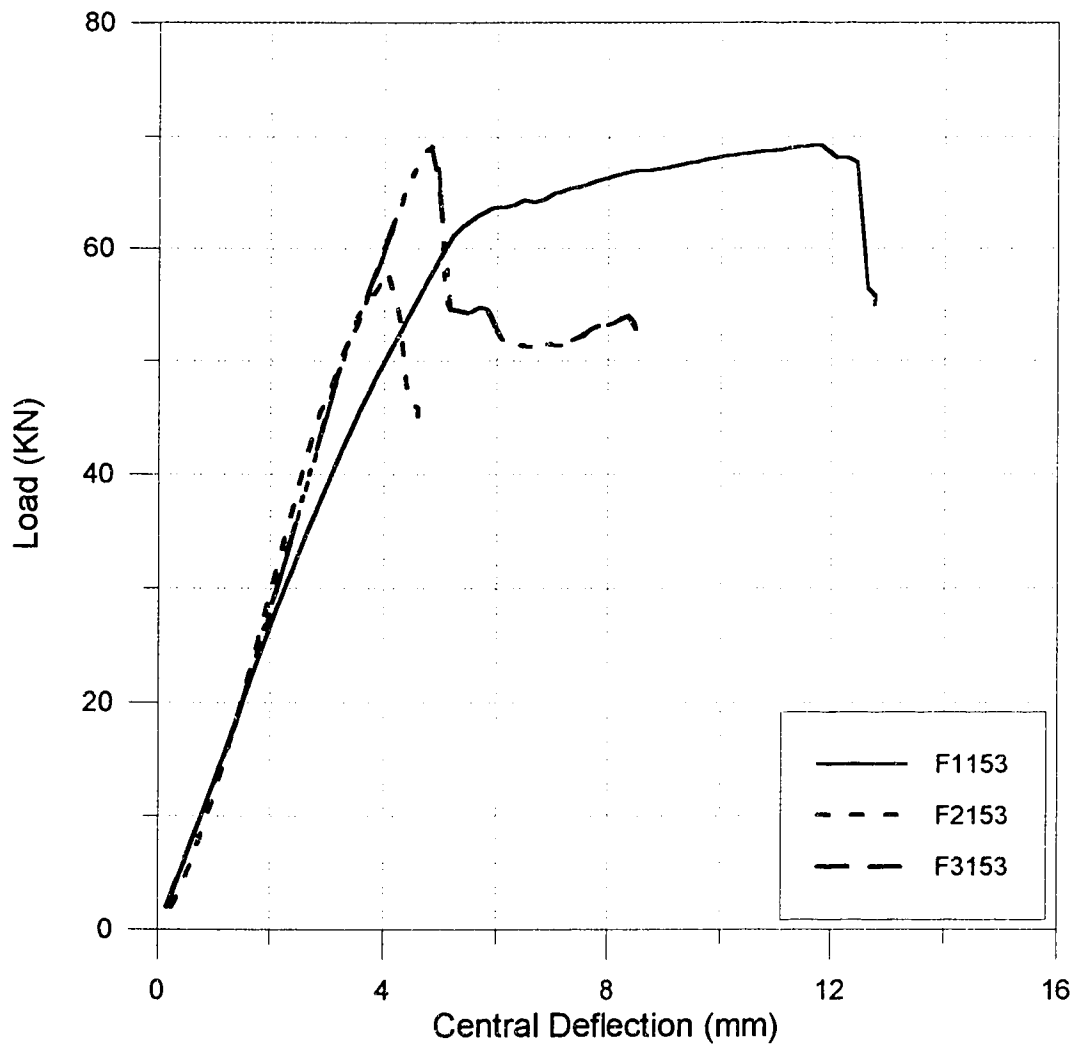


Figure 5.12: Load Vs Central Deflection for Beams repaired with 900 mm long steel plates of thickness 1, 2, and 3 mm respectively on the soffit of beam having stirrups at 30 mm c/c each

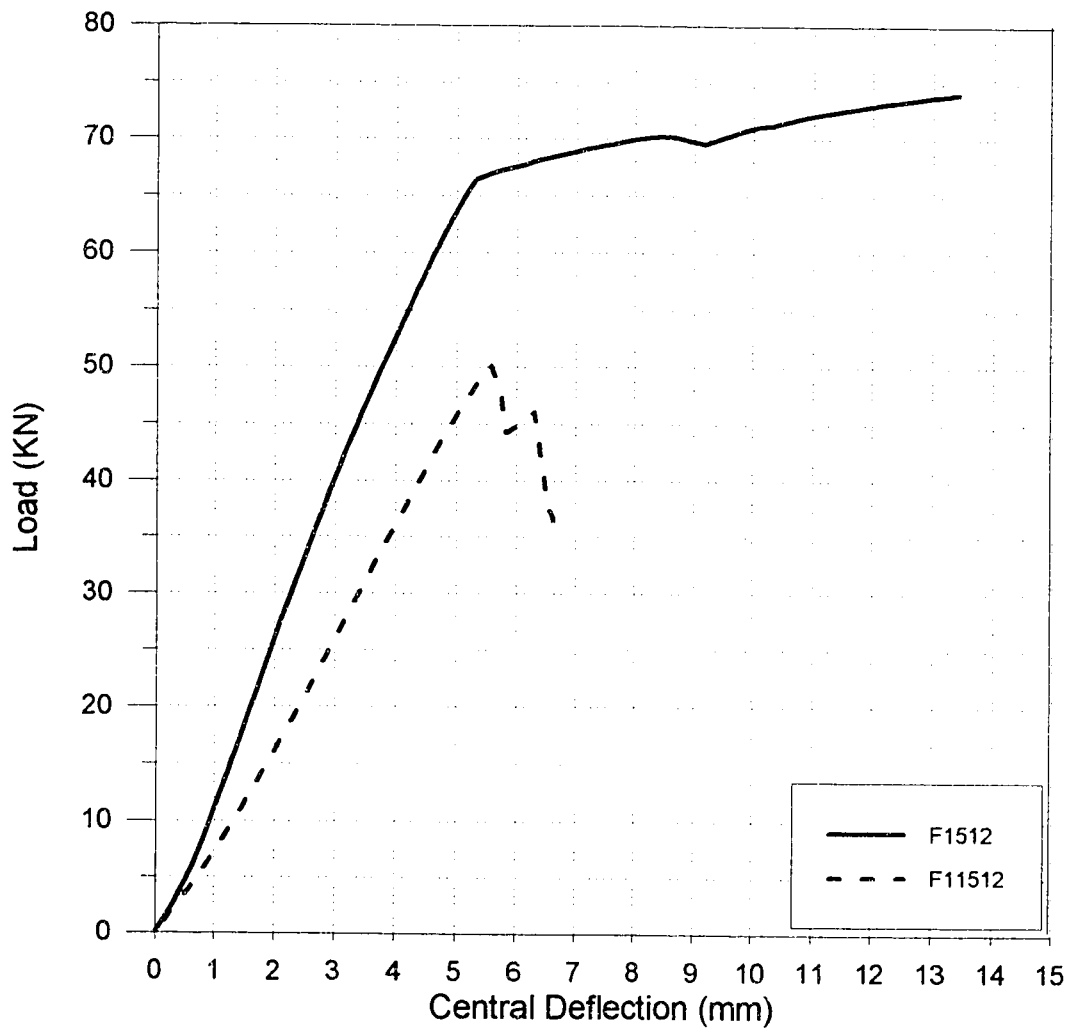


Figure 5.13: Load Vs Central Deflection for Beams repaired with 900 mm and 1100 mm long steel plates of 1 mm thickness on the soffit of beam having stirrups at 120 mm c/c

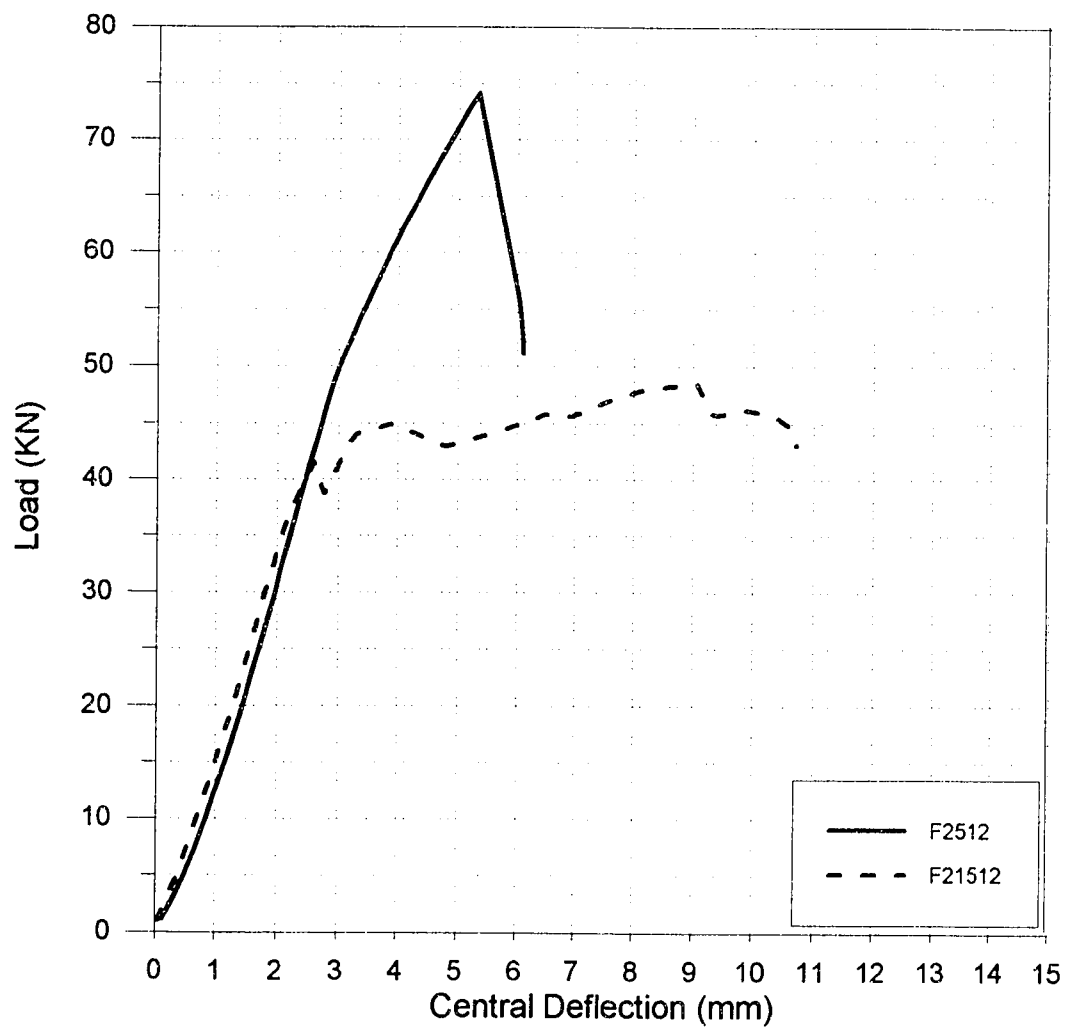


Figure 5.14: Load Vs Central Deflection for Beams repaired with 900 mm and 1100 mm long steel plates of 2 mm thickness on the soft of beam having stirrups at 120 mm c/c

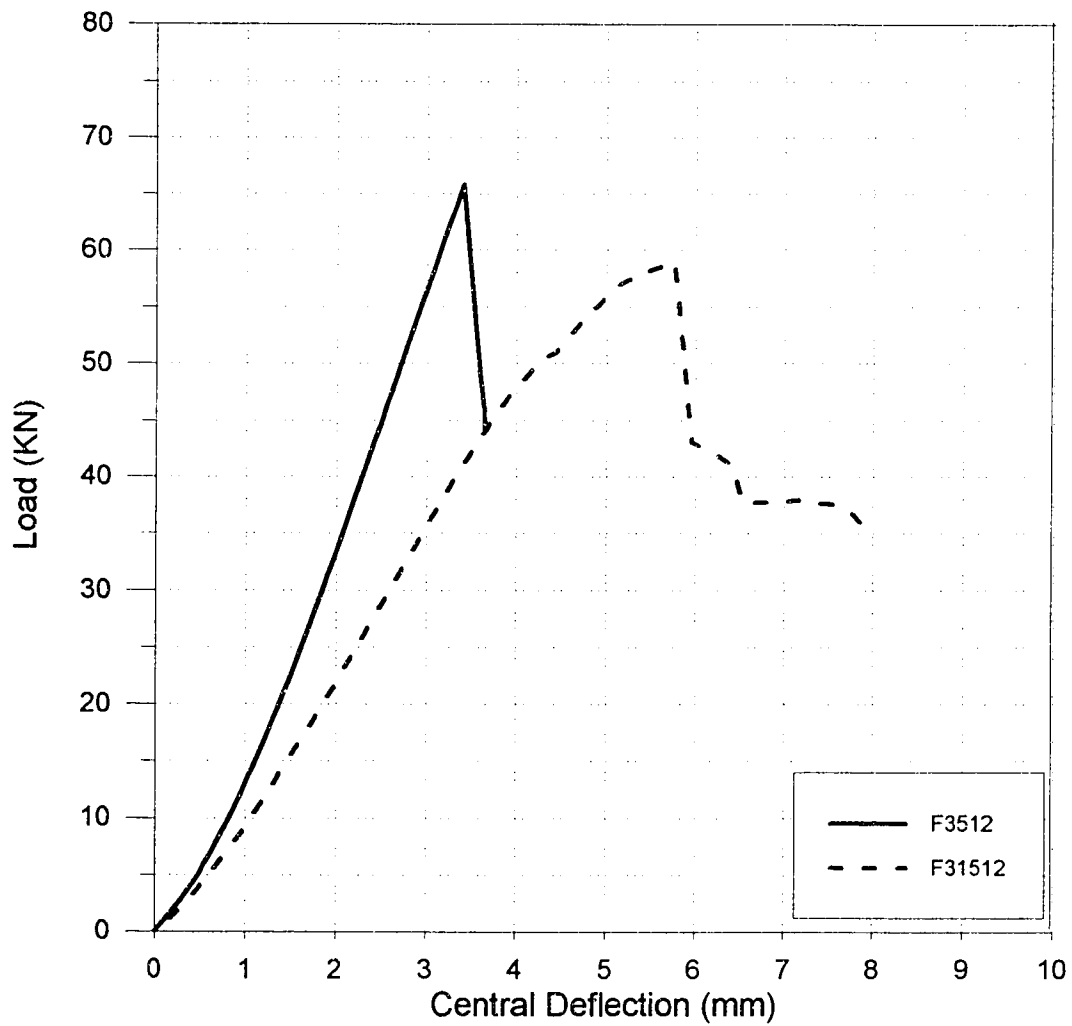


Figure 5.15: Load Vs Central Deflection for Beams repaired with 900 mm and 1100 mm long steel plates of 3 mm thickness on the soffit of beam having stirrups at 120 mm c/c

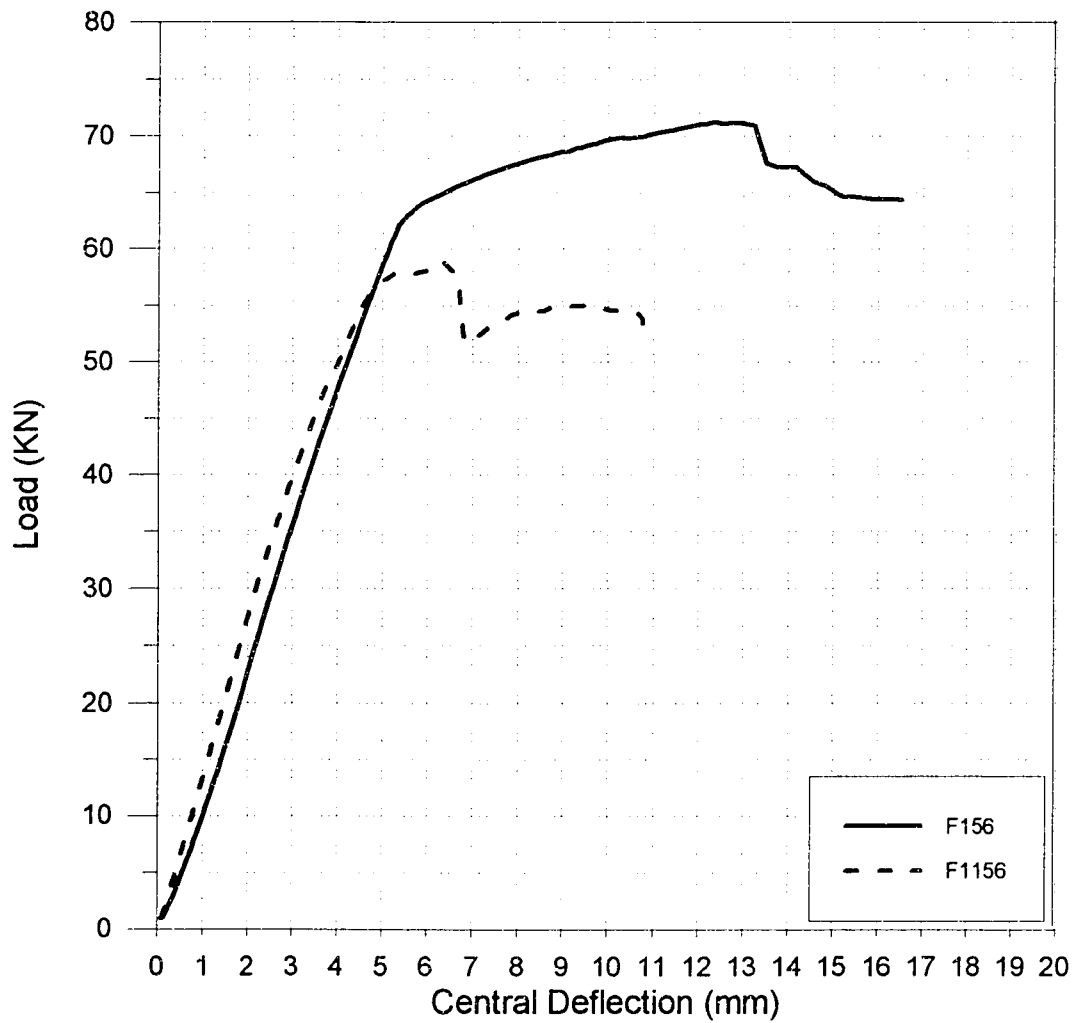


Figure 5.16: Load Vs Central Deflection for Beams repaired with 900 mm and 1100 mm long steel plates of 1 mm thickness on the soffit of beam having stirrups at 60 mm c/c

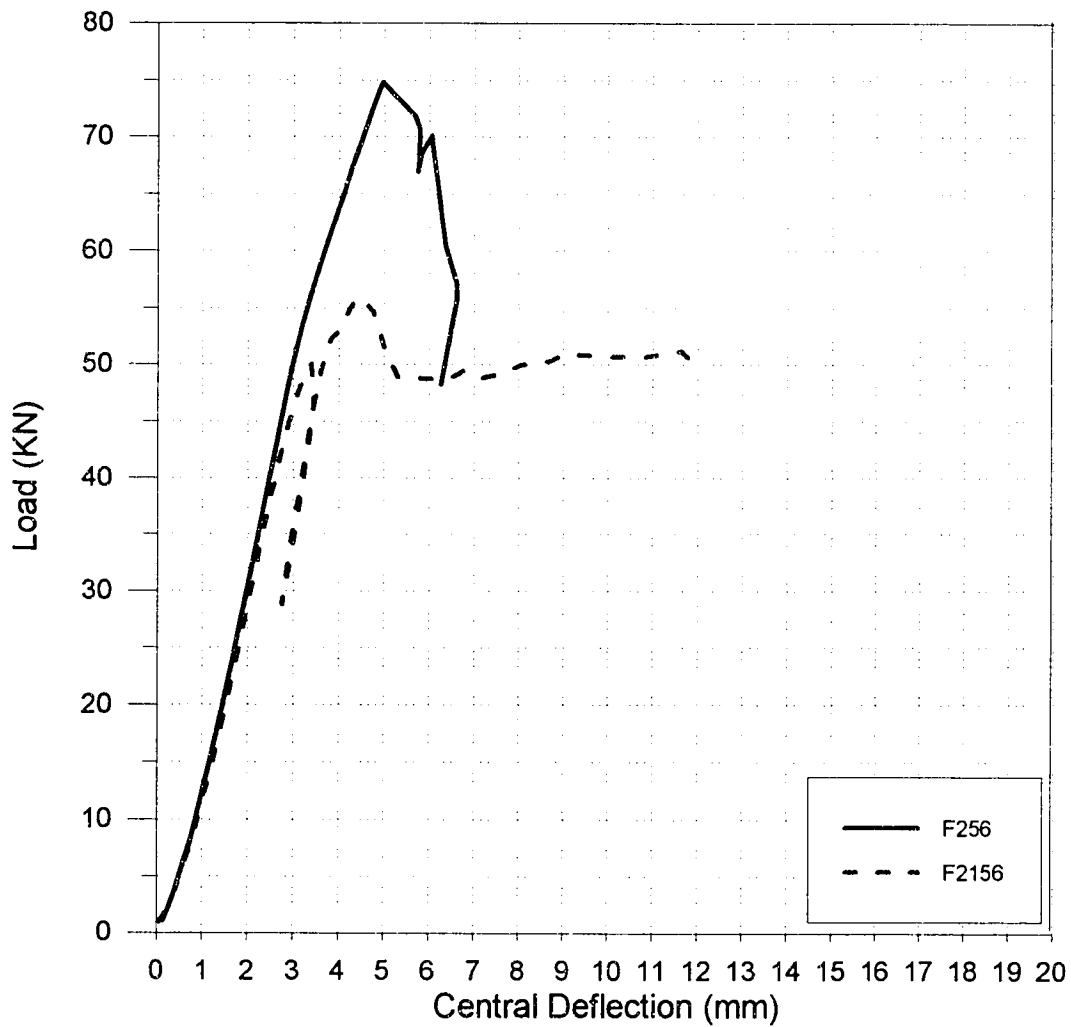


Figure 5.17: .Load Vs Central Deflection for Beams repaired with 900 mm and 1100 mm long steel plates of 2 mm thickness on the soffit of beam having stirrups at 60 mm c/c

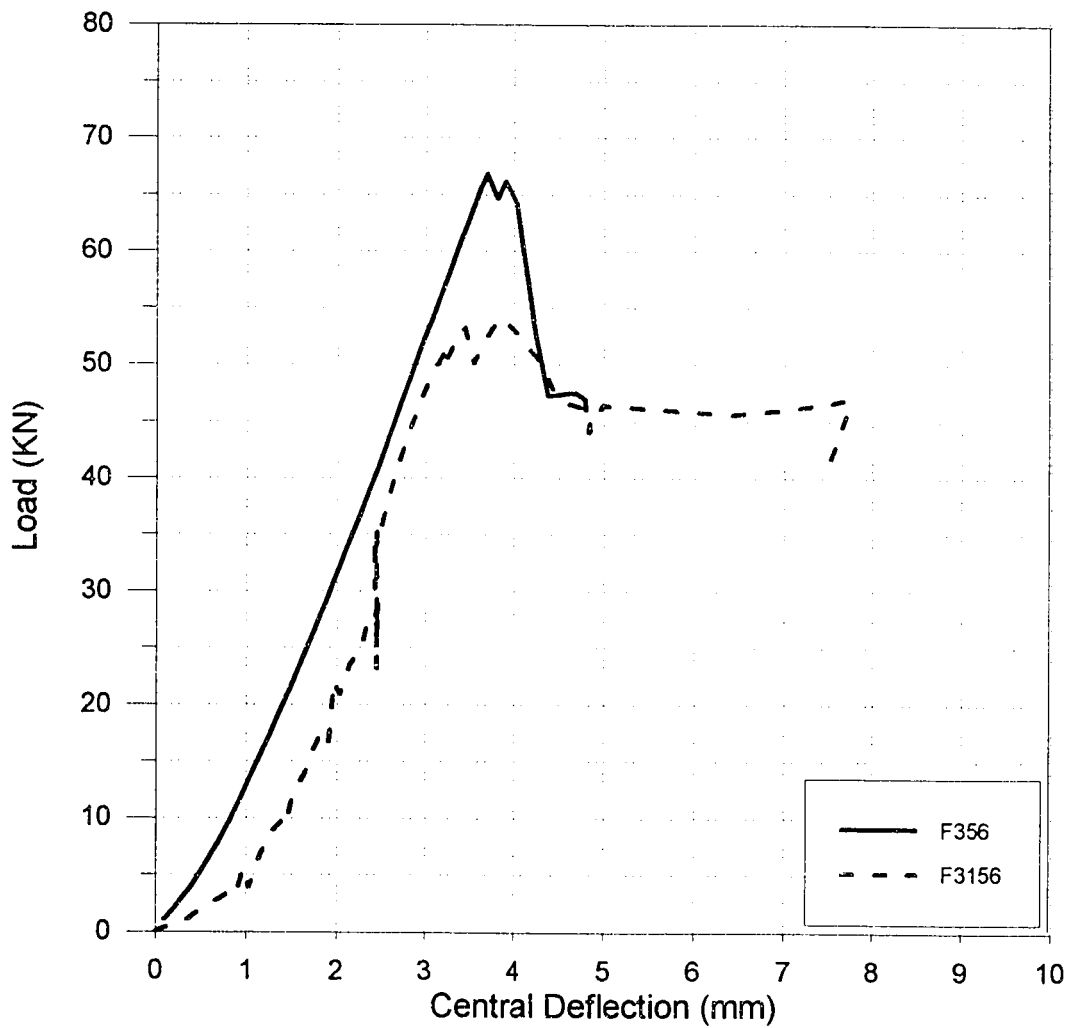


Figure 5.18: Load Vs Central Deflection for Beams repaired with 900 mm and 1100 mm long steel plates of 3 mm thickness on the soffit of beam having stirrups at 60 mm c/c

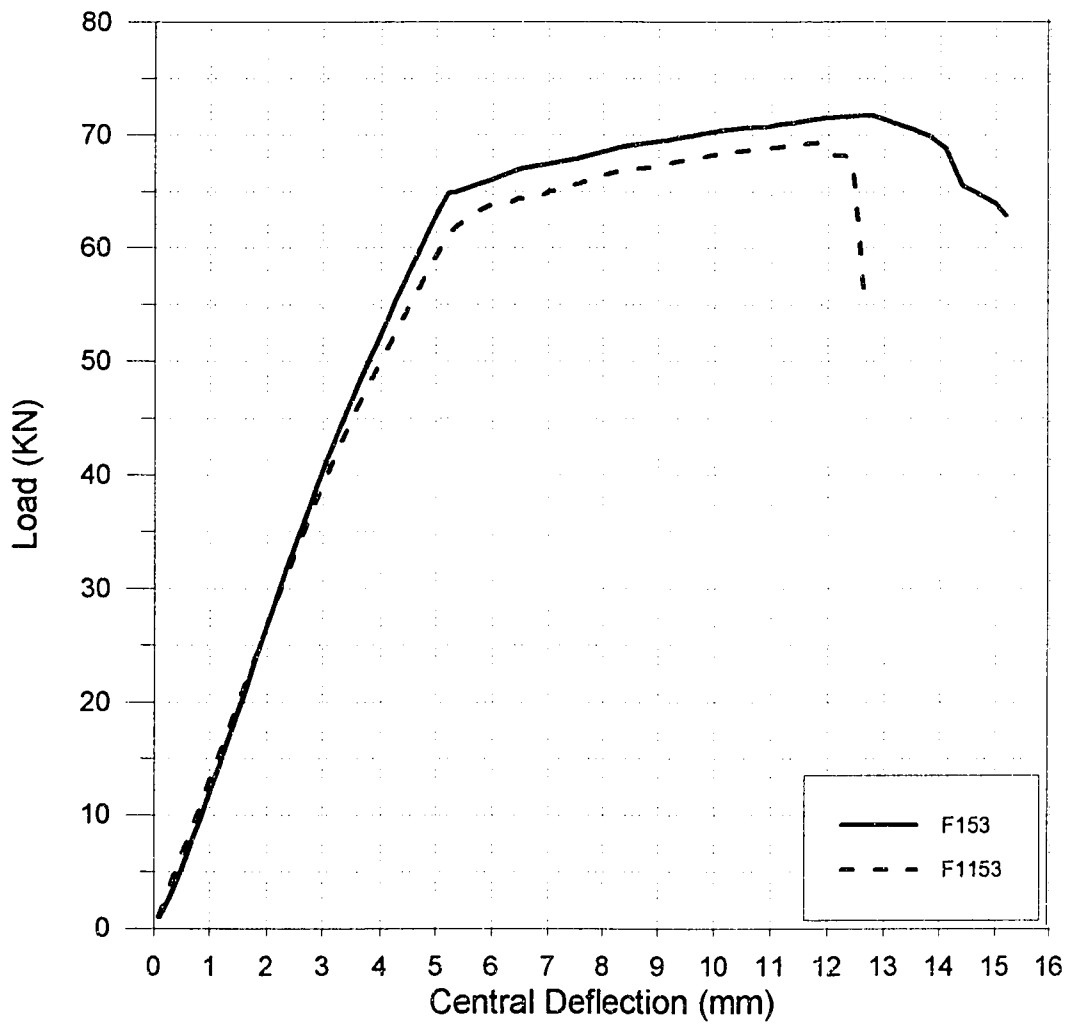


Figure 5.19: Load Vs Central Deflection for Beams repaired with 900 mm and 1100 mm long steel plates of 1 mm thickness on the soffit of beam having stirrups at 30 mm c/c

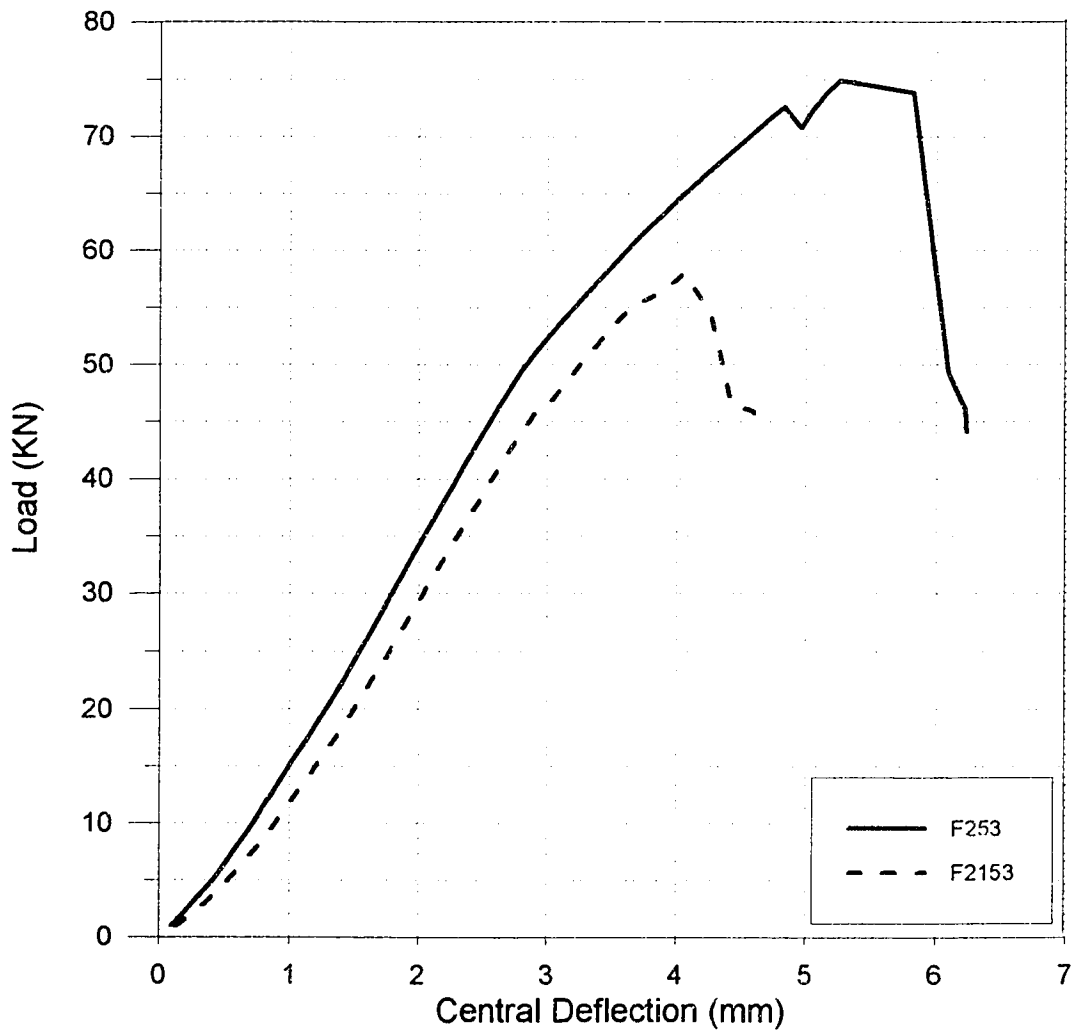


Figure 5.20: Load Vs Central Deflection for Beams repaired with 900 mm and 1100 mm long steel plates of 2 mm thickness on the soffit of beam having stirrups at 30 mm c/c

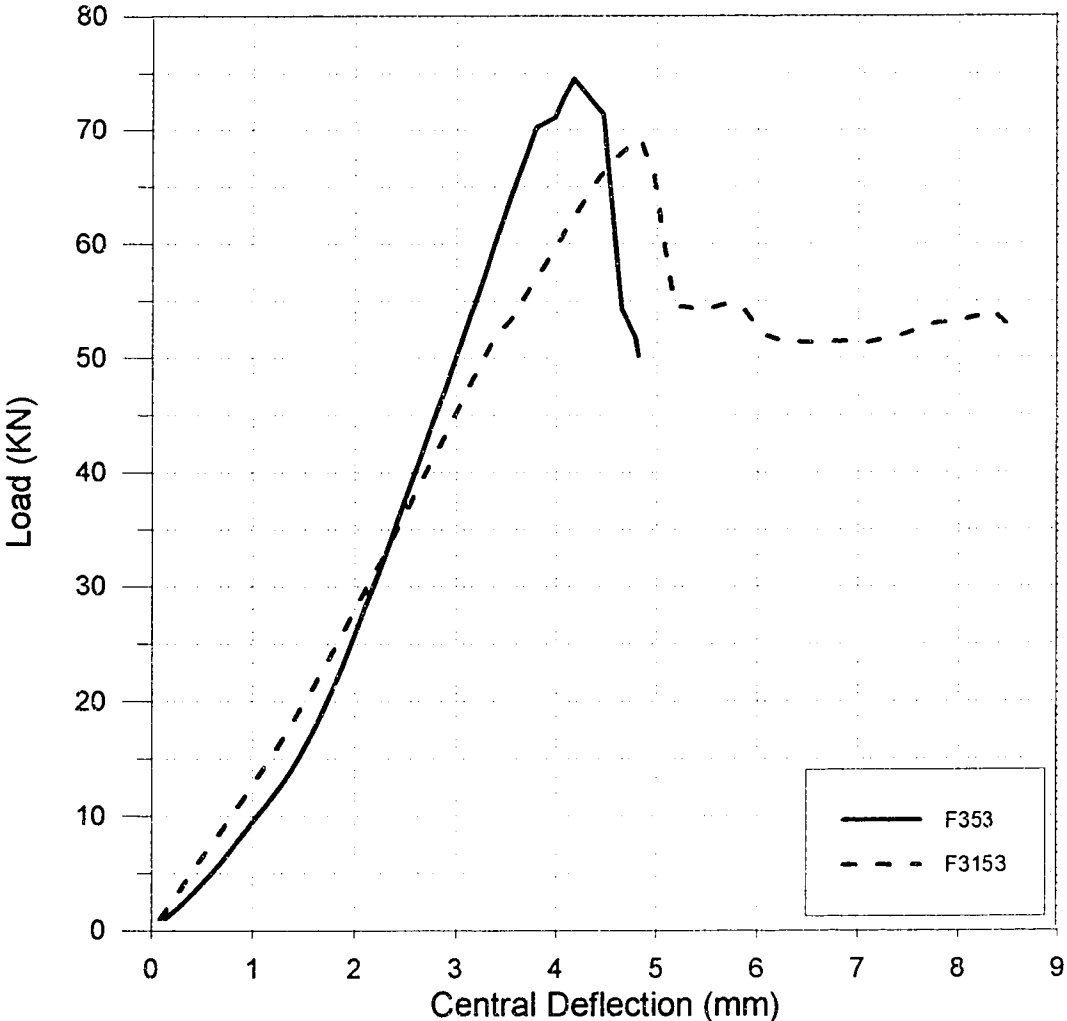


Figure 5.21: Load Vs Central Deflection for Beams repaired with 900 mm and 1100 mm long steel plates of 3 mm thickness on the soffit of beam having stirrups at 30 mm c/c

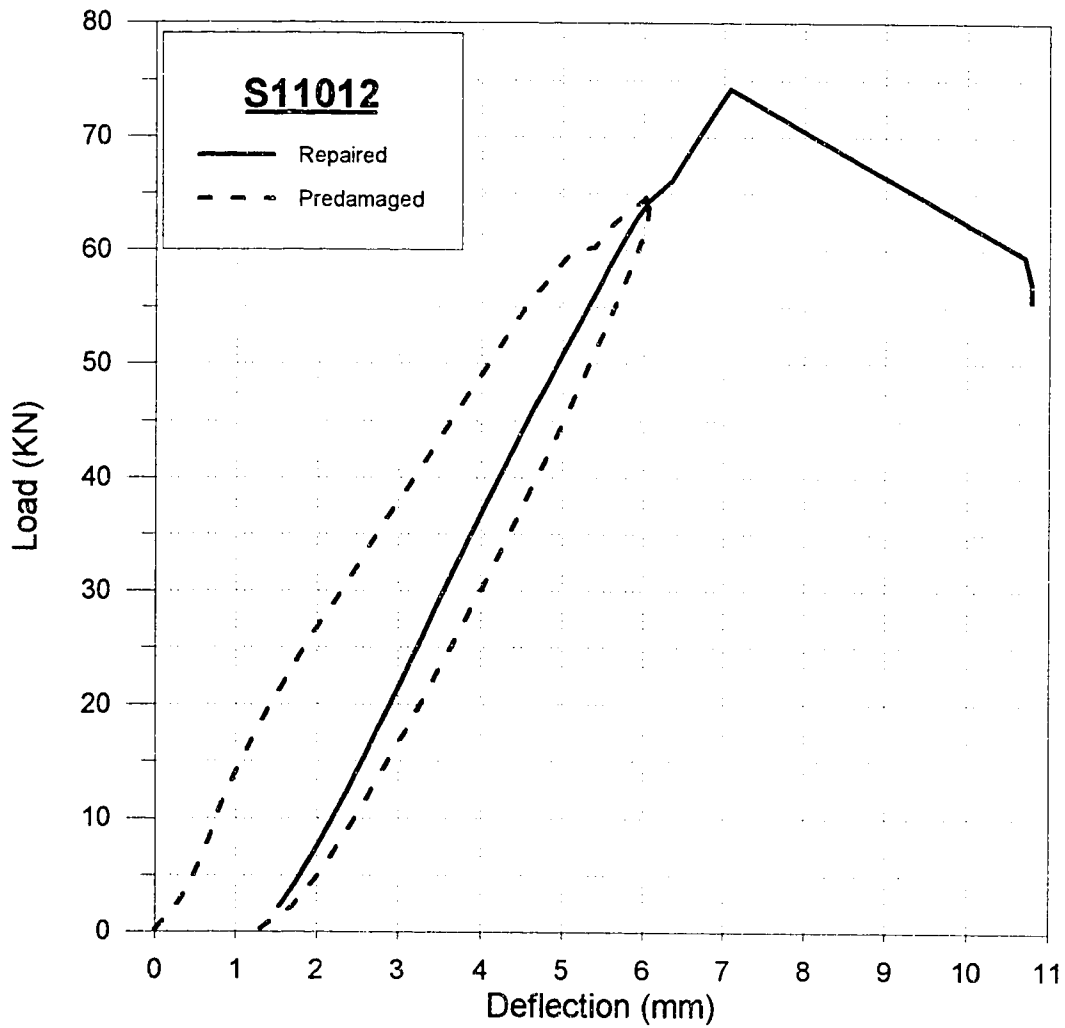


Figure 5.22: Load Vs Central Deflection for Beam (S11012) repaired with 1000 mm long steel plates of 1 mm thickness on the soffit of beam having stirrups at 120 mm c/c

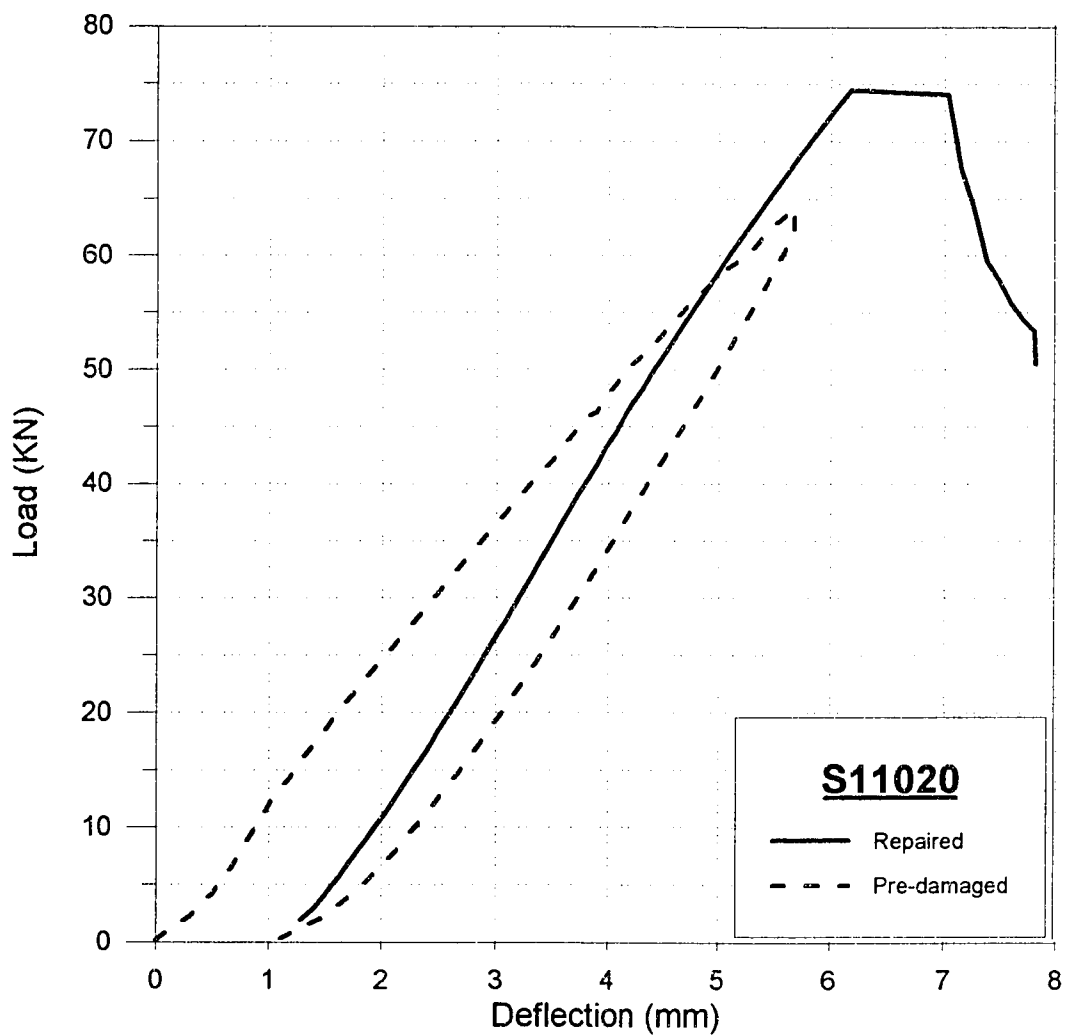


Figure 5.23: Load Vs Central Deflection for Beam (S11020) repaired with 1000 mm long steel plates of 1 mm thickness on the soffit of beam having stirrups at 200 mm c/c

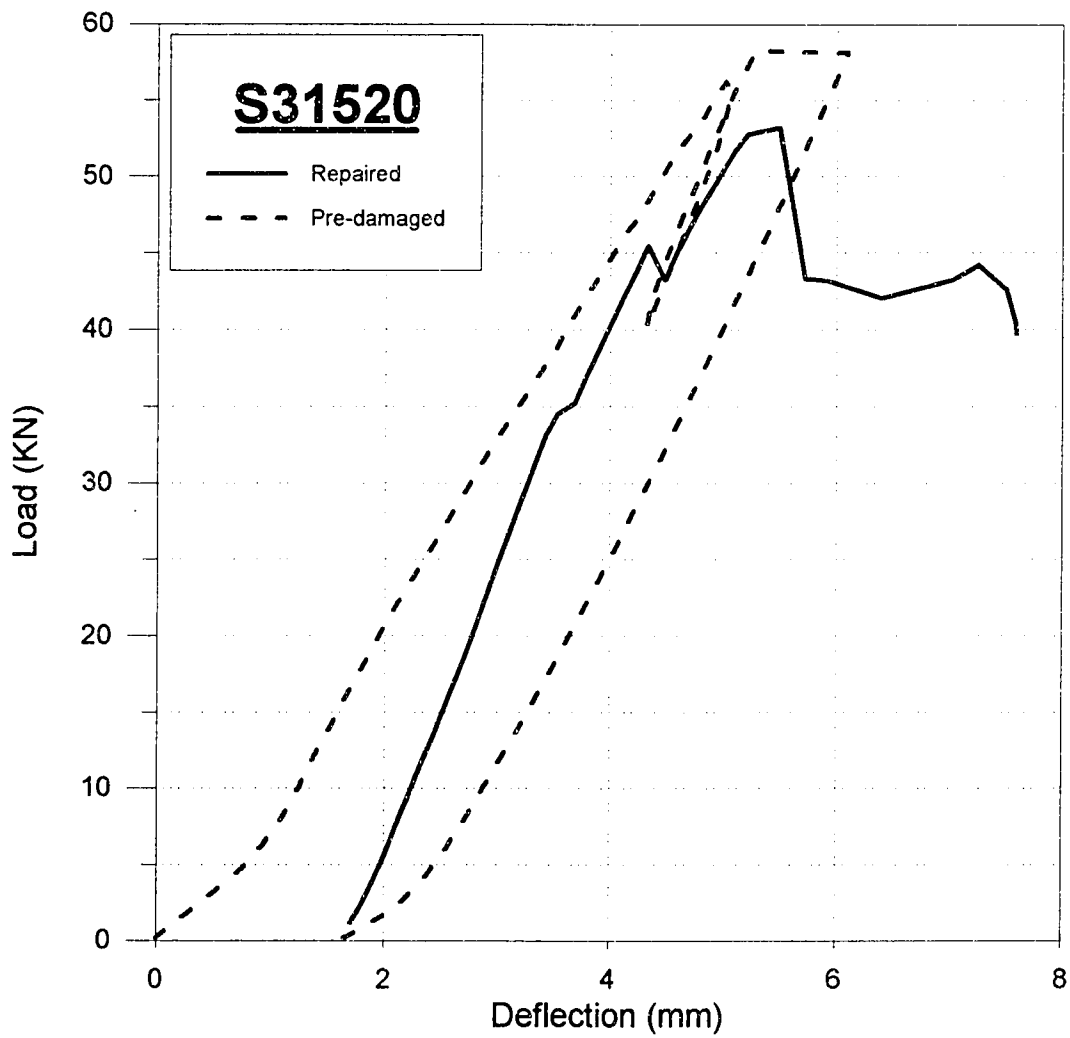


Figure 5.24: Load Vs Central Deflection for Beam (S31520) repaired with 900 mm long steel plates of 3 mm thickness on the soffit of beam having stirrups at 200 mm c/c

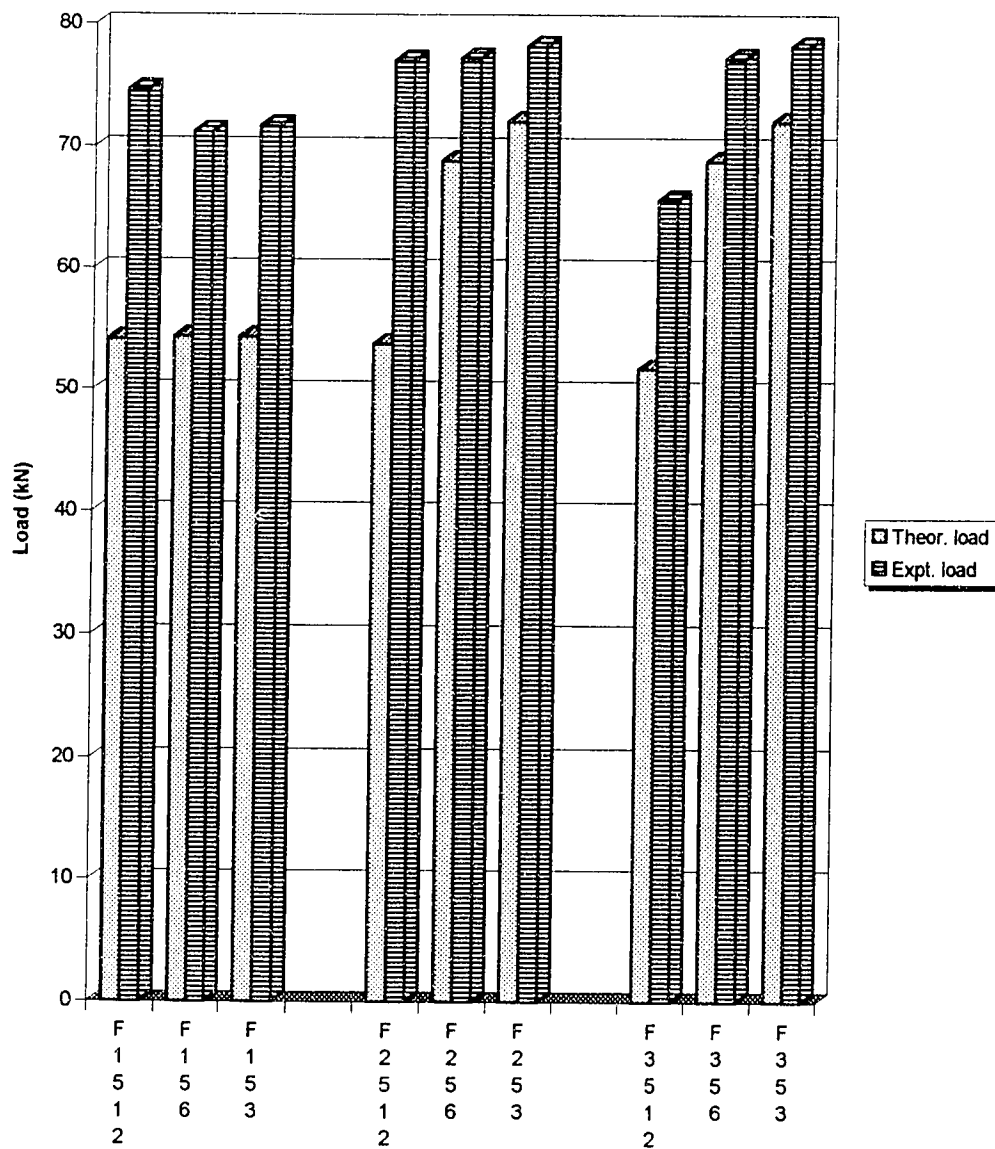


Figure 5.25: Effect of spacing of stirrups with the plate curtailed at 50 mm length (Theoretical and Experimental values)

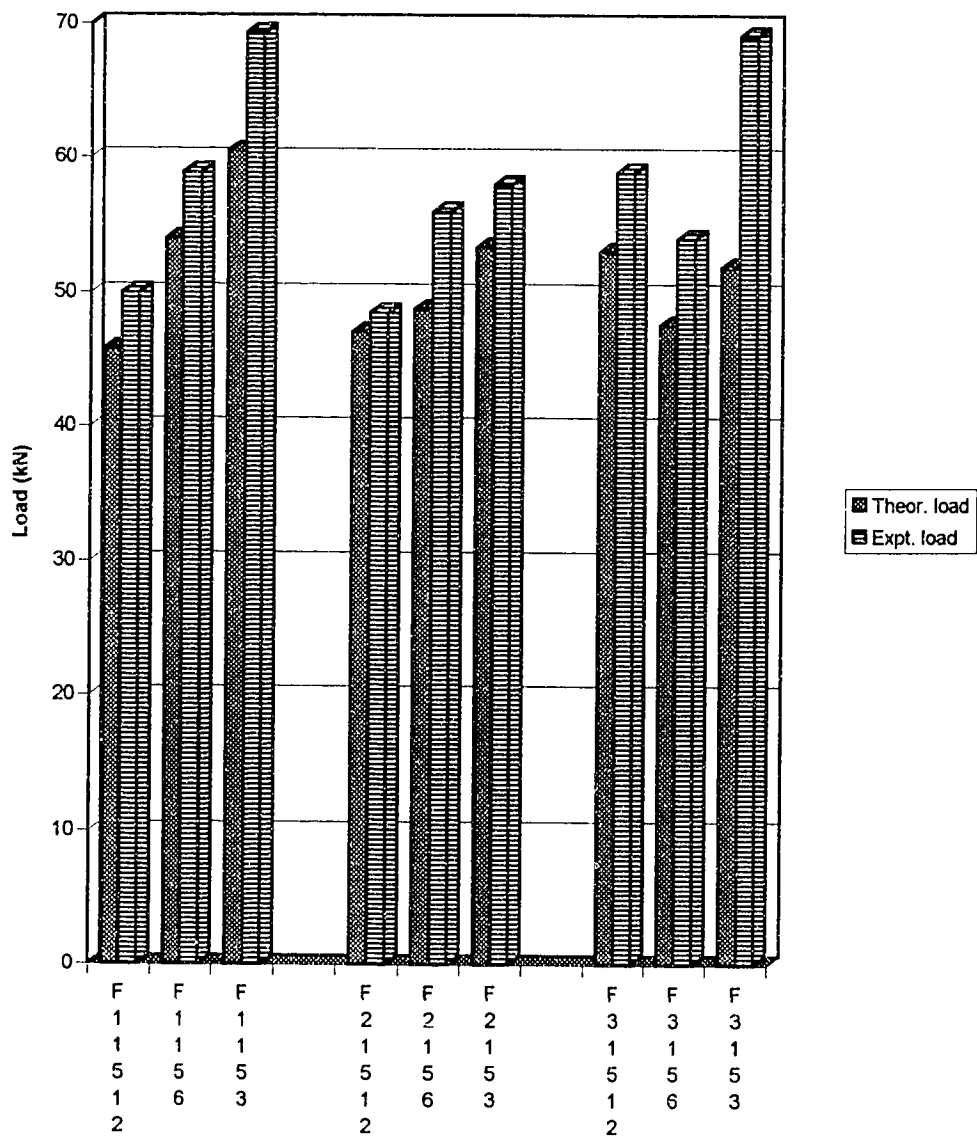


Figure 5.26: Effect of spacing of stirrups with the plate curtailed at 150 mm length (Theoretical and Experimental values)

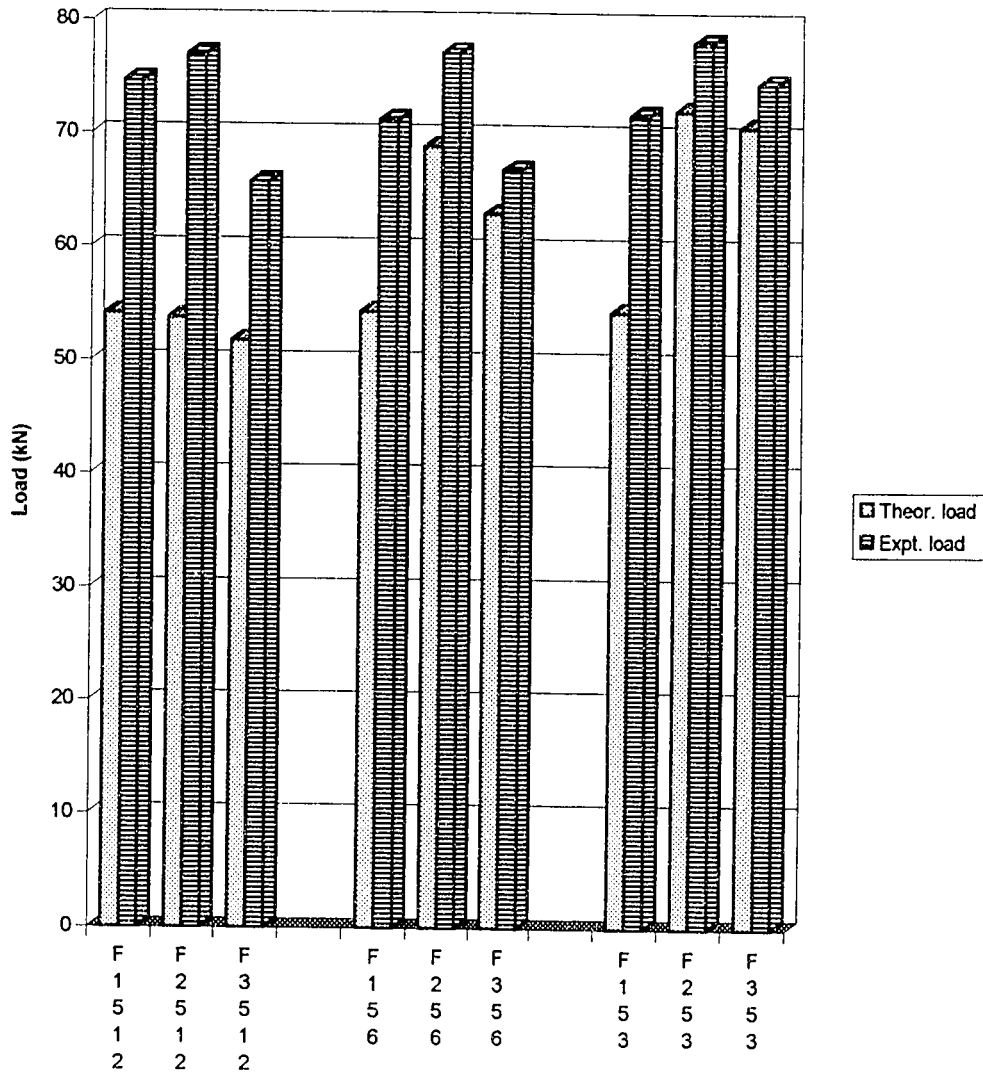


Figure 5.27: Effect of thickness of plate curtailed at 50 mm length (Theoretical and Experimental values)

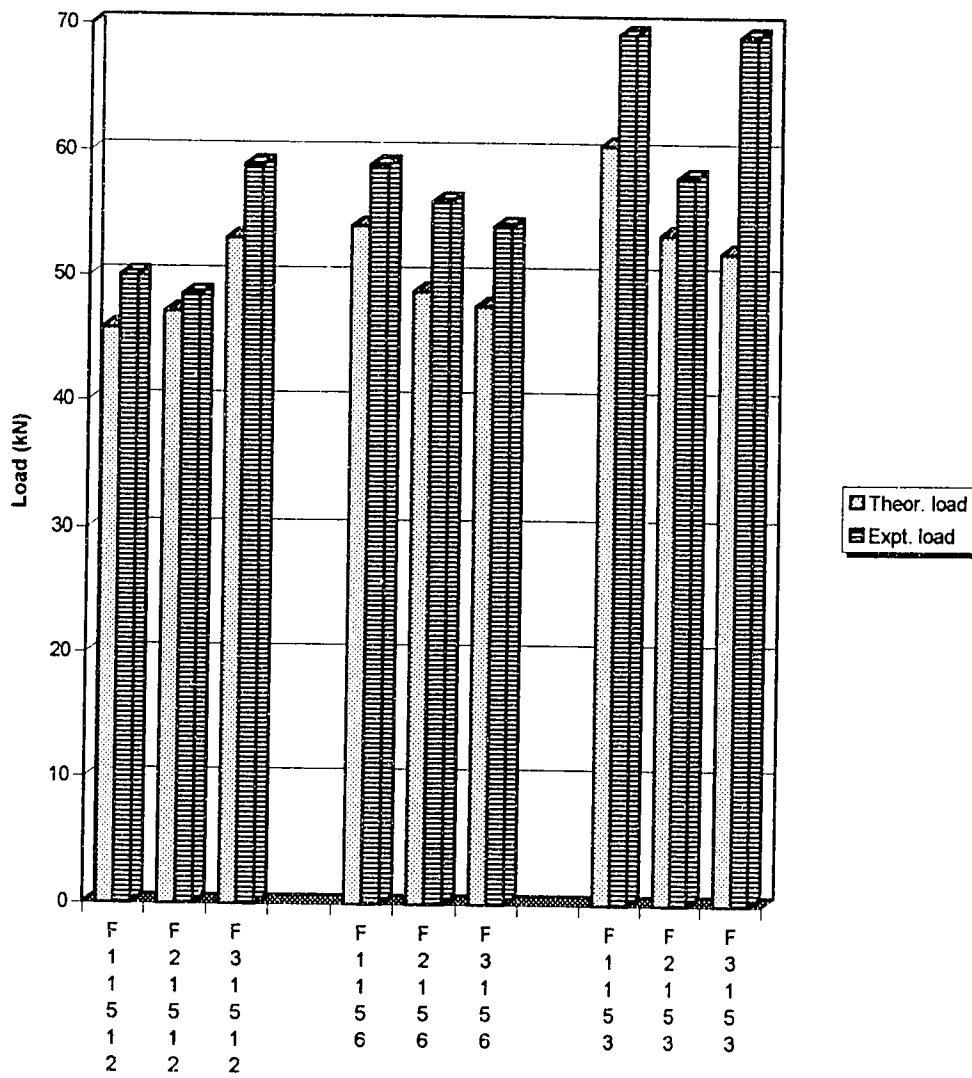


Figure 5.28: Effect of thickness of plate curtailed at 150 mm length (Theoretical and Experimental values)

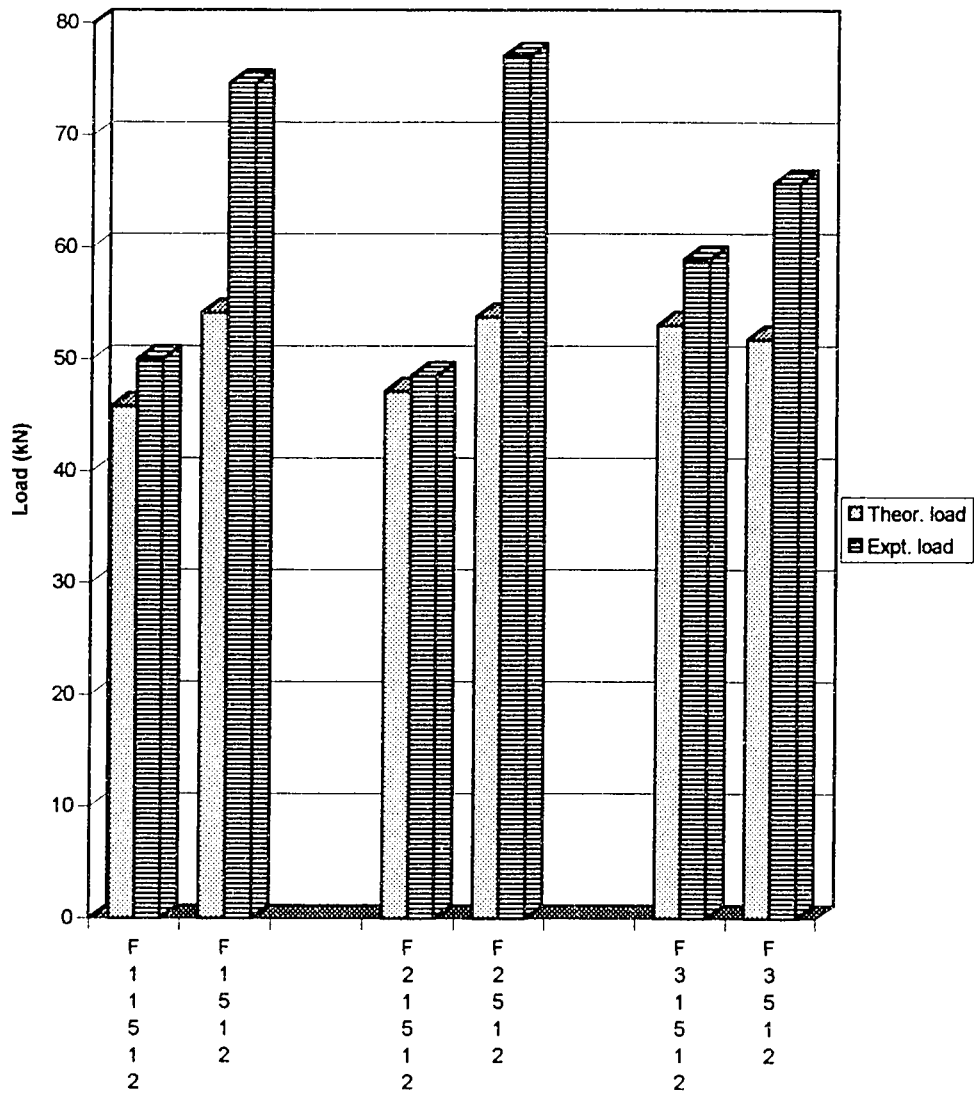


Figure 5.29: Effect of Plate curtailment with 120 mm c/c spacing of stirrups (Theoretical and Experimental values)

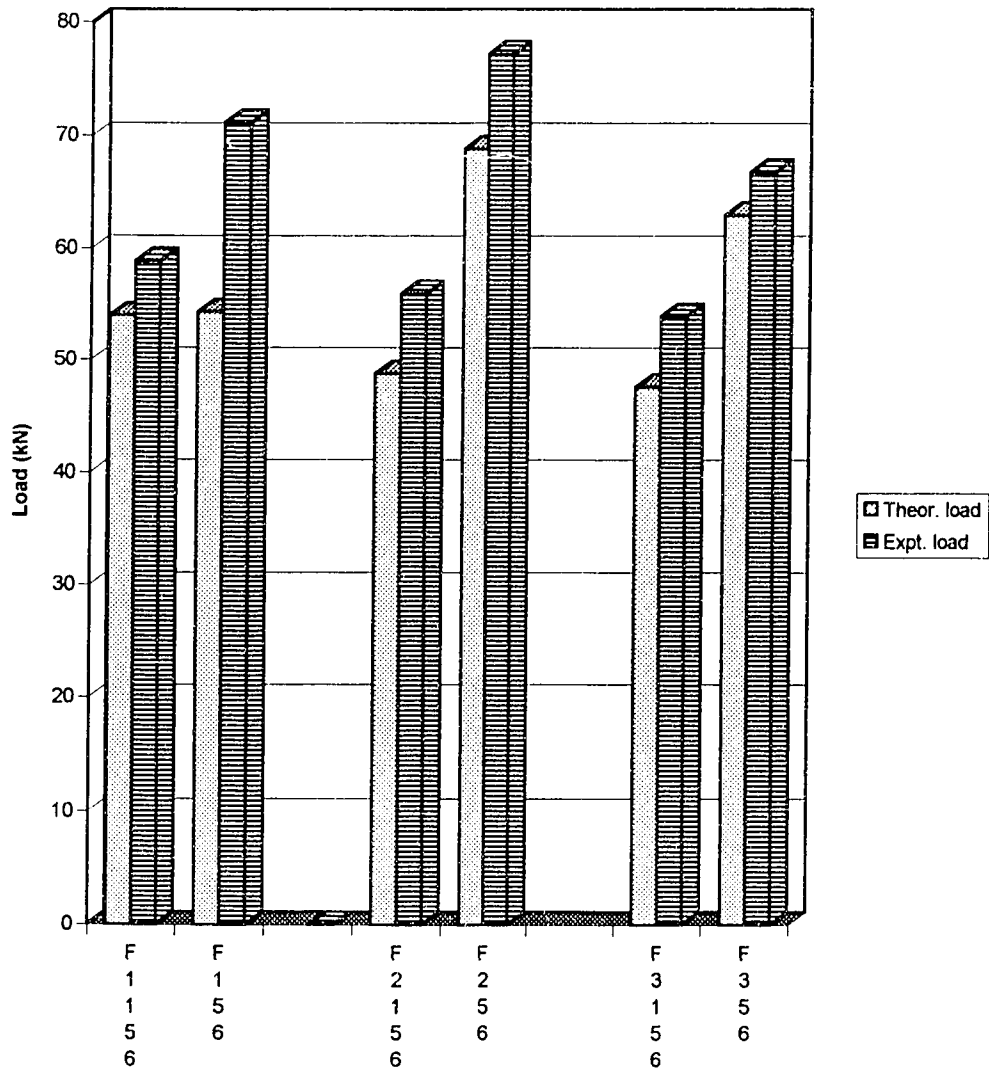


Figure 5.30: Effect of Plate curtailment with 60 mm c/c spacing of stirrups (Theoretical and Experimental values)

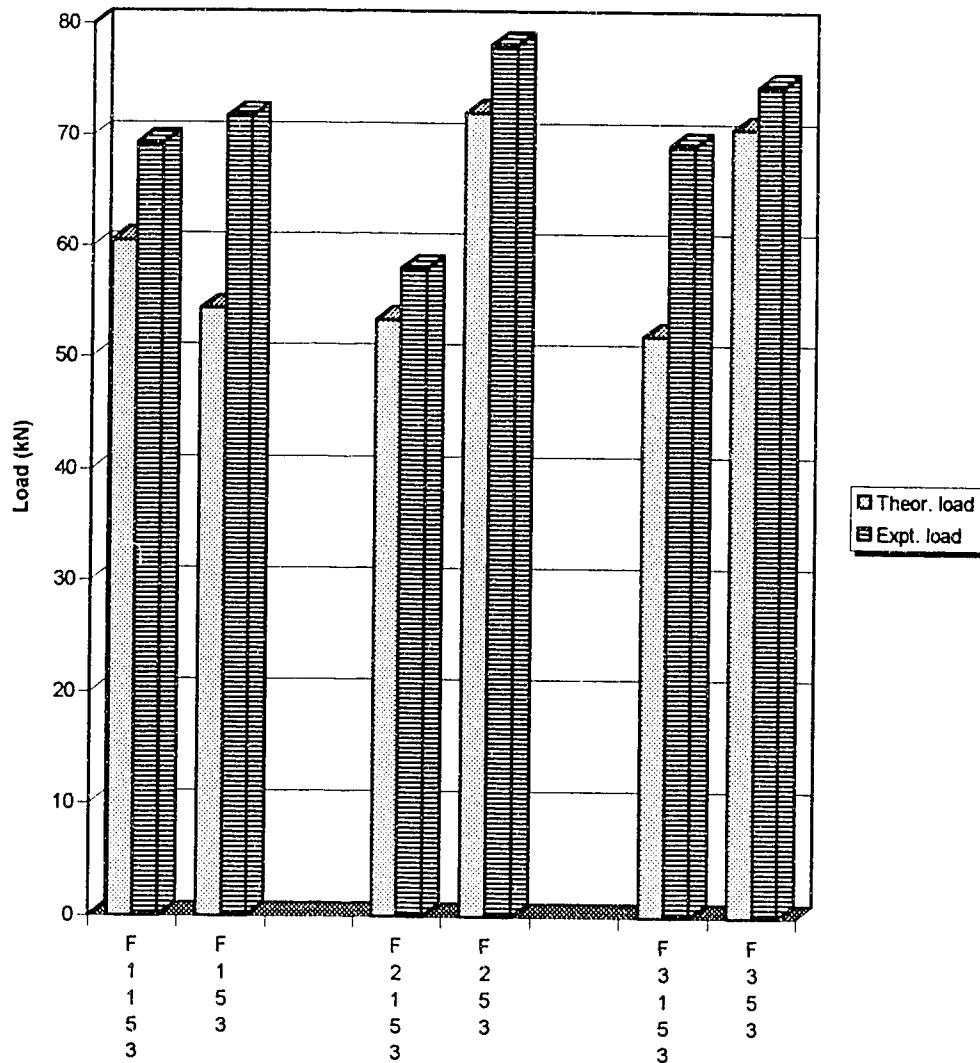


Figure 5.31: Effect of Plate curtailment with 30 mm c/c spacing of stirrups (Theoretical and Experimental values)

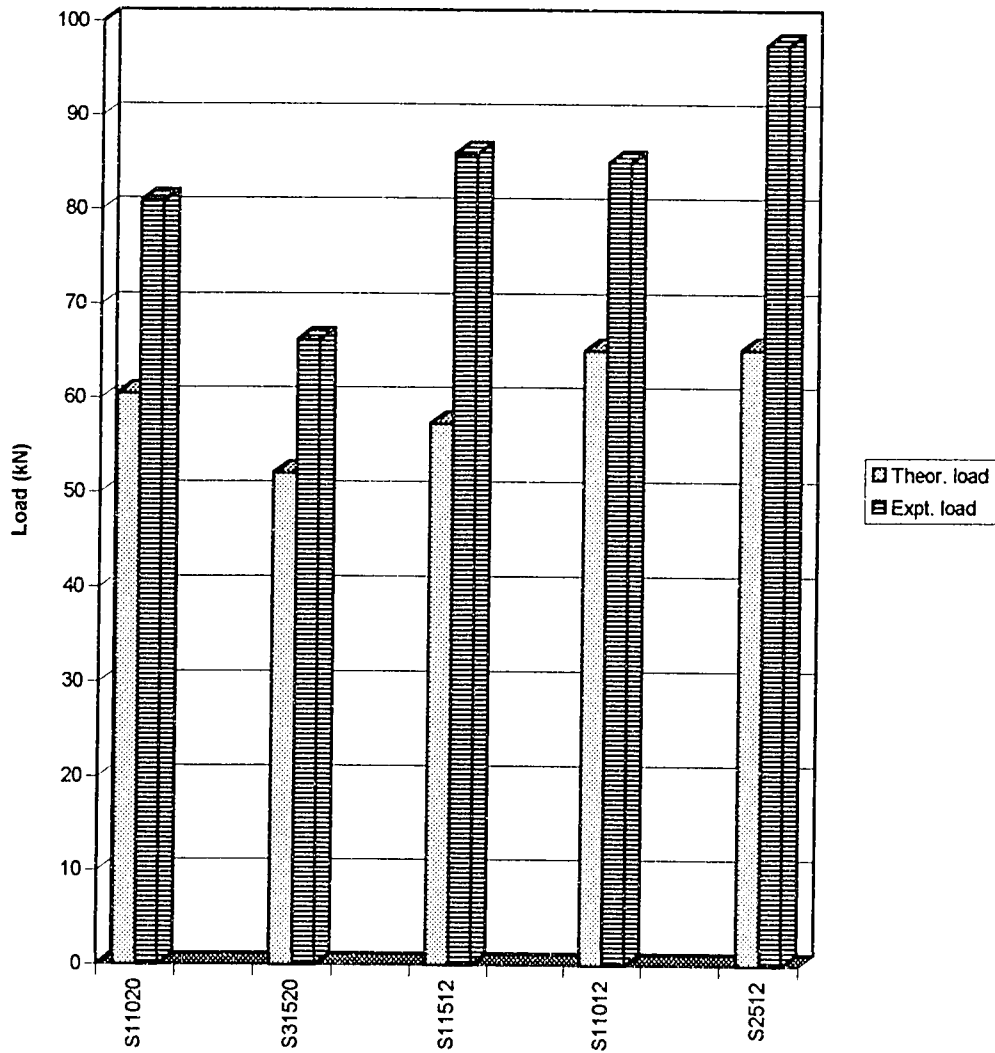


Figure 5.32: Theoretical and Experimental values for the Shear group beams based on KFUPM model [38]

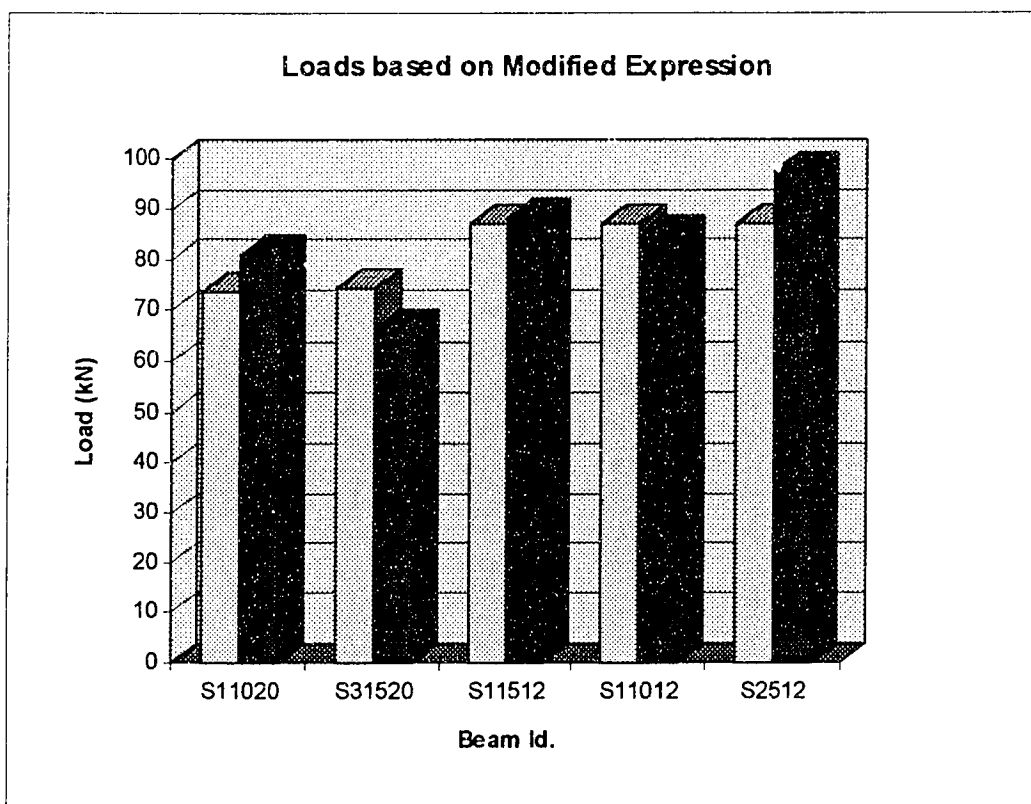


Figure 5.33: Theoretical and Experimental values for the Shear group beams based on modified ACI shear strength expression [Present Work]

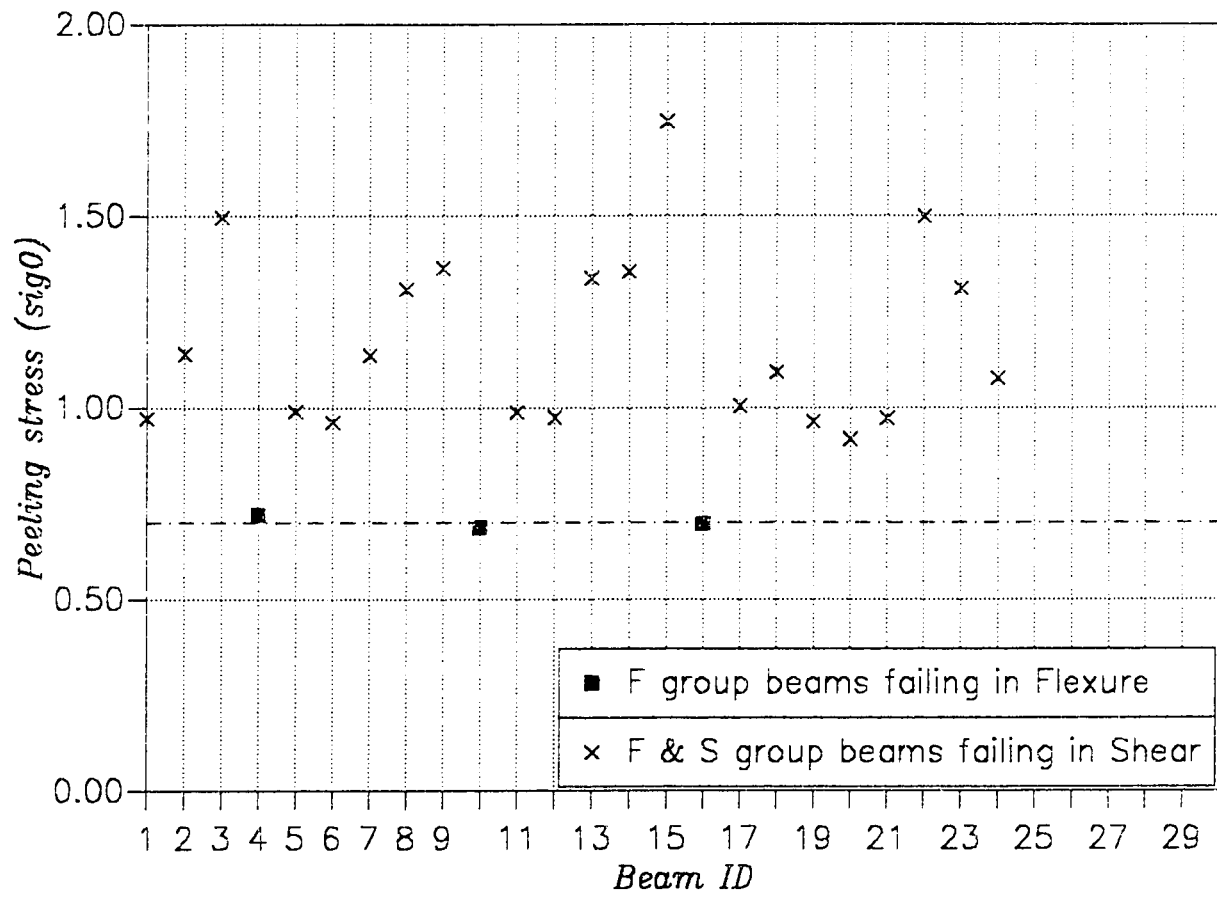


Figure 5.34: Peeling stress Vs Beam ID. based on Robert's [34] approach

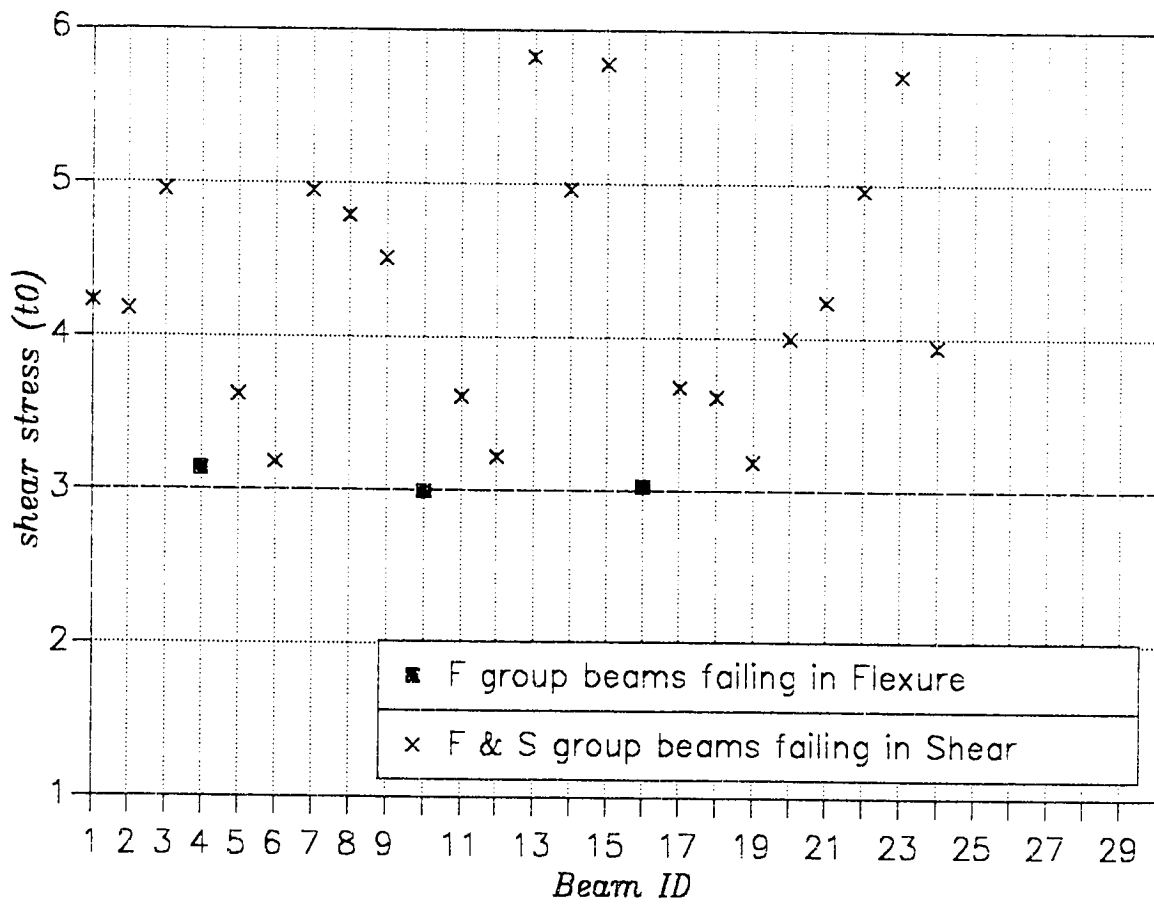


Figure 5.35: Shear stress Vs Beam ID. based on Robert's [34] approach

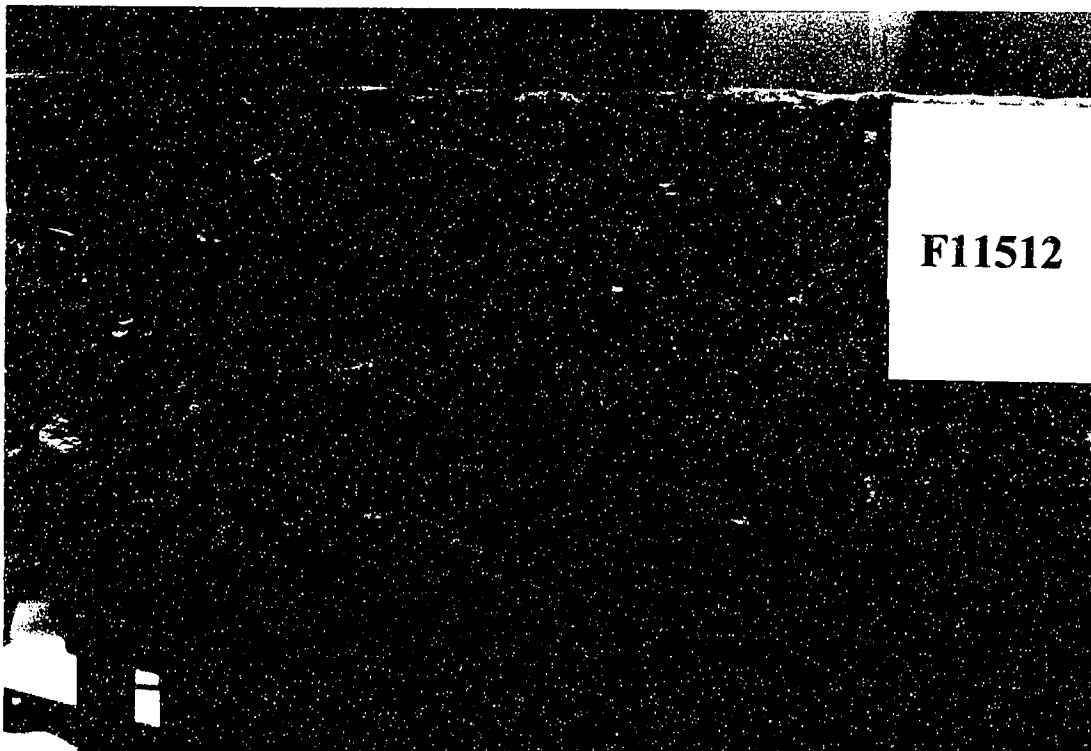


Plate 5.1: Photograph showing the mode of failure for beam F11512 strengthened by 1 mm thick, 100 mm wide and 900 mm long plate with 120 mm c/c spacing of stirrups



Plate 5.2: Photograph showing the mode of failure for beam F21512 strengthened by 2 mm thick, 100 mm wide and 900 mm long plate with 120 mm c/c spacing of stirrups

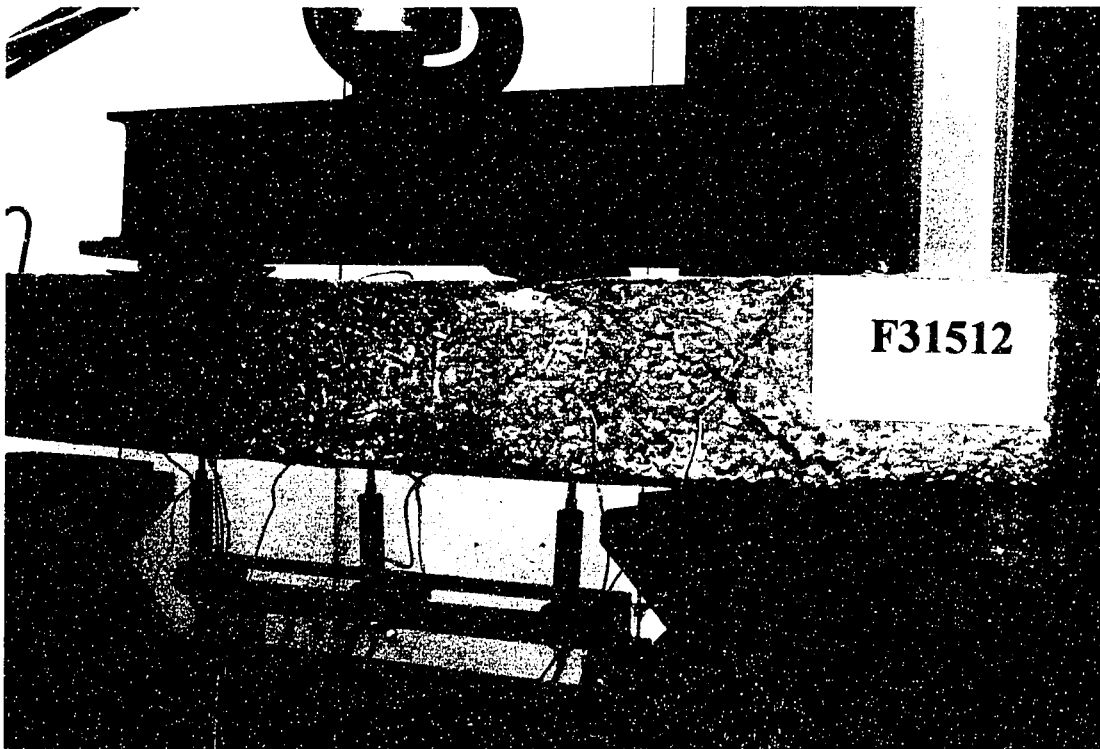


Plate 5.3: Photograph showing the mode of failure for beam F31512 strengthened by 3 mm thick, 100 mm wide and 900 mm long plate with 120 mm c/c spacing of stirrups

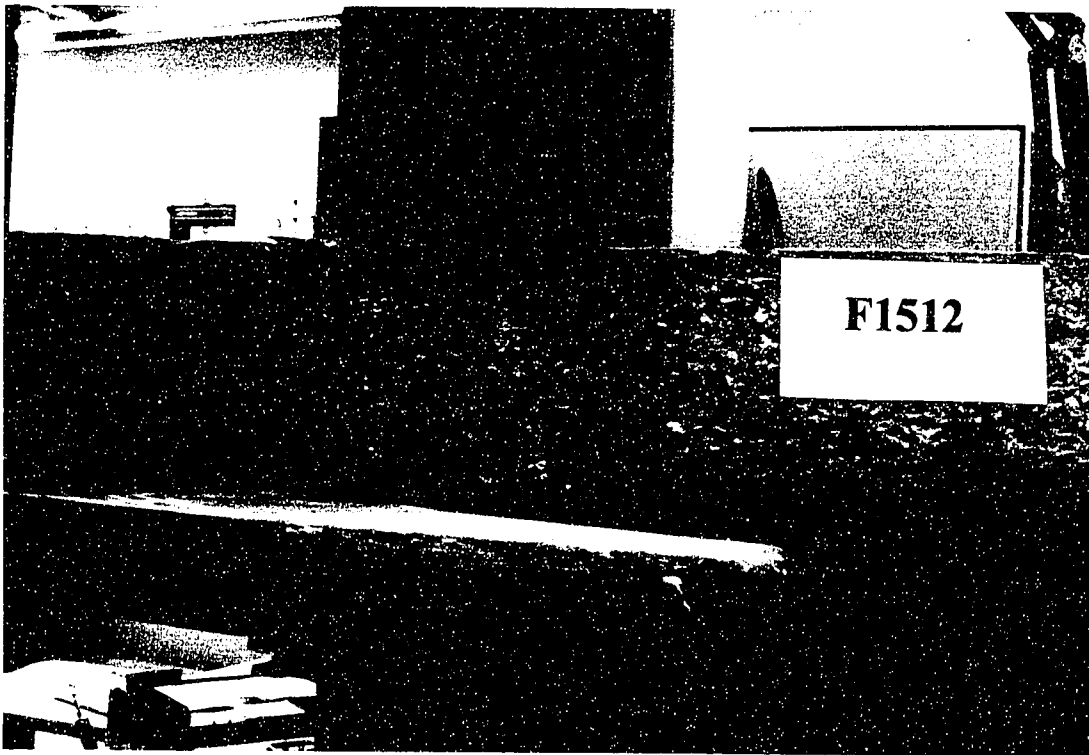


Plate 5.4: Photograph showing the mode of failure for beam F1512 strengthened by 1 mm thick, 100 mm wide and 1100 mm long plate with 120 mm c/c spacing of stirrups



Plate 5.5: Photograph showing the mode of failure for beam F2512 strengthened by 2 mm thick, 100 mm wide and 1100 mm long plate with 120 mm c/c spacing of stirrups

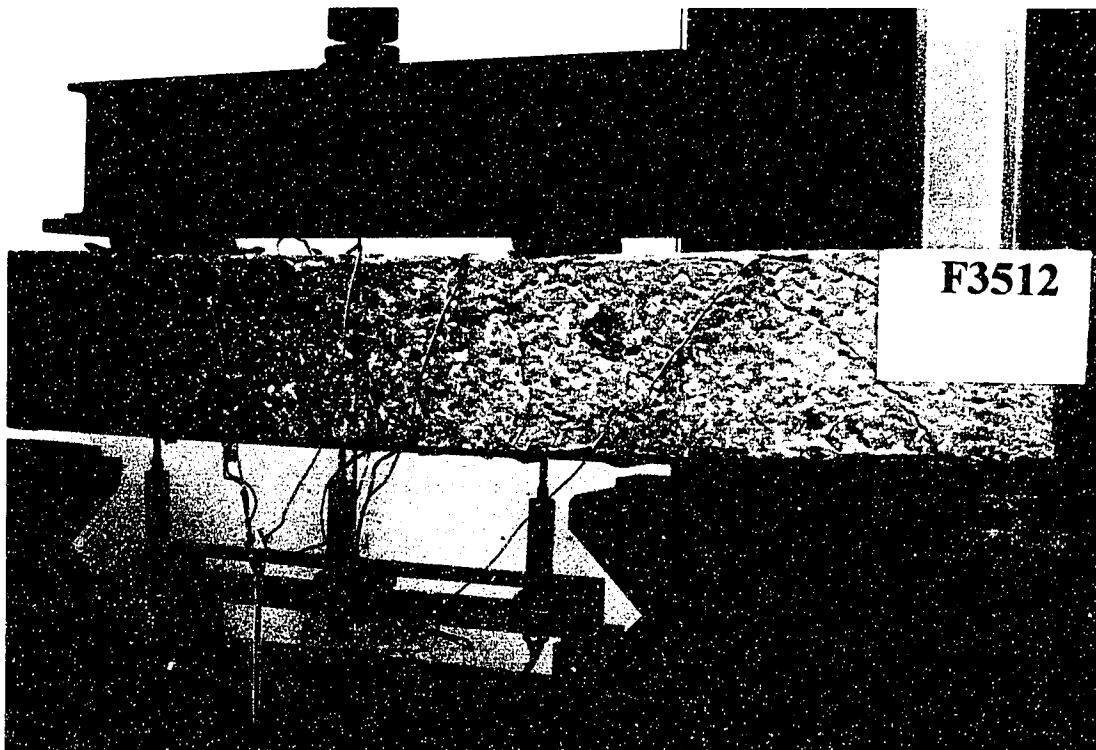


Plate 5.6: Photograph showing the mode of failure for beam F3512 strengthened by 3 mm thick, 100 mm wide and 1100 mm long plate with 120 mm c/c spacing of stirrups



Plate 5.7: Photograph showing the mode of failure for beam F1156 strengthened by 1 mm thick, 100 mm wide and 900 mm long plate with 60 mm c/c spacing of stirrups



Plate 5.8: Photograph showing the mode of failure for beam F2156 strengthened by 2 mm thick, 100 mm wide and 900 mm long plate with 60 mm c/c spacing of stirrups

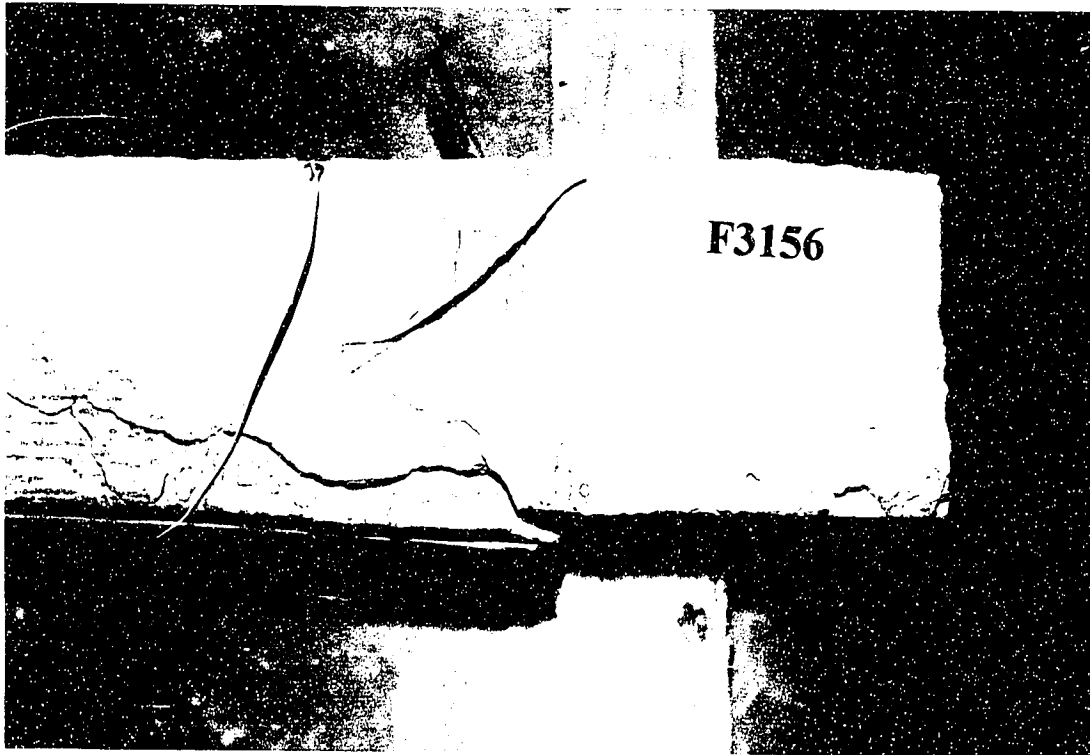


Plate 5.9: Photograph showing the mode of failure for beam F3156 strengthened by 3 mm thick, 100 mm wide and 900 mm long plate with 60 mm c/c spacing of stirrups

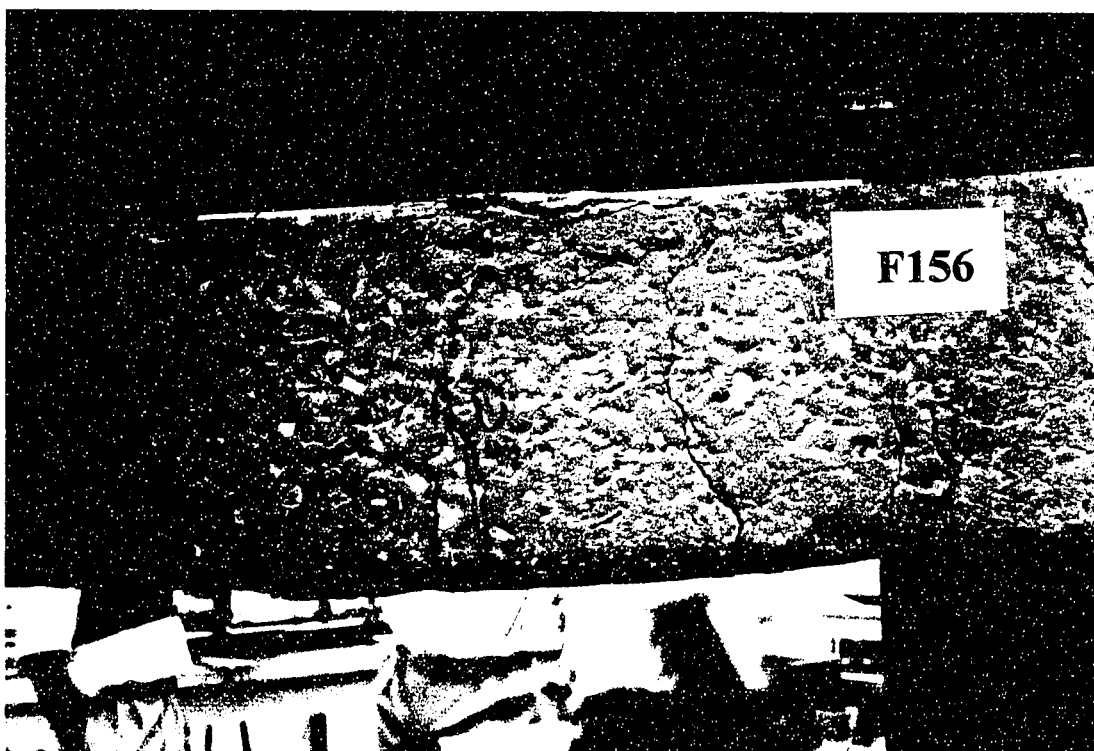


Plate 5.10: Photograph showing the mode of failure for beam F156 strengthened by 1 mm thick, 100 mm wide and 1100 mm long plate with 60 mm c/c spacing of stirrups



Plate 5.11: Photograph showing the mode of failure for beam F256 strengthened by 2 mm thick, 100 mm wide and 1100 mm long plate with 60 mm c/c spacing of stirrups



Plate 5.12: Photograph showing the mode of failure for beam F356 strengthened by 3 mm thick, 100 mm wide and 1100 mm long plate with 60 mm c/c spacing of stirrups

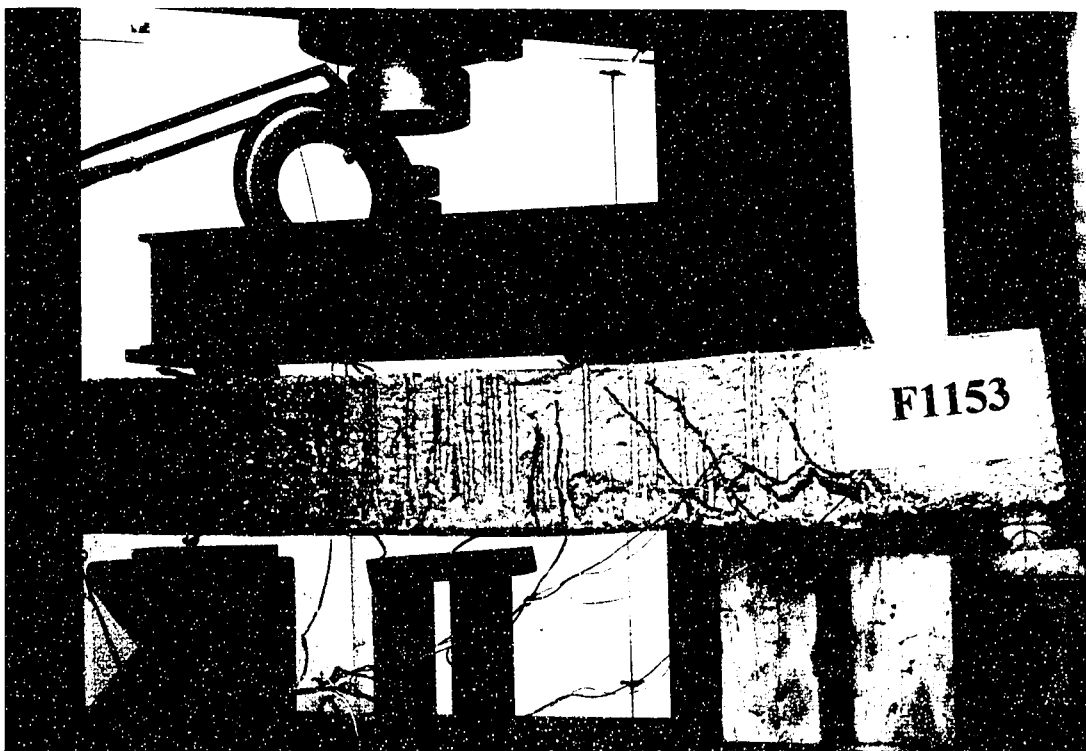


Plate 5.13: Photograph showing the mode of failure for beam F1153 strengthened by 1 mm thick, 100 mm wide and 900 mm long plate with 30 mm c/c spacing of stirrups

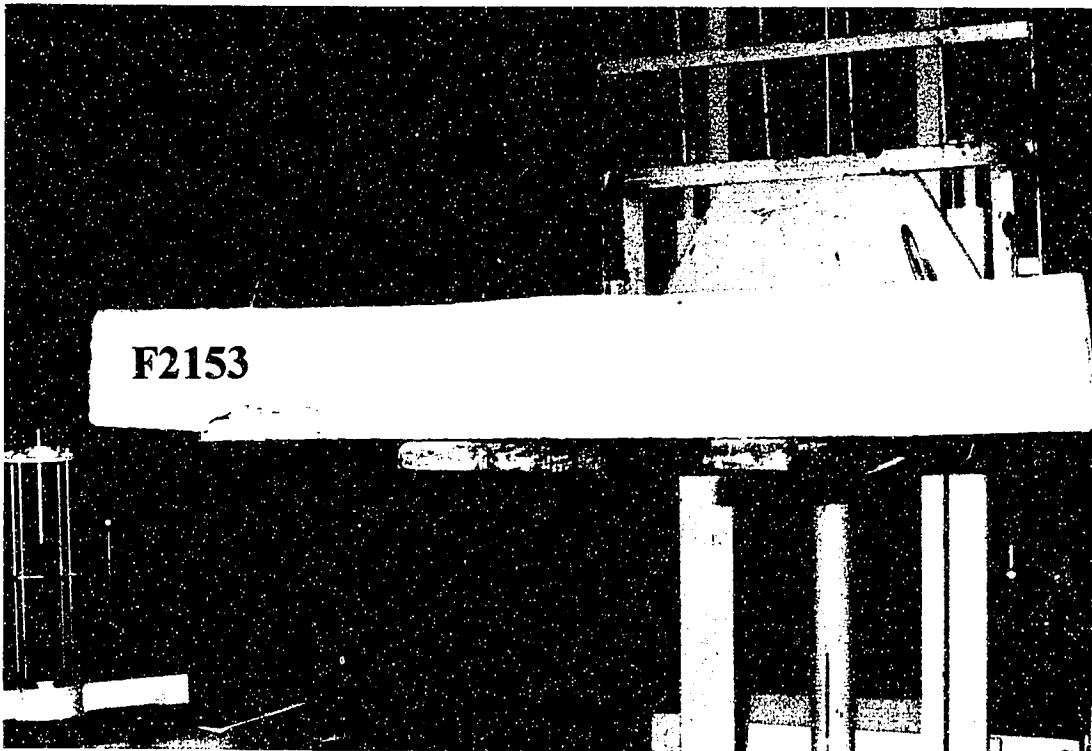
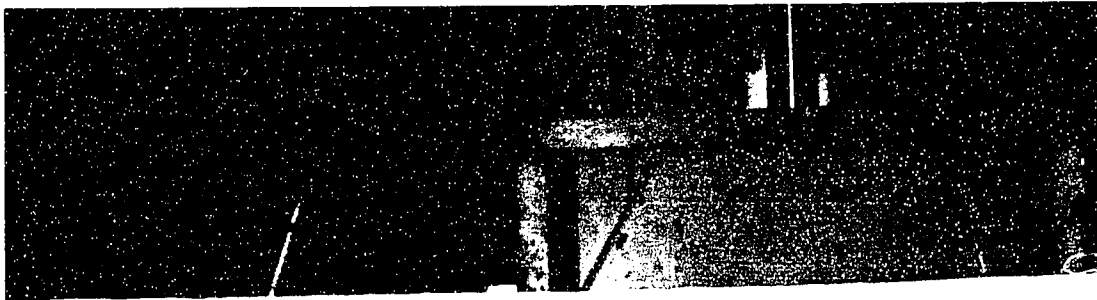


Plate 5.14: Photograph showing the mode of failure for beam F2153 strengthened by 2 mm thick, 100 mm wide and 900 mm long plate with 30 mm c/c spacing of stirrups



F3153



Plate 5.15: Photograph showing the mode of failure for beam F3153 strengthened by 3 mm thick, 100 mm wide and 900 mm long plate with 30 mm c/c spacing of stirrups

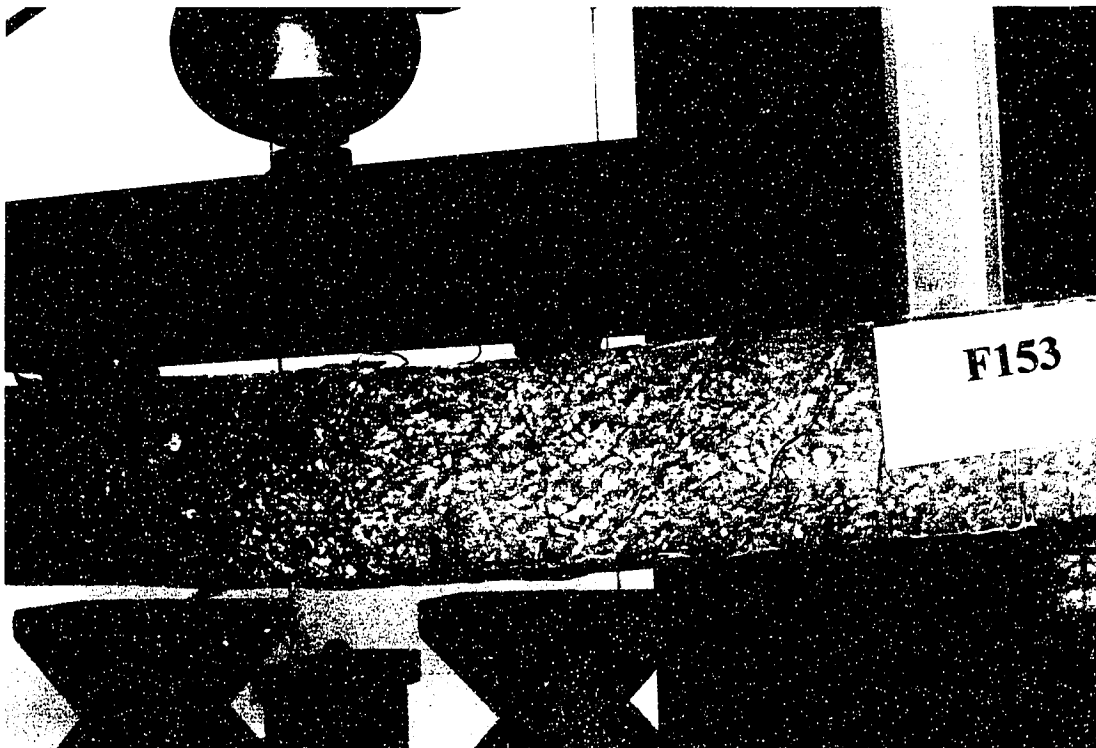


Plate 5.16: Photograph showing the mode of failure for beam F153 strengthened by 1 mm thick, 100 mm wide and 1100 mm long plate with 30 mm c/c spacing of stirrups

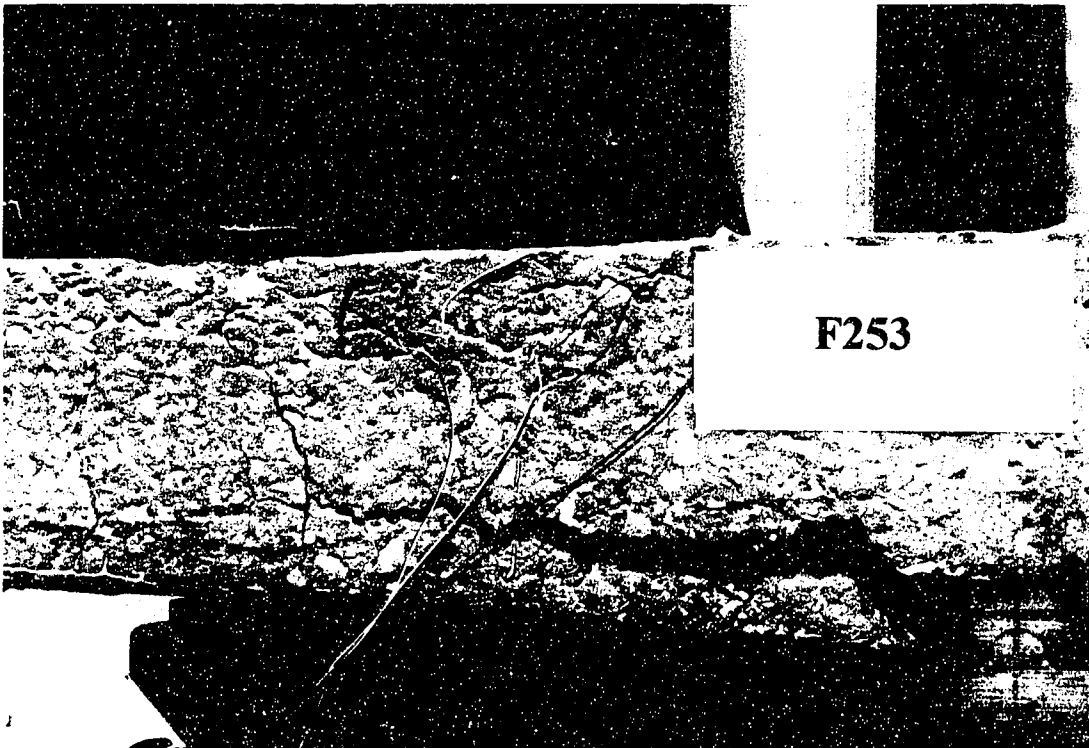


Plate 5.17: Photograph showing the mode of failure for beam F253 strengthened by 2 mm thick, 100 mm wide and 1100 mm long plate with 30 mm c/c spacing of stirrups

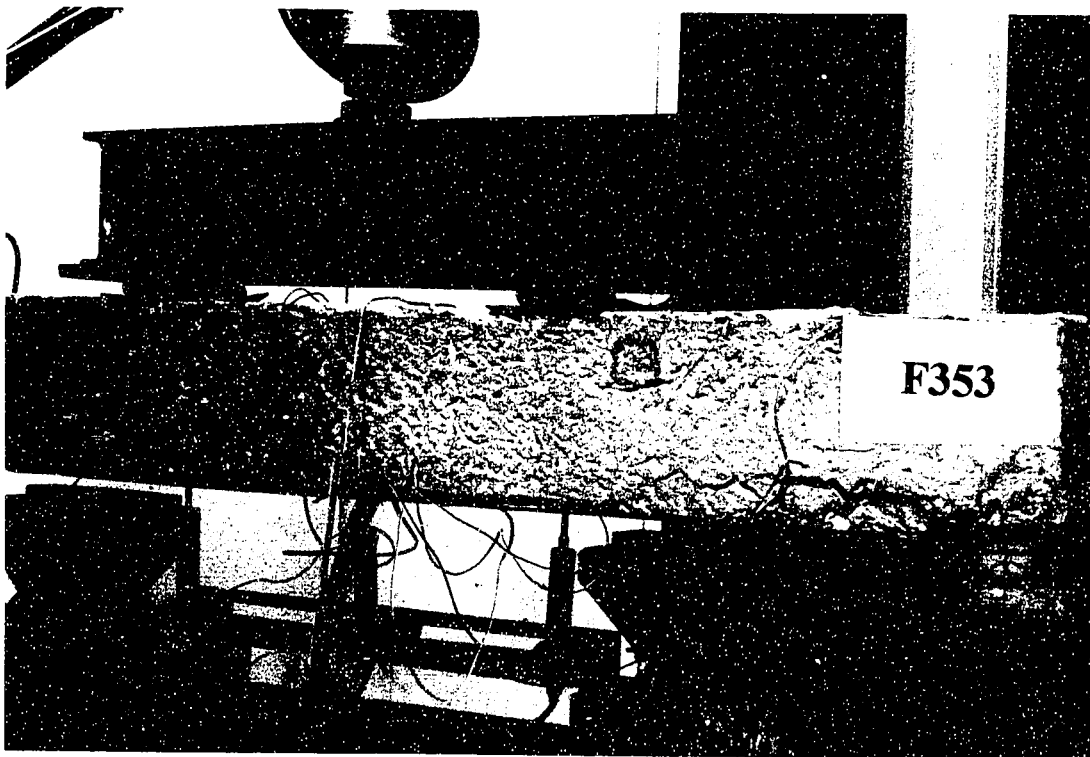


Plate .5.18: Photograph showing the mode of failure for beam F353 strengthened by 3 mm thick, 100 mm wide and 1100 mm long plate with 30 mm c/c spacing of stirrups

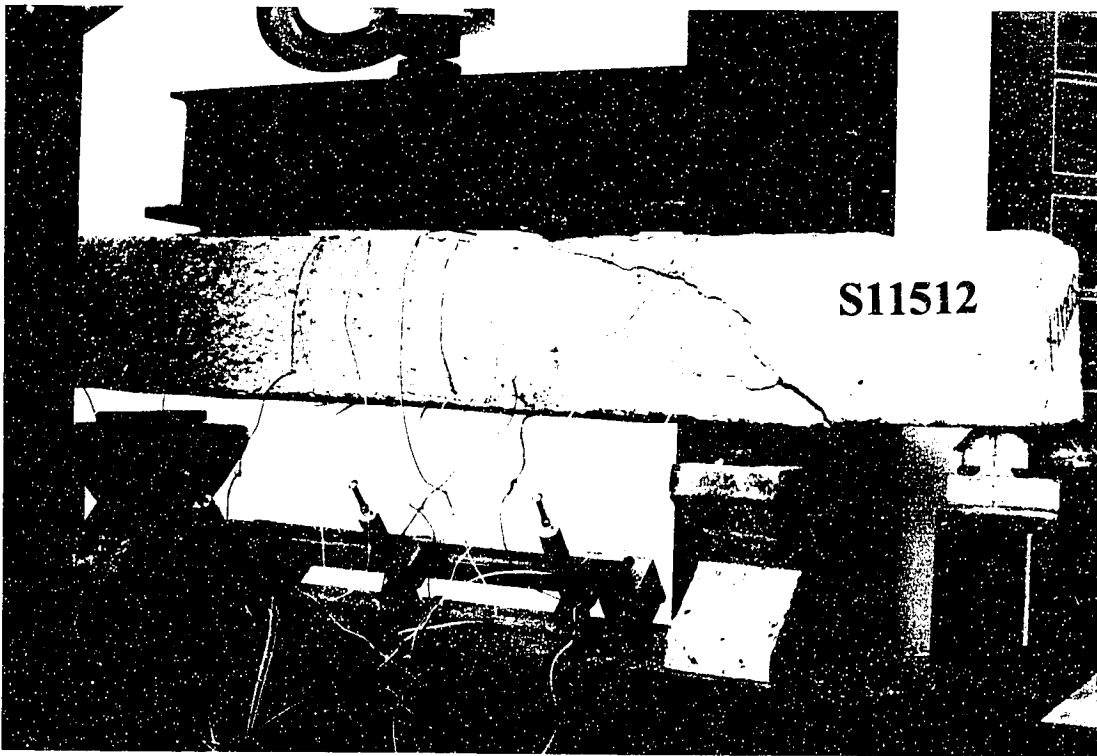


Plate 5.19: Photograph showing the mode of failure for beam S11512 strengthened by 1 mm thick, 100 mm wide and 900 mm long plate with 120 mm c/c spacing of stirrups

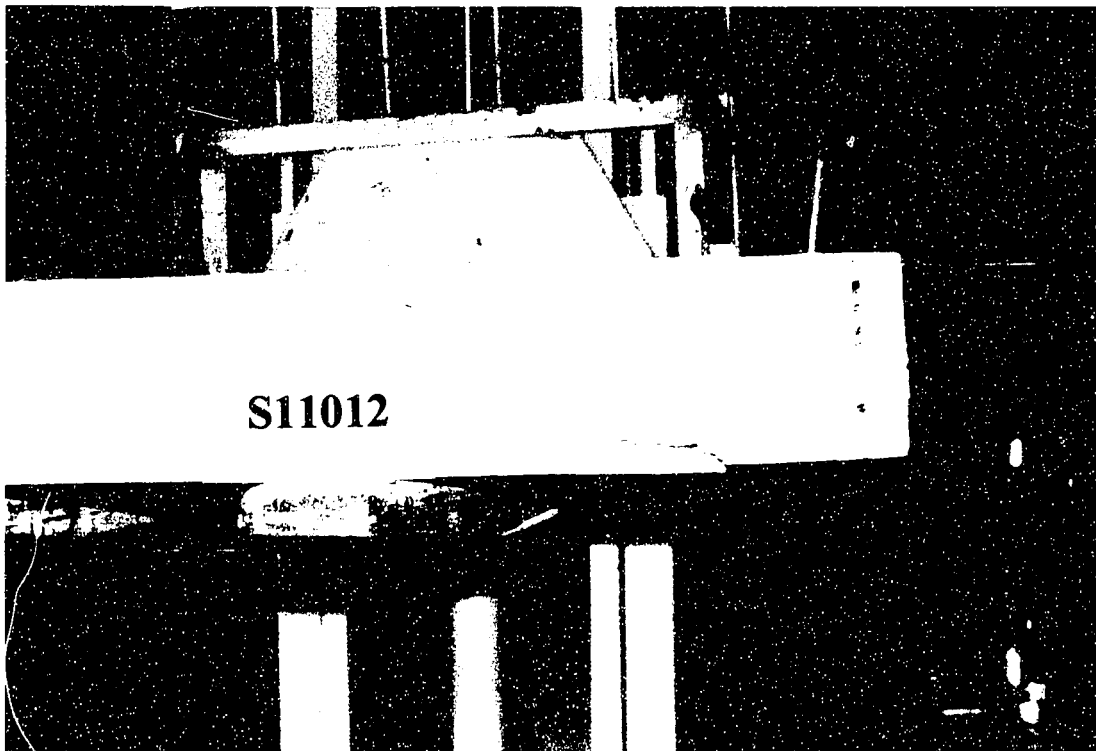


Plate 5.20: Photograph showing the mode of failure for beam S11012 strengthened by 1 mm thick, 100 mm wide and 1000 mm long plate with 120 mm c/c spacing of stirrups

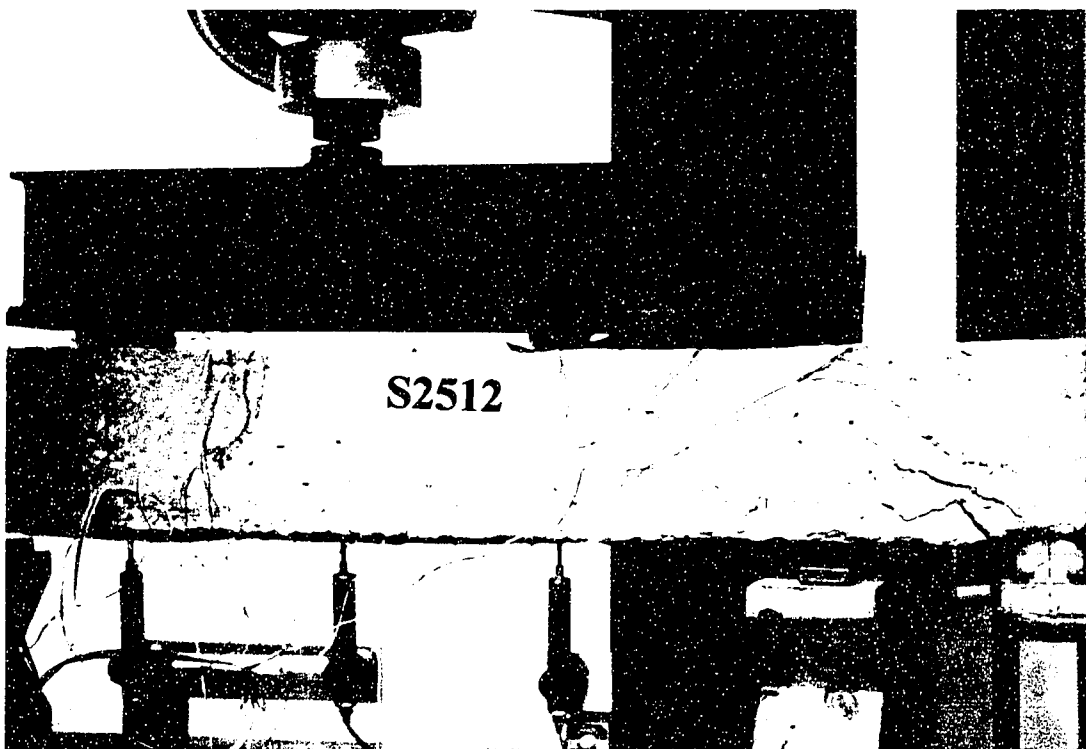


Plate 5.21: Photograph showing the mode of failure for beam S2512 strengthened by 2 mm thick, 100 mm wide and 1100 mm long plate with 120 mm c/c spacing of stirrups

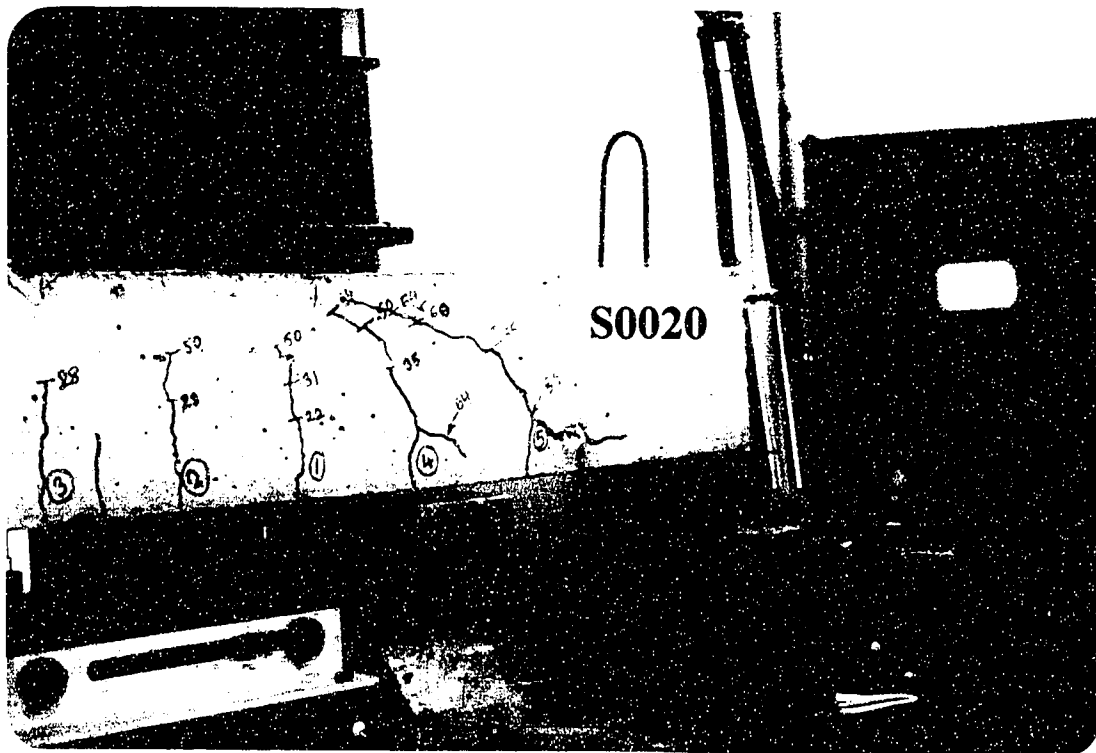


Plate 5.22: Photograph showing the mode of failure for control beam with shear stirrups at 200 mm c/c (S0020)



Plate 5.23: Photograph showing the mode of failure for beam S11020 strengthened by 1 mm thick, 100 mm wide and 1000 mm long plate with 200 mm c/c spacing of stirrups



Plate 5.24: Photograph showing the mode of failure for beam S31520 strengthened by 3 mm thick, 100 mm wide and 900 mm long plate with 200 mm c/c spacing of stirrups

Chapter VI

CONCLUSIONS AND RECOMMENDATIONS

6.1 Conclusions

Based on the results of the experimental program, the model proposed for rip-off failure has been confirmed in terms of predictions both for the ultimate load and the behavior at failure. Three independent failure modes are identified for plated R/C beams, including flexure, rip-off and diagonal tension. Characteristic parameter that distinguishes likelihood of occurrence of rip-off failure or flexure failure in contrast to diagonal tension failure is identified as comparison of the flexural capacity P_f to the shear capacity P_s of the unplated beam. If $P_f < P_s$, failure can be either by rip-off or by flexure. If $P_f > P_s$, failure will be precipitated by diagonal tension. For those repaired beams in which $P_f < P_s$, failure can be either rip-off as predicted by the KFUPM model or a flexural failure as given by ACI strength method, depending on which of the two yields a smaller load at failure. For these repaired beams in which $P_s < P_f$, failure will be by diagonal tension and an ACI modified expression is proposed for estimating the ultimate load for such beams.

$$V_u = \frac{1}{6} \left\{ \sqrt{f'_c} + 100(\rho_w + \rho_p) \frac{V_u d_s}{M_u} \right\} b_c d_s + \frac{A_v f_{yst} d_s}{s} \quad (4.31)$$

In beams with $P_s < P_f$, although initial cracks emanate from location of plate curtailment due to existence of high peeling and shear stresses these cracks are arrested due to presence of high amount of flexural reinforcement and the rip-off

failure is preempted. Thus, loads based on rip-off model underestimate the capacity of such beams, whose actual failure is precipitated in a classical diagonal tension mode. These load are predicted with reasonable accuracy by modifying the ACI expression for shear strength of R/C beams to account for the beneficial effect of the steel plate on the shear capacity of the beam.

Plate curtailment length ' L_c ' which plays a significant role in rip-off failure has an insignificant role in beams that fail under diagonal tension. Failure in both rip-off and in diagonal tension modes of failure is brittle and should be avoided from a design point of view, although strengthening may be attained as manifested by ultimate loads greater in repaired section than those in the unplated ones. Rational design should strive for a plate thickness t_p and curtailment length L_c that will ensure a flexural failure ensuring increased capacity and ductile mode of failure.

6.1.1 FOR PLATED WITH ($P_f < P < P_s$)

1. Failure is Rip-off (Starting at plate curtailment). This horizontal crack traverses below the main steel and joins up with an existing, highly stressed flexural crack. This combined crack then moved up suddenly to cause brittle failure.
2. KFUPM Group Model's predictor equation for Rip-off failure is an accurate estimate of load at failure.

$$P = 2 (kV_s + V_c)$$

Where,

$$k = 2.4 e^n$$

$$n = -0.08 C_{R1} C_{R2} * 10^6$$

3. Curtailment length plays a significant role in magnitude of load at failure as L_c increases $P \implies P_f$.
4. If plate thickness designed appropriately, then at failure, plate should be yielding i.e Flexural failure. This failure will not be brittle but a desirable ductile mode.
5. Preferred optimum design is to select plate thickness and curtailment length such that $P > P_f$ and failure ductile.
6. At failure, stress in stirrups $<$ yield stress (f_Y), and Rip-off failure crack does not traverse across stirrups. Hence, one cannot use the ACI expression for shear strength of R/C beams.

6.1.2 BEAMS WITH ($P_s < P < P_f$)

1. Rip-off crack originating at cut-off point meeting any lowly stressed flexural cracks is arrested due to presence of large amount of main reinforcement.
2. Secondary cracking will be in form of diagonal tension failure, similar to shear failure of unplated R/C beams. This load 'P' at failure will be $> P_s$, and given by following suggested expression (similar to ACI).
3. Failure is also brittle as in all shear failure, since there is no yielding of either main steel or plate.

4. Increase in P over P_s is nominal. Hence, repairing a beam weak in shear by a plate at the soffit is not recommended. In fact, we suggest use of web jackets in the shear span region.
5. Curtailment length plays no role in these beams.

6.2 Recommendations

The following are the suggestions for further studies:-

1. Concepts developed for simply supported members should be extended to continuous beams.
2. Two way slabs repaired by bonded plates should be studied for use in bridge decks and building floors.
3. Influence of cyclic loading on interface layer between plate and RC beam should be studied.
4. Use of Fiber glass and other advanced composite materials should be considered in environments conducive to corrosion of steel plate.

REFERENCES

1. Van Gemert, D. A., "Repairing of Concrete Structures by Externally Bonded Steel Plates", Proceedings ICP/RILEM/IBK International Symposium on Plastics in *Material and Structural Engineering*, Prague, June 1981, Elsevier Scientific Publishing Company, 1982, pp 519-526.
2. "Bresson, J., Realisation Pratique d'un Reinforcement Par Collage D'armatures", Annales de I, *Annales de I, ITBTP*, Suppl. 278, Feb 1971, pp 50-52.
3. Bresson, J., "Reinforcement par Collage d' Armatures du Passage Inferieur Du ed 126 Sous 1, Autoroute du sud. Annales de l'Institute du Batiment et des Travaux Publics", *Concrete and Reinforcement Series No. 122* Supplement No. 297, Sept 1972.
4. Lino, T., and Otokawa, K., "Application of Epoxy Resins in Strengthening of Concrete Structures", *Proceedings Third International Congress on Polymers in Concrete*, Japan, May 1981, Vol. II, pp 997-1011.
5. Ryback, M., "Reinforcement of Bridges by Gluing Reinforcing Steel", *Materials and Structures*, 16, No. 91, RILEM, Jan 1981, pp 13-17.
6. Fleming, C.J., and King, G.E.M., "The Development of the Structural Adhesives for Three Original Uses in South Africa", *International Symposium, Synthetic Resins in Building Construction*, RILEM, Paris, 1967, pp 75-92.
7. Hugenschmidt, H., "Epoxy Adhesive for Concrete and Steel", *Proceedings First International Congress on Polymers in Concrete*, London, May 1975, The Construction Press Limited, Hornby, 1976, pp 195-209.
8. Ladner, M., and Weber, C., "Concrete Structures with Bonded External Reinforcement", *EMPA Report No. 206*, Dubendorf, 1981
9. Mander, R.F "Bonded External Reinforcement, A Method of Strengthening Structures", *Department of Environment report on Quinton Interchange of the M5 Motorway*, 1974.

10. Davis, B.L., Powel, and J., "Strengthening of Brinsworth Road Bridge, Rotherham", *IABSE, 12th Congress, Vancouver, base coarse*, Sept. 1984, pp 401-407.
11. Barrett, N "Plates Steel Leads Floor", *New Civil Engineer*, June 1985, pp 18.
12. L'Hermite, R.L., and Bresson, J., "Beton Arme par Collage Des Armatures", *Resins in Building Construction, Part 2, International Symposium, RILEM, Paris 1967*, pp 172-203.
13. Lerchental, H., "Bonded Sheet Metal Reinforcement For Concrete Slabs", *Resins in Building Construction, Part 2, International Symposium, RILEM, Paris 1967*, pp 165-173.
14. Kajfasz, S., "Concrete Beams with External Reinforcement Bonded by Gluing", *Resins in Building Construction, Part 2, International Symposium, RILEM, Paris 1967*, pp 142-151.
15. "Reinforcing Methods for Bridges", *Proceedings 23rd Annual Meeting of Civil Engineering, Nov. 1975, Public Works Institute, Ministry of Construction, Japan*.
16. L'Hermite, R., and Devars du Mayne, R., "Le Collage Structural et le Renforcement Par Resines Des Structures De La Construction", *Annals De l'Institute Technique Du Batiment Et Das Travaux Publics, No. 349, Apl 1977. General Construction Series No. 62*.
17. Sommerard, T., "Swanley Steel Patch-Up", *New Civil Engineer 1977, No. 247, 16 June 1977*.
18. Raithby, K. D., "External Strengthening of Concrete Bridges With Bonded Steel Plates", Department of the Environment, Department of the Transport, *Supplimentary Report 612, TRRL, Crowthore, Birkshire, 1980*.
19. "External Reinforcement of Concrete Structures" *CIBA-GEIGY June 1985*.
20. Ladner, M. Flueler, P., Lauterbach, H., and Tausky, R.U.A., "Verstarkung Von Tragkonstruktionen Mit Geklebter Armierung, Schweizerische Bauzeitung", Vol. 92, No. 19, 9 May 1974, pp 457-474.
21. Felix Hugenschmidt, "Strengthening of Existing Concrete Structures with Bonded Reinforcements", *CIBA-GIEGY, June 1985*.

22. Jones, R., R. N. Swamy, and Charif A, "Plate Separation and Anchorage of Reinforced Concrete Beams Strengthened by Epoxy Bonded-Steel Plates", *The Structural Engineer*, Volume 66, No. 5, March 1988.
23. Irwin, C.A. K., "The Strengthening of Concrete Beams by Bonded Steel Plates", *TRRL Supplementary Report 160UC. Bridge Design Division, Structural Department*, Crowthorne, Birkshire, 1975.
24. Calder, "Exposure Tests on Externally Reinforced Concrete Beams-First Two Years", *Transport and Road Research Laboratory, TRRL Supplementary Report 529* 1979, pp 1-34.
25. Jones, R., R.N. Swamy, J. Bloxham and A. Bouderbalah, "Composite Behaviour of Concrete Beams With Epoxy Bonded External Reinforcement", *The International Journal of Cement Composites*, Vol 2, No. 2, May 1980 pp 91-107.
26. Cusens, D.W. Smith., "A Study of Epoxy Resin Adhesive Joints in Shear" *The Structural Engineer* Vol 58A, No.1, Jan 1980 pp 13-18.
27. Macdonald, "The Flexural Performance of 3.5 m Concrete Beams With Various Bonded External Reinforcements" May 1982, pp 1-16.
28. Lloyd and A.J.J. Calder "The Microstructure of Epoxy Bonded Steel-to-Concrete Joints" *Transport and Road Research Laboratory, TRRL Supplementary Report 705* Berkshire, 1982, pp 1-8.
29. Jones, R., R.N. Swamy and T.H. Ang "Under and Over Reinforced Concrete Beams with Glued Steel Plates", *The International Journal of Cement Composites and Lightweight Concrete* Feb. 1982, pp 19-32.
30. Jones, R., R.N. Swamy and J. Bloxham, "Crack Control of Reinforced Concrete Beams Through Epoxy Bonded Steel Plates", 1987, pp 542-555.
31. Swamy, R.N., R. Jones and J.W. Bloxham, "Structural Behaviour of Reinforced Concrete Beams Strengthened by Epoxy-Bonded Steel Plates", *The Structural Engineer*, Vol 65A, No.2, Feb. 1987, pp 59-68.
32. Jones, R.N., R. Swamy, and A. Charif, "Plate Separation and Anchorage of Reinforced Concrete Beams Strengthened by Epoxy-Bonded Steel Plates", *The Structural Engineer*, Vol 66, No. 5, March 1988, pp 85-94.

33. Swamy, R.N., R. Jones and A. Charif, "The Effect of External Plate Reinforcement on the Strengthening of Structurally Damaged RC Beams", *The Structural Engineer*, Vol 67, No. 3, Feb 1989 pp 45-56.
34. Roberts, T.M., "Approximate Analysis of Shear and Normal Stress Concentrations in the Adhesive Layer of Plated RC Beams", *The Structural Engineer*, Vol 67, No. 12, June 1989, pp 229-233.
35. Alan E. Vardy, and Arumugam Anadarajah, "Bonded Joint End Conditions: A Laboratory Specimen", *The Structural Engineer*, pp 359-364.
36. D.Van Gemert and M. Vanden Bosch, "Long-Term Performance of Epoxy bonded Steel-Concrete Joints", *The Structural Engineer*, pp 518-527.
37. Munawar Hussain "Flexure and Shear Behaviour of Damaged RC Beams Repaired by Plate Bonding", *M.S Thesis*, KFUPM: July 1992.
38. Zirabia, Y.N., "Non-Linear Finite Element Analysis of R/C Beams Repaired by Plate Bonding", *P.hd Dissertation*, KFUPM: June 1993.
39. Arthur H. Nilson, and George Winter, "Design of Concrete Structures" *McGraw-Hill International Editions*, 1991.
40. Chu-Kia Wang, and Charles G.Salmon, "Reinforced Concrete Design", *Happer & Row Publishers*, New York: 1985.
41. Baluch, M.H, Ziraba, Y. N, Azad, A. K, Sharif, A. M, Al-Sulaimani, G. J, and Basunbul, I. A, "Shear Strength of Plated R/C Beams," *Magazine of Concrete Research*, UK, to appear, 1995.
42. Al-Sulaimani, G. J, Sharif, A. M, and Basunbul, I. A, Baluch, M.H, and Ghaleb, B. N, "Shear Repair for Reinforced Concrete by Fiberglass Plate Bonding," *ACI Structural Journal*, V. 91, No.4, July-Aug 1994, pp. 458-464.
43. Al-Farabi Sharif, Al-Sulaimani, G. J, Basunbul, I. A, Baluch, M.H, and Ghaleb, B. N, "Strengthening of Initially Loaded Reinforced Concrete Beams Using FRP Plates," *ACI Structural Journal*, V. 91, No.2, March-April 1994, pp. 160-168.
44. Ziraba, Y. N, Baluch, M.H, Basunbul, I. A, Sharif, A. M, , Azad, A. K, Al-Sulaimani, G. J, "Guidelines Towards the Design of Reinforced Concrete (RC) Beams with External Plates, " *ACI Structural Journal*, V. 91, No.6, Nov-Dec. 1994, pp. 639-646.

45. Ziraba, Y. N, Baluch, M.H, Basunbul, I. A, Azad, A. K, Al-Sulaimani, G. J and Sharif, A. M, "Combined Experimental-Numerical Approach to Characterization of Steel/Glue/Concrete Interface," *Materials and Structures Journal, RILEM*, France, to appear, 1995.
46. Ziraba, Y. N, Baluch, M.H, Sharif, A.M, Azad, A. K, Al-Sulaimani, G. J and Basunbul, I. A,"Modelling of Damaged RC Beams Strengthened by Fiber Composite Plates," *Journal of Engineering Computations*, to appear, 1995.
47. Alfarabi Sharif, Al-Sulaimani, G. J, Basunbul, I. A, Baluch, M.H, and Hussain, M, "Strengthening of Shear Damaged RC Beams by Externally Bonding Steel Plates," *Magazine of Concrete Research*, to appear, 1995
48. Baluch, M.H., "Strengthening by plate bonding", notes of short course- Repair and Rehabilitation of Concrete Structures, KFUPM, Saudi Arabia, Dec., 1994.

APPENDIX-A

This section gives a sample calculation for the evaluation of flexure and shear capacity for Beam S2512. The dimensions and material properties used are as follows:

f'_c	=	5737 psi (39.5 Mpa)
b_c	=	150 mm
h_c	=	150 mm
E_c	=	$57,000 \sqrt{f'_c} = 29,746$ Mpa
b_p	=	100 mm
$t_p = d_p$	=	2 mm
E_p	=	200,000 Mpa
b_a	=	100 mm
E_a	=	278.6 MPa
G_a	=	120.1 MPa
A_s	=	330.3 mm ²
E_s	=	200,000 MPa
$d_s = h_s$	=	113 mm
h_p	=	152.5 mm
f_{ys}	=	414 MPa
A_{st}	=	56 mm ²
f_{yst}	=	380 MPa
f_{yp}	=	276 MPa
P_{exp}	=	97.6 kN

Unrepaired Beam

Calculations for P_f and P_s based on Unplated beam properties:

Flexural Capacity (P_f)

$$A_s = \frac{\pi}{4} d^2 = 339.3 \text{ mm}^2$$

The depth of the concrete rectangular stress block is given by

$$\bar{a} = \left(\frac{A_s f_{ys}}{0.85 f'_c b_c} \right) = \frac{339.3 * 414}{0.85 * 39.5 * 150} = 27.9$$

$$M_n = A_s f_{ys} \left(d_s - \frac{\bar{a}}{2} \right)$$

$$M_n = 339.3 * 414 * \left(113 - \frac{27.9}{2} \right) = 13.9 * 10^6 \text{ N} - \text{mm}$$

The load corresponding to flexure is given by

$$\frac{P_f}{2} a' = M_n$$

$$P_f = \frac{2M_n}{a'}$$

$$P_f = \frac{2 * 13.9 * 10^6}{400} = 70 \text{ kN} * *$$

*** Actual (P_f) approximately 35 % greater due to strain hardening

Shear Capacity (P_s)

Shear strength provided by concrete V_c is,

$$V_c = \frac{1}{6} \left[\sqrt{f'_c} + 100 \rho_w \left(\frac{V_u d_s}{M_u} \right) \right] b_c d_s$$

$$V_c = \frac{1}{6} \left[\sqrt{39.5} * 150 * 113 + 100 * 339.3 \right] = 23.40 \text{ kN}$$

$$\rho_w = \frac{A_s}{b_c d_s}$$

Shear strength in the web steel is,

$$V_s = \frac{A_v f_{ys} d_s}{s}$$

$$V_s = \frac{56 * 380 * 113}{120} = 20.04 \text{ kN}$$

Total shear force V_n applied at a given section is given by

$$V_n = V_c + V_s$$

$$V_n = 23.40 + 20.04 = 43.44 \text{ kN}$$

The load corresponding to shear

$$P_s = 2 V_n$$

$$P_s = 2 * 43.44 = 86.9 \text{ kN}$$

For this case, $P_s < P_f$, therefore, repaired beam will fail in diagonal tension.

Repaired Beam

Flexural Capacity (P_{flex})

The depth of the concrete rectangular stress block is,

$$\bar{a} = \frac{A_s f_{ys} + b_p t_p f_{yp}}{0.85 f'_c b_c}$$

$$\bar{a} = \frac{339.3 * 414 + 100 * 2 * 276}{0.85 * 39.5 * 150} = 38.85$$

$$h_p = h_c + d_a + \frac{t_p}{2}$$

$$h_p = 150 + 1.5 + 1.0 = 152.5 \text{ mm}$$

Assuming yielding of both internal and external reinforcement at failure, moment equilibrium at ultimate load conditions requires:

$$M_n = A_s f_{ys} \left(d_s - \frac{\bar{a}}{2} \right) + t_p b_p f_{yp} \left(h_p - \frac{\bar{a}}{2} \right)$$

$$M_n = 339.3 * 414 \left(113 - \frac{38.85}{2} \right) + 2 * 100 * 276 \left(152.5 - \frac{38.85}{2} \right) = 20.49 * 10^6 \text{ N} - \text{mm}$$

$$P_{flex} = \frac{2M_n}{a}$$

$$P_{flex} = \frac{2 * 20.49 * 10^6}{400} = 102.45 \text{ kN} **$$

** Represents maximum flexural capacity if repaired beam was to fail in flexure.

Shear Capacity (P_{shear})

Investigation for Concrete Rip-off

In order to check on the shear capacity of the plated R/C beams, the following quantities are computed according to ACI strength method:

Shear strength provided by concrete V_c is,

$$V_c = \frac{1}{6} \left[\sqrt{f'_c} + 100 \rho_w \left(\frac{V_u d_s}{M_u} \right) \right] b_c d_s$$

$$V_c = \frac{1}{6} \left[\sqrt{39.5} + \frac{100 * 339.3}{150 * 113} \right] * 150 * 113 = 23.40 \text{ kN}$$

$$\rho_w = \frac{A_s}{b_c d_s}$$

Shear strength in the web steel is,

$$V_s = \frac{A_v f_{ys} d_s}{s} = 20.04 \text{ kN}$$

Total shear force V_n applied at a given section is given by

$$V_n = V_c + V_s = 23.40 + 20.04 = 43.44 \text{ kN}$$

The load corresponding to shear

$$P_s = 2 V_n = 2 * 43.44 = 86.88 \text{ kN}$$

$$P_{\text{expt}} = 97.6 \text{ kN}$$

$$K_{\text{sf}} = \frac{\left(\left(\frac{P_{\text{expt}}}{2} \right) - V_c \right)}{V_s} = 1.267$$

Expression for Shear Capacity

Rip-Off Failure

Using the strength of materials approach, the maximum shear and peeling stresses at the interface for the beam using Robert's approach [34] at the maximum load sustained by the beam are represented by τ_o and σ_o respectively. In addition to the material properties and beam dimension, the other parameters are determined as follows:

$$A = \frac{E_c b_c}{2E_p} = \frac{29746 * 150}{2 * 200000} = 11.15 \text{ mm}$$

$$B = \frac{E_s A_s}{E_p} + b_p t_p = \frac{200000 * 339.3}{200000} + 100 * 2 = 539.3 \text{ mm}^2$$

$$C = \frac{A_s d_s E_s}{E_p} + h_p b_p t_p = \frac{113 * 339.3 * 200000}{200000} + 152.5 * 2 * 100 = 68840.90$$

$$X = \frac{-B + (B^2 + 4AC)^{1/2}}{2A}$$

$$X = \frac{-539.3 + \sqrt{(539.3)^2 + 4 * 11.15 * 68840.9}}{2 * 11.15} = 58.03$$

$$M^* = \frac{P}{2y} \left(X + \frac{d_c + t_p}{2} \right)$$

$$V = \frac{P}{2}$$

$$I_p = \frac{b_p t_p^3}{12} = \frac{100 * 2^3}{12} = 66.67 \text{ mm}^4$$

The second moment of Inertia (I) of the fully composite transformed equivalent steel section is given by

$$I = \frac{E_c b_c X^3}{3E_p} + \frac{A_s E_s (h_s - X)^2}{E_s} + b_p t_p (h_p - X)^2$$

$$I = \frac{29,746 * 150 * (58.03)^3}{3 * 200,000} + \frac{339.3 * 200,000 * (113 - 58.03)^2}{200,000} + 100 * 2 * (152.5 - 58.03)^2$$

$$I = 4,263,382 \text{ mm}^4$$

The shear stiffness of the interface layer

$$K_s = \frac{G_a b_a}{d_a} = \frac{120.1 * 100}{15} = 8006 \text{ MPa}$$

Normal stiffness of the interface layer

$$K_n = \frac{E_a b_a}{d_a} = \frac{278.6 * 100}{15} = 18,573 \text{ MPa}$$

The peak shear stress τ_o is given as

$$\tau_o = \alpha_1 f'_t \left(\frac{C_{rl} V_o}{f'_c} \right)^{5/4}$$

Tensile strength of concrete is given by

$$f'_t = 0.324 (f'_c)^{2/3} = 3.804 \text{ MPa}$$

$$\tau_o = 35 * 3.804 \left(\frac{7.567 * 10^{-5} * \frac{97.6 * 10^3}{2}}{39.5} \right)^{5/4} = 6.88 \text{ MPa}$$

Where,

- α_1 = 35, an empirical regression coefficient determined from numerical parametric study
- f_t = tensile strength of concrete, Mpa
- V_o = global shear force at location of plate cutoff

In contrast, using a linear strength of materials model, Robert's [34] suggested use of the following expression to evaluate the peak shear interface stress

$$\bar{\tau}_o = C_{r1} V_o$$

Where

$$C_{r1} = \left[1 + \left(\frac{K_s}{E_p b_p d_p} \right)^{1/2} L_c \right] \frac{b_p d_p}{I b_a} (h_p - h)$$

$$C_{r1} = \left[1 + \left(\sqrt{\frac{8006.67}{200000 * 100 * 2}} \right) 50 \right] \frac{100 * 2 * (152.5 - 58.03)}{4263,382 * 100} = 7.567 * 10^{-5}$$

Where,

- L_c = M_o / V_o at plate cutoff location
- h = depth to neutral axis of cracked section of plated beam
- I = second moment of area of equivalent transformed steel section about neutral axis for cracked section
- G_a, b_a, d_a shear modulus, width, and depth of adhesive

The peak peeling stress σ_o required is given by

$$\sigma_o = \alpha_2 C_{R2} \tau_o$$

$$\sigma_o = 1.10 * 0.2732 * 6.88 = 2.068 \text{ MPa}$$

The factor C_{R2} is calculated using

$$C_{R2} = d_p \left(\frac{K_n}{4E_p I_p} \right)^{1/4}$$

$$C_{R2} = 2 \left(\frac{18573}{4 * 200000 * 66.67} \right)^{1/4} = 0.2732$$

Where,

I_p = second moment of area of steel plate about its own centroid

E_a = elastic modulus of adhesive

The capacity of a plated R/C beam prone to concrete rip-off failure has been detailed in Ref [38] and can be approximated (in N-mm) as

$$V_u = (V_c + kV_s)$$

$$V_c = \frac{1}{6} \left(\sqrt{f'_c} + 100 \rho_w \frac{V_u d_s}{M_u} \right) b_c d_s$$

$$V_s = \frac{A_v f_{yst} d_s}{s}$$

$$k = 2.4 e^n$$

$$k = 2.4 e^{-0.08 * 7.567 * 10^{-5} * 0.2732 * 10^6} = 0.459$$

$$n = -0.08 C_{R1} C_{R2} * 10^6$$

$$n = -0.08 C_{R1} C_{R2} * 10^6$$

Where

f'_c = concrete strength, Mpa

$$\rho_w = \frac{A_s}{b_c d_s}$$

$$\frac{V_u d_s}{M_u} > 1.0$$

b_w, d_s = width and effective depth of unplated R/C section

A_v = amount of shear reinforcement

f_{yst} = stirrup yield strength

s = stirrup spacing

$$P_{shear} = 2 V_n$$

$$P_{shear} = 2(V_c + kV_s) = 2*(23.40 + 0.4591*20.04)$$

$$P_{shear} = 65.20 \text{ kN}$$

The maximum shear stress at interface τ_o at the point of plate curtailment based on

Robert's approach [34] is given by:

$$\tau_o = \left(V_n + \sqrt{\left(\frac{K_s}{E_p b_p d_p} \right) M^*} \right) b_p t_p \left(\frac{h_p - h}{b_a J} \right)$$

The maximum peeling (normal) stress at interface σ_o on the basis of Rober's expression [34] is given by:

$$\sigma_o = \tau_o t_p \left(\frac{K_n}{4E_p I_p} \right)^{1/4}$$

$$\sigma_o = C_{R1} C_{R2} \left(\frac{P_{cxpt}}{2} \right) = 7.567 * 10^{-5} * 0.2732 * \frac{97.6 * 10^3}{2} = 1.0088 \text{ MPa}$$

$$\tau_o = \frac{\sigma_o}{C_{R2}} = \frac{1.0088}{0.2732} = 3.67 \text{ MPa}$$

Diagonal Tension Failure

The ultimate shear capacity when diagonal tension failure is anticipated in the plated R/C beam is found by:

$$V_n = \frac{1}{6} \left\{ \sqrt{f'_c} + 100 \left(\rho_w + \rho_p \right) \frac{V_u d_s}{M_u} \right\} b_c d_s + \frac{A_v f_{yst} d_s}{s}$$

$$V_n = \frac{1}{6} \left[\sqrt{39.5} + 100 \left(\frac{339.3}{150 * 113} + \frac{100 * 2}{150 * 113} \right) * 1 \right] * 150 * 113 + \frac{56 * 380 * 113}{120} = 46.7$$

$$P_{shear} = 2 * V_n = 2 * 46.78 = 93.56 \text{ kN}$$

Example 2

This section gives a sample calculation for the evaluation of flexure and shear capacity for Beam F353 (F group beam). The dimensions and material properties used are as follows:

$$\begin{aligned}
 f'_c &= 6087 \text{ psi (41.97 Mpa)} \\
 b_c &= 150 \text{ mm} \\
 h_c &= 150 \text{ mm} \\
 E_c &= 57,000 \sqrt{f'_c} = 30,661 \text{ Mpa} \\
 b_p &= 100 \text{ mm} \\
 t_p = d_p &= 3 \text{ mm} \\
 E_p &= 200,000 \text{ Mpa} \\
 b_a &= 100 \text{ mm} \\
 E_a &= 278.6 \text{ MPa} \\
 G_a &= 120.1 \text{ MPa} \\
 A_s &= 157.08 \text{ mm}^2 \\
 E_s &= 200,000 \text{ MPa} \\
 d_s = h_s &= 113 \text{ mm} \\
 h_p &= 153 \text{ mm} \\
 f_{ys} &= 414 \text{ MPa} \\
 A_{st} &= 56 \text{ mm}^2 \\
 f_{yst} &= 380 \text{ MPa} \\
 f_{yp} &= 276 \text{ MPa} \\
 P_{exp} &= 74.5 \text{ kN}
 \end{aligned}$$

Unrepaired Beam

Calculations for P_f and P_s based on Unplated beam properties:

Flexural Capacity (P_f)

$$A_s = \frac{\pi}{4} d^2 = 157.08 \text{ mm}^2$$

The depth of the concrete rectangular stress block is given by

$$\bar{a} = \left(\frac{A_s f_{ys}}{0.85 f'_c b_c} \right) = \frac{157.08 * 414}{0.85 * 41.97 * 150} = 12.15$$

$$M_n = A_s f_{ys} \left(d_s - \frac{\bar{a}}{2} \right)$$

$$M_n = 157.08 * 414 * \left(113 - \frac{12.15}{2} \right) = 6.95 * 10^6 \text{ N} - \text{mm}$$

The load corresponding to flexure is given by

$$\frac{P_f}{2} a' = M_n$$

$$P_f = \frac{2 M_n}{a'}$$

$$P_f = \frac{2 * 6.95 * 10^6}{400} = 35 \text{ kN} \text{ ***}$$

*** Actual (P_f) approximately 35 % greater due to strain hardening

Shear Capacity (P_s)

Shear strength provided by concrete V_c is,

$$V_c = \frac{1}{6} \left[\sqrt{f'_c} + 100 \rho_w \left(\frac{V_u d_s}{M_u} \right) \right] b_c d_s$$

$$V_c = \frac{1}{6} \left[\sqrt{41.97} * 150 * 113 + 100 * 157.08 \right] = 20.92 \text{ kN}$$

$$\rho_w = \frac{A_s}{b_c d_s}$$

Shear strength in the web steel is,

$$V_s = \frac{A_v f_{ys} d_s}{s}$$

$$V_s = \frac{(2 * 28) * 380 * 113}{30} = 80.15 \text{ kN}$$

Total shear force V_n applied at a given section is given by

$$V_n = V_c + V_s$$

$$V_n = 20.92 + 80.15 = 101 \text{ kN}$$

The load corresponding to shear

$$P_s = 2 V_n$$

$$P_s = 2 * 101 = 202 \text{ kN}$$

For this case, $P_s < P_f$, therefore, repaired beam will fail in diagonal tension.

Repaired Beam

Flexural Capacity (P_{flex})

The depth of the concrete rectangular stress block is,

$$a = \frac{A_s f_{ys} + b_p t_p f_{yp}}{0.85 f'_c b_c}$$

$$\bar{a} = \frac{157.08 * 414 + 100 * 3 * 276}{0.85 * 41.97 * 150} = 27.63$$

$$h_p = h_c + d_a + \frac{t_p}{2}$$

$$h_p = 150 + 1.5 + 1.5 = 153 \text{ mm}$$

Assuming yielding of both internal and external reinforcement at failure, moment equilibrium at ultimate load conditions requires:

$$M_n = A_s f_{ys} \left(d_s - \frac{\bar{a}}{2} \right) + t_p b_p f_{yp} \left(h_p - \frac{\bar{a}}{2} \right)$$

$$M_n = 157.08 * 414 \left(113 - \frac{27.63}{2} \right) + 3 * 100 * 276 * \left(153 - \frac{27.63}{2} \right) = 17.97 * 10^6 \text{ N} - \text{mm}$$

$$P_{flex} = \frac{2M_n}{a}$$

$$P_{flex} = \frac{2 * 17.97 * 10^6}{400} = 90 \text{ kN} **$$

** Represents maximum flexural capacity if repaired beam was to fail in flexure.

Shear Capacity (P_{shear})

Investigation for Concrete Rip-off

In order to check on the shear capacity of the plated R/C beams, the following quantities are computed according to ACI strength method:

Shear strength provided by concrete V_c is,

$$V_c = \frac{1}{6} \left[\sqrt{f'_c} + 100 \rho_w \left(\frac{V_u d_s}{M_u} \right) \right] b_c d_s$$

$$V_c = \frac{1}{6} \left[\sqrt{41.97} + \frac{100 * 157.08}{150 * 113} \right] * 150 * 113 = 20.92 \text{ kN}$$

$$\rho_w = \frac{A_s}{b_c d_s}$$

Shear strength in the web steel is,

$$V_s = \frac{A_v f_{ys} d_s}{s} = 80.15 \text{ kN}$$

Total shear force V_n applied at a given section is given by

$$V_n = V_c + V_s = 20.92 + 80.15 = 101.07 \text{ kN}$$

The load corresponding to shear

$$P_s = 2 V_n = 2 * 101.07 = 202.14 \text{ kN}$$

$$P_{\text{expt}} = 74.5 \text{ kN}$$

$$K_{\text{sf}} = \frac{\left(\left(\frac{P_{\text{expt}}}{2} \right) - V_c \right)}{V_s} = 0.204$$

Expression for Shear Capacity

Rip-Off Failure

Using the strength of materials approach, the maximum shear and peeling stresses at the interface for the beam using Robert's approach [34] at the maximum load sustained by the beam are represented by τ_o and σ_o respectively. In addition

to the material properties and beam dimension, the other parameters are determined as follows:

$$A = \frac{E_c b_c}{2E_p} = \frac{30661 * 150}{2 * 200000} = 11.50 \text{ mm}$$

$$B = \frac{E_s A_s}{E_p} + b_p t_p = \frac{200000 * 157.08}{200000} + 100 * 3 = 457.08 \text{ mm}^2$$

$$C = \frac{A_s d E_s}{E_p} + h_p b_p t_p = \frac{113 * 157.08 * 200000}{200000} + 153 * 3 * 100 = 63650$$

$$X = \frac{-B + (B^2 + 4AC)^{1/2}}{2A}$$

$$X = \frac{-457.08 + \sqrt{(457.08)^2 + 4 * 11.50 * 63650}}{2 * 11.50} = 57.13$$

$$M^* = \frac{P}{2y} \left(X + \frac{d_c + t_p}{2} \right)$$

$$V = \frac{P}{2}$$

$$I_p = \frac{b_p t_p^3}{12} = \frac{100 * 3^3}{12} = 225 \text{ mm}^4$$

The second moment of Inertia (I) of the fully composite transformed equivalent steel section is given by

$$I = \frac{E_c b_c X^3}{3E_p} + \frac{A_s E_s (h_s - X)^2}{E_s} + b_p t_p (h_p - X)^2$$

$$I = \frac{30661 * 150 * (57.13)^3}{3 * 200000} + \frac{157.08 * 200000 * (113 - 57.13)^2}{200000} + 100 * 3 * (153 - 57.13)^2$$

$$I = 4,676,921 \text{ mm}^4$$

The shear stiffness of the interface layer

$$K_s = \frac{G_a b_a}{d_a} = \frac{120.1 * 100}{15} = 8006.67 \text{ MPa}$$

Normal stiffness of the interface layer

$$K_n = \frac{E_a b_a}{d_a} = \frac{278.6 * 100}{15} = 18,573 \text{ MPa}$$

$$C_{r1} = \left[1 + \left(\frac{K_s}{E_p b_p d_p} \right)^{1/2} L_c \right] \frac{b_p d_p}{I b_a} (h_p - h)$$

$$C_{R1} = \left[1 + \left(\sqrt{\frac{8006.67}{200000 * 100 * 3}} \right) 50 \right] \frac{100 * 3 * (153 - 57.13)}{4,676,921 * 100} = 9.70 * 10^{-5}$$

$$\tau_o = \alpha_1 f'_t \left(\frac{C_{r1} V_o}{f'_c} \right)^{5/4}$$

Tensile strength of concrete

$$f'_t = 0.324 (f'_c)^{2/3} = 3.913 \text{ MPa}$$

$$\tau_o = 35 * 3.913 \left(\frac{9.70 * 10^{-5} * \frac{74.5 * 10^3}{2}}{41.97} \right)^{5/4} = 6.40 \text{ MPa}$$

In contrast, using a linear strength of materials model, Robert's [34] suggested use of the following expression to evaluate the peak shear interface stress

$$\bar{\tau}_o = C_{r1} V_o$$

The factor C_{R2} is calculated using

$$C_{R2} = d_p \left(\frac{K_n}{4E_p I_p} \right)^{1/4}$$

$$C_{R2} = 3 * \left(\frac{18573}{4 * 200000 * 225} \right)^{1/4} = 0.3023$$

The peak peeling stress σ_o required is given by

$$\sigma_o = \alpha_2 C_{R2} \tau_o$$

$$\sigma_o = 1.10 * 0.3023 * 6.40 = 2.12 \text{ MPa}$$

The capacity of a plated R/C beam prone to concrete rip-off failure has been detailed in Ref [38] and can be approximated (in N-mm) as

$$V_u = (V_c + kV_s)$$

$$V_c = \frac{1}{6} \left(\sqrt{f'_c} + 100 \rho_w \frac{V_u d_s}{M_u} \right) b_c d_s$$

$$V_s = \frac{A_v f_{yst} d_s}{s}$$

$$k = 2.4 e^n$$

$$k = 2.4 e^{-0.08 * 9.7 * 10^{-5} * 0.3023 * 10^6} = 0.23$$

$$n = -0.08 C_{R1} C_{R2} * 10^6$$

$$P_{\text{shear}} = 2 V_n$$

$$P_{\text{shear}} = 2(V_c + kV_s) = 2*(20.92 + 0.23*80.15)$$

$$P_{\text{shear}} = 78.67 \text{ kN}$$

Since, $P_{\text{shear}} < P_{\text{flex}}$ this beam will fail by concrete cover ripoff. P_u based on diagonal tension (Modified expression) not shown since $P_f < P_s$ and beam will fail either by ripoff or by flexure.

The maximum shear stress at interface τ_o at the point of plate curtailment based on Robert's approach [34] is given by:

$$\tau_o = \left(V_n + \sqrt{\left(\frac{K_s}{E_p b_p d_p} \right) M^*} \right) b_p t_p \left(\frac{h_p - h}{b_a I} \right)$$

The maximum peeling (normal) stress at interface σ_o on the basis of Robert's expression [34] is given by:

$$\sigma_o = \tau_o t_p \left(\frac{K_n}{4E_p I_p} \right)^{1/4}$$

$$\sigma_o = C_{R1} C_{R2} \left(\frac{P_{\text{expt}}}{2} \right) = 9.7 * 10^{-5} * 0.3023 * \frac{74.5 * 10^3}{2} = 1.093 \text{ MPa}$$

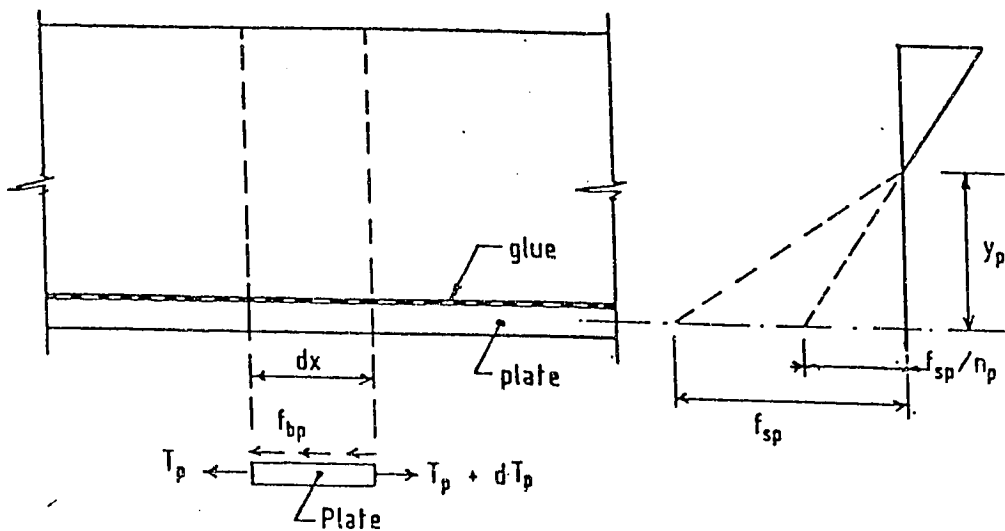
$$\tau_o = \frac{\sigma_o}{C_{R2}} = \frac{1.093}{0.3023} = 3.613 \text{ MPa}$$

APPENDIX-B

This section presents the theoretical preliminaries with regard to the Glue/Plate Interface Bond Stress, Glue/Concrete Interface Bond Stress, Effect of Plate Cutoff on Bond Stress, Effect of Peeling Forces. [48]

THEORETICAL PRELIMINARIES

1. Glue/Plate Interface Bond Stress f_{bp} [20]



f_{bp} → glue/plate interface bond stress, b_p → width of plate

$$\Sigma F_x = 0 \Rightarrow T_p + dT_p - T_p - f_{bp} dx b_p = 0$$

$$\therefore f_{bp} = \frac{1}{b_p} \frac{dT_p}{dx} \quad (1)$$

Now, using the concept of equivalent section

$$\frac{f_{sp}}{n_p} = \frac{T_p}{A_p n_p} = \frac{M y_p}{I_t} \quad (a)$$

where

A_p = cross-sectional area of plate

n_p = modular ratio $E_{plate}/E_{concrete} \approx 8.0$

y_p = distance from N.A. to mid-plane of plate

I_t = transformed second moment of area (moment of inertia)

Using incremental form of (a)

$$\frac{dT_p}{A_p n_p} = \frac{dM y_p}{I_t} \quad (b)$$

Also

$$\frac{dM}{dx} = V \Rightarrow \text{use in (b)}$$

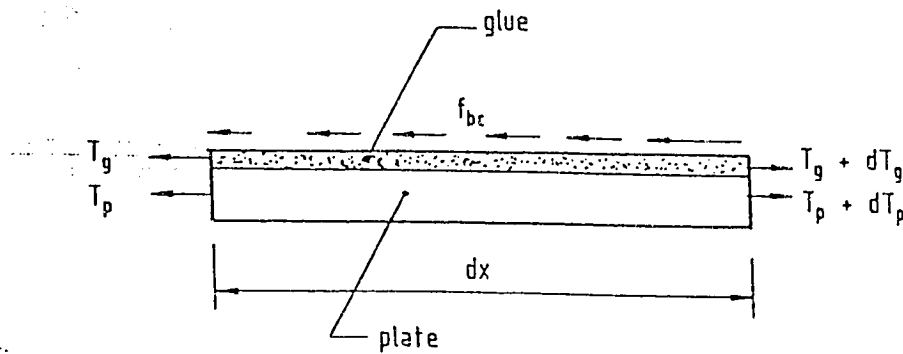
$$\frac{dT_p}{A_p n_p} = \frac{V dx y_p}{I_t}$$

$$\frac{dT_p}{dx} = \frac{V y_p A_p n_p}{I_t} \quad (c)$$

Using (c) in (1)

$$\therefore f_{bp} = \frac{V y_p A_p n_p}{I_t b_p} \quad (\text{measure of average bond stress}) \quad (2)$$

Glue/Concrete Interface Bond Stress [20]



f_{bc} = glue/concrete interface bond stress

T_g = tensile force in glue

b_g = width of glue

say b_p = width of plate

$$\Sigma F_x = 0$$

$$f_{bc} * b_p dx = (T_g + dT_g) - T_g \\ + (T_p + dT_p) - T_p$$

$$\therefore f_{bc} = \frac{dT_g + dT_p}{b_p dx} \quad (3)$$

Also, by analogy to equation (c)

$$dT_g = \frac{A_g n V y_g dx}{I_t} \quad (4)$$

where

A_g = cross-sectional area of glue layer

$n_g = E_{\text{glue}}/E_{\text{concrete}}$ which is in the range of 0.03-0.30

Then

$$\frac{dT_p}{dT_g} \approx \frac{n_p}{n_g} \text{ which is in the range of } 27-270$$

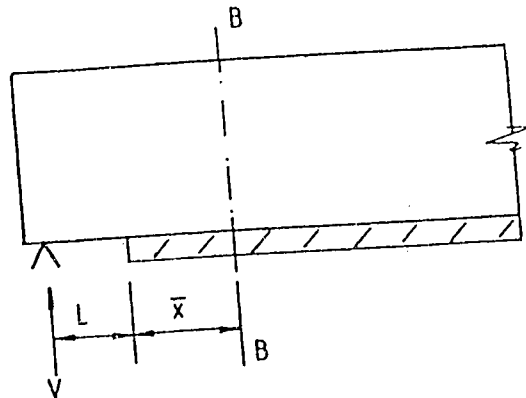
Thus

dT_g is very small compared to dT_p , then (3) becomes

$$f_{bc} = \frac{dT_p}{b_p dx} = f_{bp} \text{ from (1)}$$

Effect of Plate Cutoff on Bond Stress f_{bp}

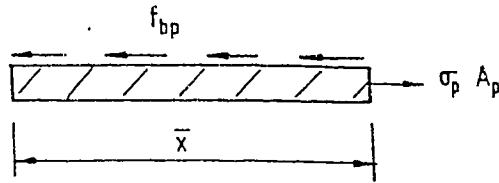
Now assume plate is fully effective at BB i.e. elastic theory applies at \bar{x} from plate curtailment.



σ_p - stress in plate at section BB $\left[\text{from } \frac{\sigma_p}{n_p} = \frac{My_p}{I_1} \text{ \& } M = V(L+\bar{x}) \right]$

$$= \frac{V(L+\bar{x}) y_p * n_p}{I_1} \quad (5)$$

For average bond stress over length \bar{x}



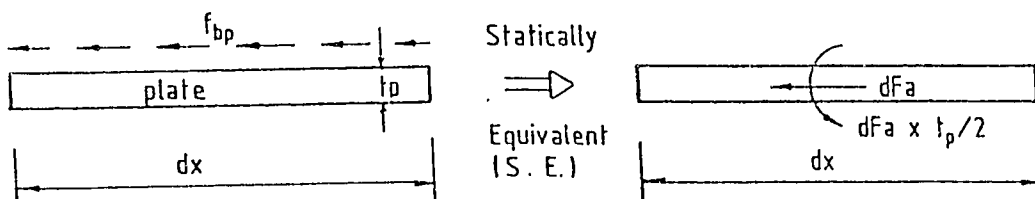
$$\Rightarrow f_{bp} \bar{x} b_p = \sigma_p A_p = \text{use (5)}$$

$$\therefore f_{bp} = \frac{V(L+\bar{x}) y_p n_p}{I_1} A_p \frac{1}{\bar{x} b_p}$$

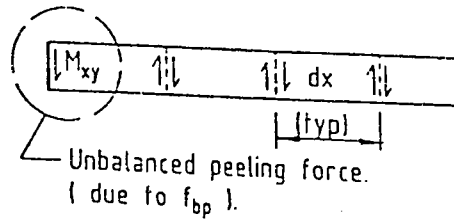
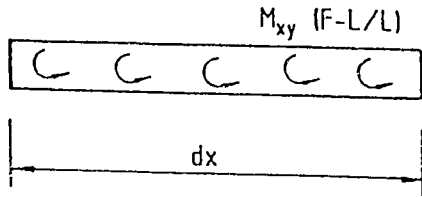
$$f_{bp} = \left[1 + \frac{L}{\bar{x}} \right] \frac{V y_p A_p n_p}{I_1 b_p} \quad (6)$$

Now if $L \approx \bar{x}$, f_{bp} as given by equation (6) in comparison to the average bond stress f_{bp} as given by equation (2) shows significant increase in bond stress near region of plate cutoff. Tests show this to be true, with non-uniform interface bond stresses & a high peak value near plate end. This f_{bp} increase plays a critical role in failure by separation.

Peeling Forces [20]



(S.E.) \Rightarrow



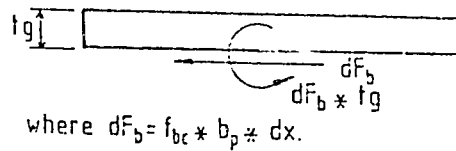
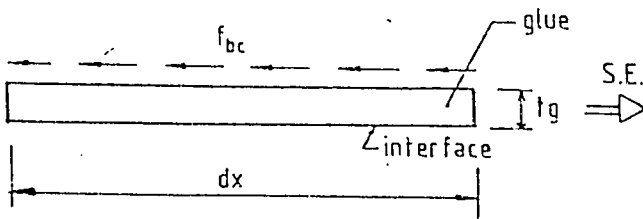
$$dF_a = f_{bp} * b_p * dx \tag{7}$$

$$M_{xy} * dx = dF_a * \frac{t_p}{2} \tag{8}$$

(M_{xy} = twisting moment per unit length)

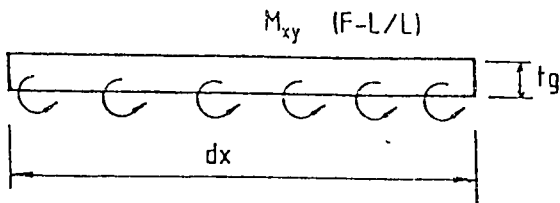
Using (7) in (8)

$$M_{xy} = f_{bp} * b_p * \frac{t_p}{2} \tag{9.1}$$

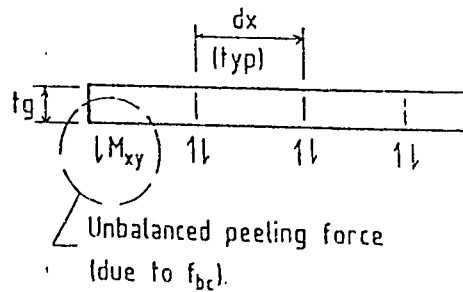


where $dF_b = f_{bc} * b_p * dx$.

S.E. \Rightarrow



S.E. \Rightarrow



$$M_{xy} dx = dF_b * t_z = f_{bc} * b_p * dx * t_z$$

$$\therefore M_{xy} = f_{bc} * b_p * t_z \quad (9.2)$$

Total unbalanced peeling force = (9.1) + (9.2)

$$M_{xy} (F-L/L) - b_p \left[t_z + \frac{t_p}{2} \right] f_{bp} \quad (f_{bp} - f_{bc})$$

$$\Rightarrow (6) - b_p \left[t_z + \frac{t_p}{2} \right] \left[1 + \frac{L}{x} \right] \frac{V y_p A_p n_p}{I_t b_p}$$

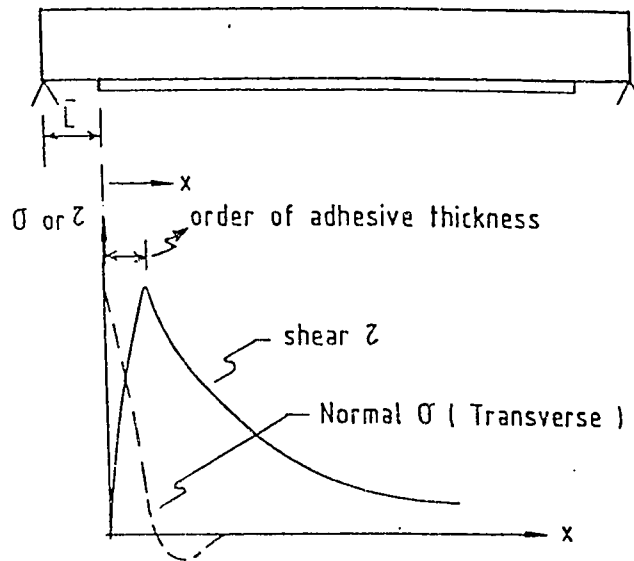
or

$$M_{xy} - V y_p n_p A_p \left[t_z + \frac{t_p}{2} \right] \left[1 + \frac{L}{x} \right] \quad (10)$$

- * Note: Effect of interface bond stress (f_{bp}) is statically equivalent to applying a set of vertical forces $M_{xy} (F-L/L)$, which yields an unbalanced M_{xy} at location of plate cutoff. This is a tensile force and is responsible for horizontal tearing of concrete below the level of main (internal) reinforcement, causing what is known as concrete rip-off failure.

2. Analysis for Determination of Shear & Peeling Stresses in Adhesive Layer [22]

- Premature failures may occur because of shear + normal stress concentrations at the ends of the steel plates, resulting in debonding or ripping off the concrete cover along the level of conventional internal reinforcement



- τ, σ stress concentrations depend on K_s, K_n of adhesive
- τ, σ stress concentrations depend on t_p & \bar{L} (point of termination)

Can reduce stress concentrations significantly by

- using more flexible adhesive
- reducing t_p
- for simply supported beam, terminating steel plate as close to supports as possible

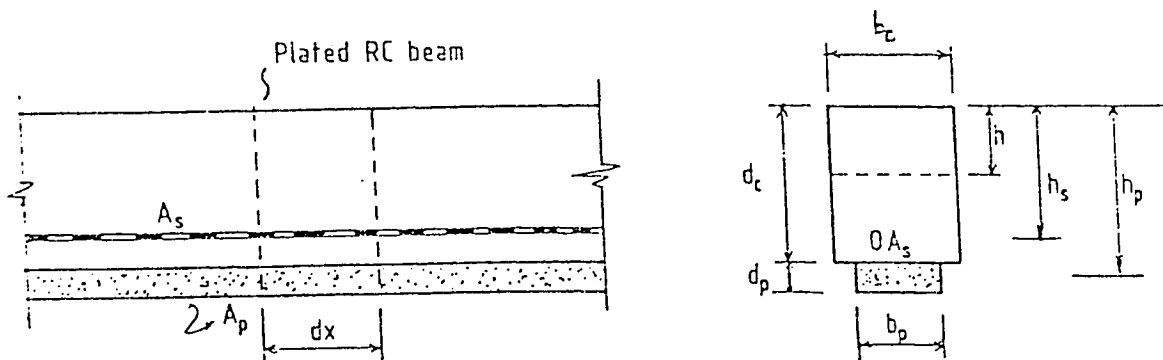
Three Stage Analysis

STAGE 1 : assume fully composite action between RC beam & adhesive bonded steel plate and calculate stresses at sections removed from the boundary

STAGE 2 : } \Rightarrow Analysis modified to take account of actual boundary
 STAGE 3 : } conditions at ends of steel plate

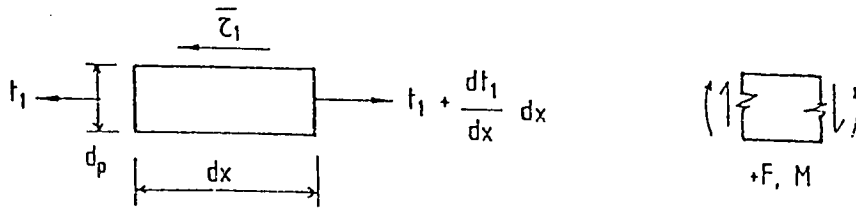
We need to superpose the three stages for complete solution of the problem.

STAGE 1 Calculation of σ, τ removed from b' dry



$h \Rightarrow$ depth of NA, based on assumed elastic b'vior & fully composite action
 (but allowing for cracking of concrete in tension)

$I \Rightarrow$ moment of inertia of transformed equivalent steel section about NA



$t_1 \Rightarrow$ axial force in plate

$\bar{\tau}_1 \Rightarrow$ shear flow/unit length in adhesive layer

$$\Sigma F_x = 0 \Rightarrow \frac{dt_1}{dx} dx - \bar{\tau}_1 dx \Rightarrow \bar{\tau}_1 = \frac{dt_1}{dx}$$

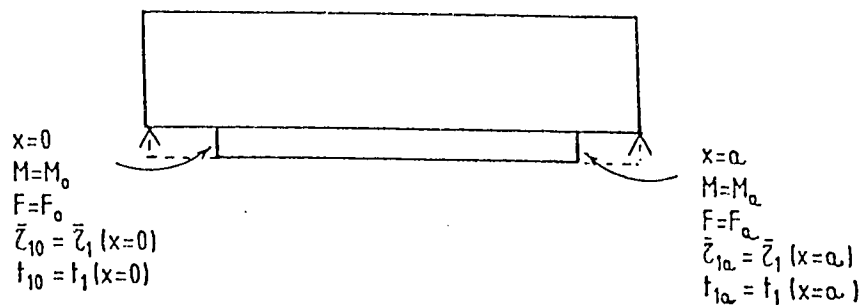
$$\& \quad F = \frac{dM}{dx} \quad (\Sigma M = 0)$$

Also

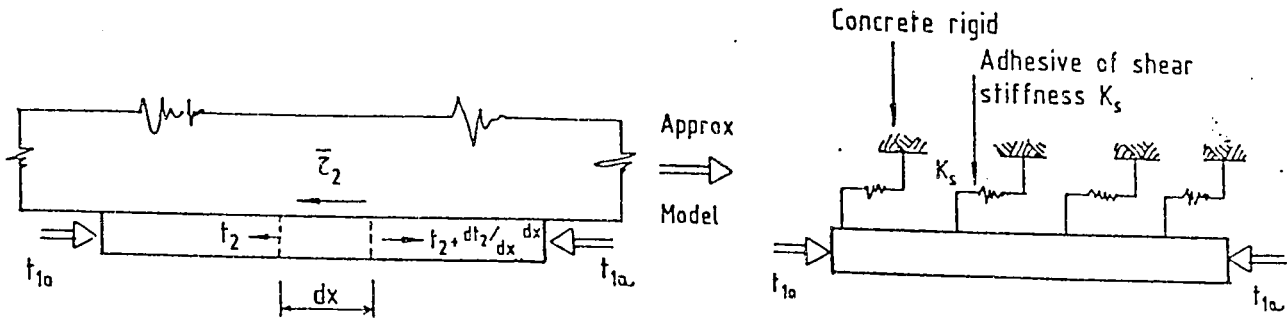
$$\bar{\tau}_1 \Rightarrow \frac{FQ}{I} \Rightarrow \frac{F [b_p d_p (h_p - h)]}{I}$$

(A)

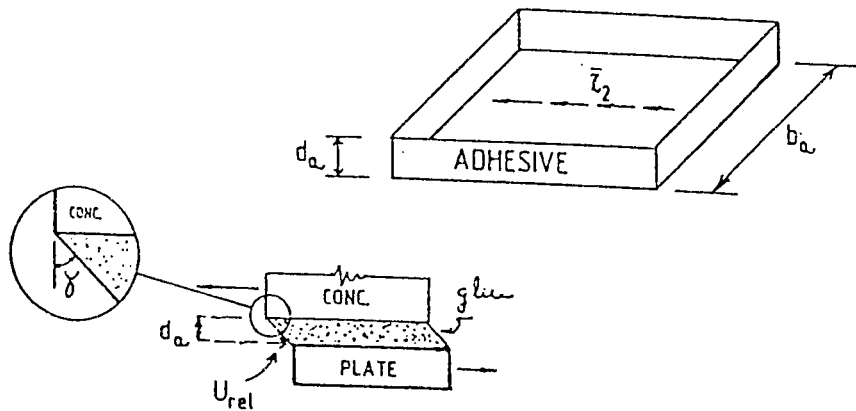
$$\& \quad t_1 = \sigma_1 A_p = \frac{M(h_p - h)}{I} b_p d_p$$



STAGE 2 Clear axial forces t_{10} and t_{1x} .



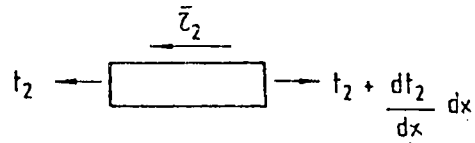
$K_s = ?$



$$\tau_{gluc} = \frac{\bar{\tau}_2}{b_a} = G_{gluc} \gamma = G_g \frac{U_{rel}}{d_a}$$

$$\therefore \left(\frac{F}{L} \right) \left(\frac{\bar{\tau}_2}{b_a} \right) = \frac{G_g b_a}{d_a} U_{rel} = \left(K_s \right) \left(U_{rel} \right)$$

$$\therefore K_s = \text{shear stiffness} = \frac{G_s b_s}{d_s}$$



$$\frac{dt_2}{dx} dx = \bar{\tau}_2 dx$$

$$\therefore \bar{\tau}_2 = \frac{dt_2}{dx} \quad (1)$$

$$\& \bar{\tau}_2 = K_s u_{rel} = K_s u$$

$$\& t_2 = \sigma A_p$$

$$= E_p \epsilon_x d_p b_p$$

$$= E_p \frac{du}{dx} d_p b_p \quad (2)$$

($u \rightarrow$ plate disp. in x-direction)

Using (2) in (1)

$$K_s u = \frac{d}{dx} \left[E_p \frac{du}{dx} b_p d_p \right]$$

$$\therefore \frac{d^2u}{dx^2} - \frac{K_s}{E_p b_p d_p} u = 0 \quad (3)$$

$$\text{Let } \alpha^2 = \frac{K_s}{E_p b_p d_p}$$

\therefore Solution of (3) subject to bc's that $t_2(x=0) = -t_{10}$ & $t_2(x=a) = -t_{1a}$

$$u = \frac{-t_{10} \sinh \alpha x}{E_p b_p d_p \alpha} + \frac{t_{10} \cosh \alpha a - t_{1a}}{E_p b_p d_p \alpha \sinh \alpha a} \cosh \alpha x \quad (4)$$

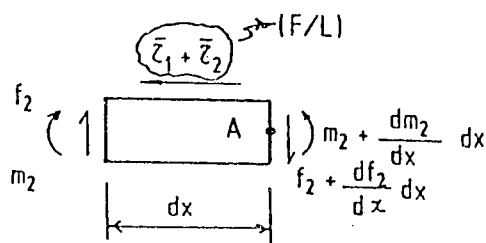
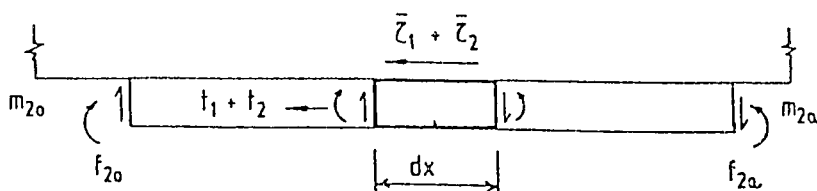
Then

$$\bar{\tau}_2 = K_s u \Rightarrow \text{use (4)}$$

$$= \left\{ \frac{K_s}{E_p b_p d_p} \right\}^{1/2} \left\{ -t_{10} \sinh \alpha x + \frac{(t_{10} \cosh \alpha a - t_{1a})}{\sinh \alpha a} \cosh \alpha x \right\} \quad (5)$$

(Note clearing axial forces has created MORE shear stress)

Resultant Forces in steel plate at end of STAGE 2:



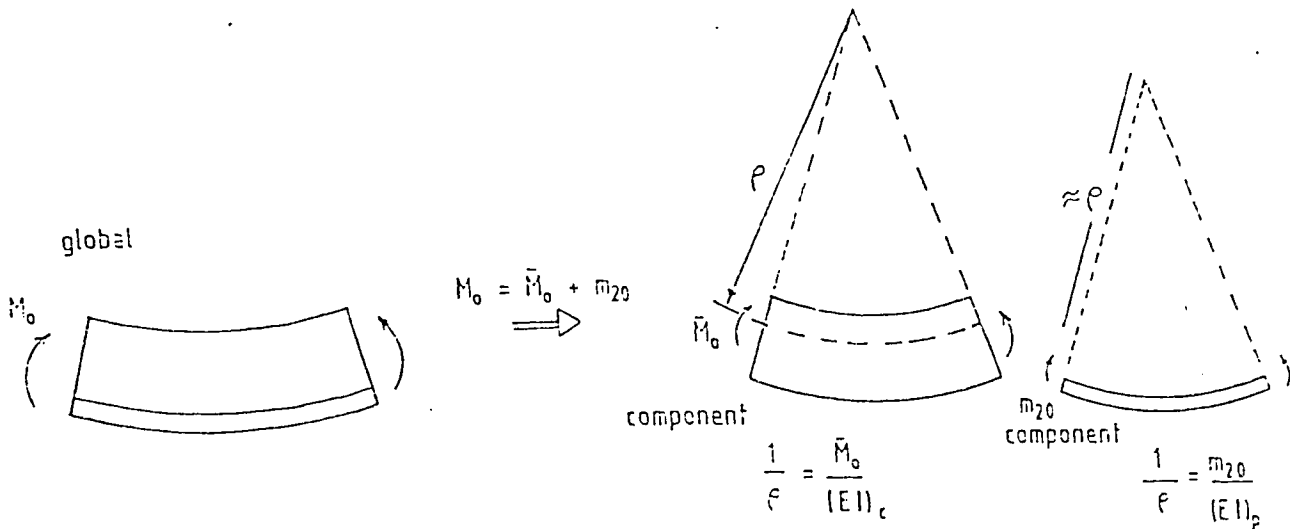
(\therefore shear & moment not cleared from ends)

$$\Sigma M_A = 0$$

$$\frac{dm_2}{dx} dx - f_2 dx + (\bar{r}_1 + \bar{r}_2) \frac{d_p}{2} dx = 0$$

$$\therefore f_2 = \frac{dm_2}{dx} + (\bar{r}_1 + \bar{r}_2) \frac{d_p}{2} \quad (6)$$

Consider the following:



(I_p, I_c are second moments of area of steel plate & concrete beam about their individual centroids.)

Then

$$\frac{\bar{M}_o}{(EI)_c} = \frac{m_{20}}{(EI)_p}$$

$$\therefore \frac{M_o - m_{20}}{(EI)_c} = \frac{m_{20}}{(EI)_p}$$

$$\therefore \frac{M_o}{(EI)_c} = m_{20} \left[\frac{(EI)_c + (EI)_p}{(EI)_c (EI)_p} \right]$$

$$\therefore m_{20} = \frac{(EI)_p}{(EI)_c + (EI)_p} M_o \tag{7}$$

Using (7) in (6) (at $x = 0$)

$$f_2(x=0) = f_{20} = \frac{(EI)_p}{(EI)_c + (EI)_p} \left(\frac{dM_c}{dx} \right) + (\bar{\tau}_{10} + \bar{\tau}_{20}) \frac{d_p}{2}$$

$\rightarrow = F_o$

$$\therefore f_{20} = \left\{ \frac{(EI)_p}{(EI)_c + (EI)_p} \right\} F_o + (\bar{\tau}_{10} + \bar{\tau}_{20}) \frac{d_p}{2} \quad \text{(shear force at end } x = 0)$$

(8)

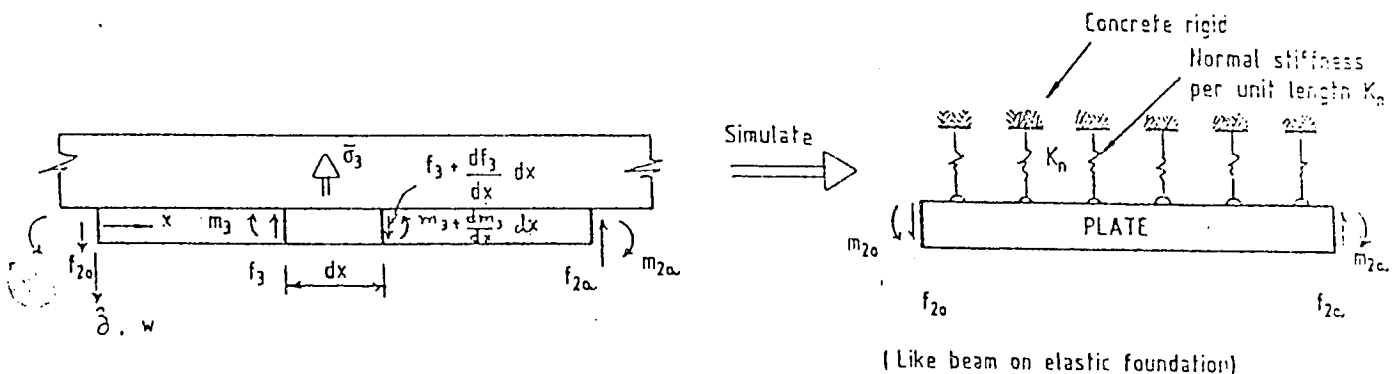
$$\& \quad m_{20} = \frac{(EI)_p}{(EI)_c + (EI)_p} M_o \tag{7}$$

(For f_{2a} , M_{2a} , we need appropriate values M_a , F_a , $\bar{\tau}_{1a}$, $\bar{\tau}_{2a}$ in (7) & (8))

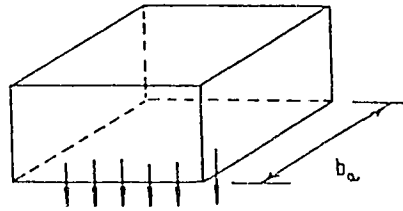
STAGE 3 (Clear f_{20} , m_{20} & f_{2a} , m_{2a})

Since moments m_{20} & m_{2a} & shear forces f_{20} & f_{2a} do not exist in practice, the next stage

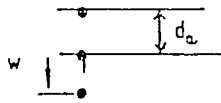
of the solution is to apply opposite moments & shears at $x = 0$ & $x = a$.



$$K_n = ?$$



$\bar{\sigma}$ = normal force / unit length in adhesive.



$$\therefore \frac{\bar{\sigma}}{b_a} = \text{average normal stress in adhesive}$$

$$= \sigma = E_a * \epsilon_{\text{relative}}$$

$$\frac{\bar{\sigma}}{b_a} = E_a * \frac{w}{d_a}$$

$$\therefore \bar{\sigma} = \underbrace{\frac{E_a b_a}{d_a}}_{K_n} w$$

$$\therefore \bar{\sigma}(F/L) = K_n * w \quad (9)$$

Then treating the model of stage 3 like a beam on an elastic foundation, the governing differential equation becomes

$$\frac{d^4 w}{dx^4} + 4\gamma^4 w = 0 \quad (10)$$

$$\left[\gamma^4 - \frac{K_n}{4E_p I_p} \right]$$

Solving (9) under assumption that $\lim_{x \rightarrow \text{big}} w = 0$ & that at $x = 0$

$$\left. \begin{aligned} m_3 &= -E_p I_p \frac{d^2 w}{dx^2} = -m_{20} \\ & \text{ \& } f_3 = -E_p I_p \frac{d^3 w}{dx^3} = -f_{20} \end{aligned} \right\} \quad (11)$$

The solution becomes

$$w(x) = \frac{e^{-\gamma x}}{2E_p I_p \gamma^4} \left\{ (f_{20} \gamma + m_{20} \gamma^2) \cos \gamma x - m_{20} \gamma^2 \sin \gamma x \right\} \quad (12)$$

Using (12) in (9)

$$\bar{\sigma} = 2e^{-\gamma x} \left\{ (f_{20} \gamma + m_{20} \gamma^2) \cos \gamma x - m_{20} \gamma^2 \sin \gamma x \right\} \quad (13)$$

COMPLETE SOLUTION

$$\bar{\tau} = \bar{\tau}_1 + \bar{\tau}_2 \quad (\text{Eqn. (A.1) } \div (5))$$

$$\& \quad \bar{\sigma} \Rightarrow \text{equation (13)}$$

& unit shear & normal stresses in adhesive are given by

$$\tau = \frac{\bar{\tau}}{b_a} \quad ; \quad \sigma = \frac{\bar{\sigma}}{b_a} \quad (\text{peeling stress}) \quad (14)$$

APPROXIMATE EXPRESSIONS

neglect (conservative)

$$\bar{\tau}_2(x=0) \Rightarrow (5) = \left\{ \frac{K_s}{E_p b_p d_p} \right\}^{1/2} \left\{ \frac{t_{10} \cosh \alpha a - t_{1a}}{\sinh \alpha a} * 1 \right\}$$

(Also $\cosh \alpha a \approx \sinh \alpha a$)

$$\& \quad t_{10} \Rightarrow (A.2) = \frac{M_o b_p d_p}{I} (h_p - h)$$

$$\therefore \bar{\tau}_2(x=0) = \left[\frac{K_s}{E_p b_p d_p} \right]^{1/2} \frac{M_o b_p d_p}{I} (h_p - h) \quad (15)$$

Then $\bar{\tau}(x=0) \Rightarrow$ EQN. (A.1) + (15)

$$= \frac{F_o b_p d_p}{I} (h_p - h) + \left[\frac{K_s}{E_p b_p d_p} \right]^{1/2} \frac{M_o b_p d_p}{I} (h_p - h)$$

$$\therefore \tau_o = \frac{\bar{\tau}(x=0)}{b_s} = \left[F_o + \left\{ \frac{K_s}{E_p b_p d_p} \right\}^{1/2} M_o \right] \frac{b_p d_p}{I b_s} (h_p - h) \quad (16)$$

$$\& \quad \text{if we assume } \frac{E_p I_p}{E_p I_p + E_c I_c} \approx 0$$

then $m_{20} \approx 0$ (from (7))

$$\& \quad f_{20} \cong (\bar{\tau}_{10} + \bar{\tau}_{20}) \frac{d_p}{2} \quad (17)$$

Then

$$\sigma_o = \frac{\bar{\sigma}(x=0)}{b_s} \Rightarrow \text{using (13)} = \frac{1}{b_s} [2 f_{20} \gamma] \Rightarrow \text{using (17)}$$

$$= \frac{1}{b_s} (\bar{\tau}_{10} + \bar{\tau}_{20}) d_p \gamma \Rightarrow \text{using (A.1) and (15)}$$

$$= d_p \gamma \left\{ \frac{F_o b_p d_p (h_p - h)}{I b_s} + \left[\frac{K_s}{E_p b_p d_p} \right]^{1/2} \frac{M_o b_p d_p}{I b_s} (h_p - h) \right\}$$

$$\Rightarrow \text{using (16)} = d_p \gamma \tau_o \Rightarrow \text{use } \gamma^4 = \frac{K_n}{4 E_p I_p}$$

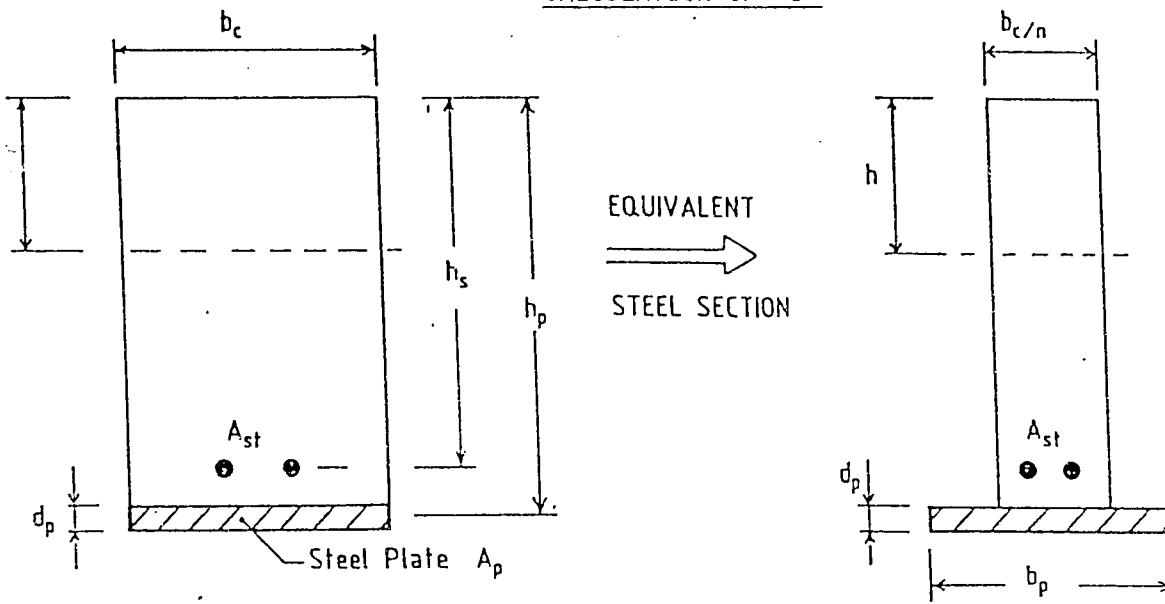
$$\therefore \sigma_o = \tau_o d_p \left\{ \frac{K_n}{4 E_p I_p} \right\}^{1/4}$$

SUMMARY

$$\left. \begin{aligned} \tau_o &= \left[F_o + \left\{ \frac{K_s}{E_p b_p d_p} \right\}^{1/2} M_o \right] \frac{b_p d_p}{I b_s} (h_p - h) \\ \sigma_o &= \tau_o d_p \left\{ \frac{K_n}{4 E_p I_p} \right\}^{1/4} \end{aligned} \right\}$$

Robert's expressions
[22]

CALCULATION OF 'I'



For NA Location

$$\frac{b_c}{n} \frac{h^2}{2} = A_{st}(h_s - h) + A_p(h_p - h)$$

or

$$\underbrace{\left(\frac{b_c}{2n}\right)}_A h^2 + h \underbrace{(A_{st} + A_p)}_B - \underbrace{(A_{st}h_s + A_ph_p)}_C = 0$$

$$\therefore h = \left(-B + \sqrt{B^2 + 4AC} \right) / 2A$$

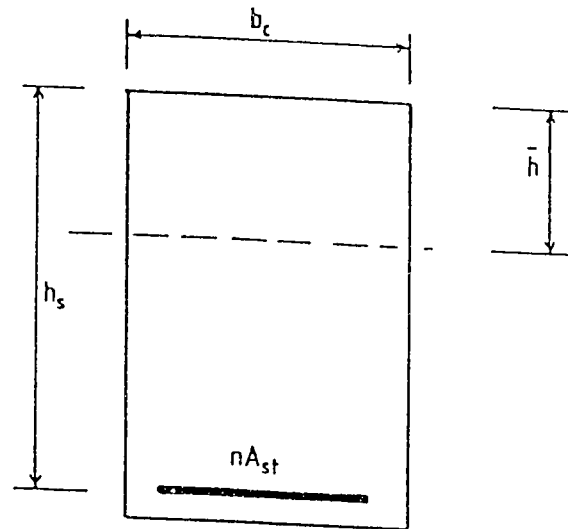
&

$$I = \frac{b_c}{n} \frac{h^3}{3} + A_{st}(h_s - h)^2 + A_p(h_p - h)^2$$

$$= \frac{b_c h^3}{3E_p/E_c} + A_{st}(h_s - h)^2 + b_p d_p (h_p - h)^2$$

- RC beam alone for calculation of $(EI)_c$

Consider equivalent section in concrete



$$\frac{b_c \bar{h}^2}{2} = nA_{st}(h_s - \bar{h}) \quad \left(n = \frac{E_p}{E_c} \right)$$

$$\bar{A} \left(\frac{b_c}{2n} h^2 + \underbrace{A_{st}}_{\bar{B}} \bar{h} - \underbrace{A_{st}}_{\bar{C}} h_s \right) = 0$$

$$\bar{h} = \frac{-\bar{B} + \sqrt{\bar{B}^2 + 4\bar{A}\bar{C}}}{2\bar{A}}$$

Then

$$I_c = \frac{b_c \bar{h}^3}{3} + nA_{st}(h_s - \bar{h})^2$$

&

$$E_c I_c = \frac{E_c b_c \bar{h}^3}{3} + E_p A_{st} (h_s - \bar{h})^2 \quad \textcircled{1}$$

(Alternatively: if used equivalent in steel

$$\bar{I}_c = \frac{b_c \bar{h}^3}{3n} + A_{st} (h_s - \bar{h})^2$$

& Then

$$E_p \bar{I}_c = \frac{E_p b_c \bar{h}^3}{3E_p/E_c} + E_p A_{st} (h_s - \bar{h})^2$$

$$= \frac{E_c b_c \bar{h}^3}{3} + E_p A_{st} (h_s - \bar{h})^2 \quad (2)$$

(2) is SAME as (1) i.e. EI of unplated RC beam.)

VITAE

Mohammed Ashrafuddin

Born on 21st August, 1968 in Hyderabad, India.

Received B.S. in Civil Engineering in 1991 from Osmania University, Hyderabad, India.

Received M.S. (Structures) in Civil Engineering in 1995 from King Fahd University of Petroleum & Minerals, Dhahran, Saudi Arabia.